The Production of Granular Activated Carbon from Agricultural Waste Products

By

Lizelle Doreen van Dyk

Thesis submitted in partial fulfilment of the requirements for the degree of Master of Science in Engineering (Extractive Metallurgical Engineering) in the Department of Chemical Engineering at the University of Stellenbosch.

Supervisor: Prof. Izak Nieuwoudt

Stellenbosch

October 2000

Declaration

I, the undersigned, hereby declare that the work contained in this thesis is my own original work and that I have not previously in its entirety or in part submitted it at any university.

Lizelle Doreen van Dyk 13 October 2000

Summary

Peach and apricot shells are agricultural waste products. These waste products accumulate around canneries and food-processing plants in South Africa. No effort is being made to utilise these waste products. This study is the first part of the product development from these products i.e. peach shell activated carbon and apricot shell activated carbon. By producing activated carbon from peach and apricot shells the solid waste problem is addressed, but most of all a profit can be made.

But why activated carbon? Activated carbons are unique and versatile adsorbent with a vast amount of adsorption applications. It can be produced via a simple oxidation reaction with steam and the nature of peach and apricot shells are such that it is expected that activated carbons with good adsorption properties can be produced from it. The single largest consumer of activated carbon in South Africa is the gold mining industry that uses imported coconut shell activated carbon for gold adsorption in the gold recovery process. Activated carbon is also used as water purification adsorbents.

During this study activated carbons were produced in a fluidized bed reactor at various activation conditions: 700 – 900°C, 0.0425 – 0.0629 g steam/g char.min and 30 – 60 min. This was done in order to find the optimum activation conditions within the activation parameter range. The optimal activated carbons were defined as peach and apricot shell activated carbons that showed good microporous as well as mesoporous character. The optimal activated carbons produced are: peach shell activated at 875°C, 0.0533 g steam/g char.min, 60 min and apricot shell activated carbon at 850°C, 0.0533 g steam/g char.min, 60min.

The possible use of these optimal activated carbons and two other activated carbons produced (Peach shell activated carbon 900°C, 0.0425 g steam/g char.min, 60 min and apricot shell activated carbon 900°C, 0.0425 g steam/g char.min, 60min) were tested in gold recovery and water purification. The gold adsorption properties of peach and apricot shell activated carbons were found to be better than two commercial coconut shell activated carbons (Chemquest 650 and GRC 22). No definite conclusions could, however, be drawn about the replacement of coconut shell

activated carbon with peach or apricot shell activated carbon, because abrasion test work and thermal regeneration of the experimental carbons still have to be performed.

The experimental activated carbons displayed good phenol adsorption characteristic, although further test work is required.

Opsomming

Perske- en appelkoospitte is landbouafvalprodukte. Hierdie afvalprodukte versamel rondom inmaakfabrieke en voedselververkingsaanlegte. Tans word daar geen poging in Suid-Afrika aangewend om hierdie afvalprodukte te benut nie. Hierdie studie is die eerste deel van die ontwikkeling van die produkte: Perskepitdop-geaktiveerde koolstof en appelkoospitdop-geaktiveerde koolstof. Deur geaktiveerde koolstof van die perske- en appelkoospitdoppe te maak, word nie net 'n antwoord op die vastestofafvalsprobleem gevind nie, maar daar kan ook geld gemaak word.

Hoekom geaktiveerde koolstof? Aktiveerde koolstowwe is veelsydige en unieke adsorbente met 'n groot verskeidenheid adsorpsie toepassings. Dit kan vervaardig word via 'n eenvoudige oksidasie reaksie met stoom en die aard van die perske- en appelkoospitdoppe is sodanig, dat verwag kan word om geaktiveerde koolstowwe met goeie adsorpsie eienskappe daarvan te kry. Die grootste enkelverbruiker van geaktiveerde koolstof in Suid-Afrika is die goudmynbedryf, wat kokosneutdop geaktiveerde koolstof invoer om goud te herwin. Geaktiveerde koolstof word ook gebruik vir watersuiwering.

Tydens hierdie studie is geaktiveerde koolstowwe by verskillende aktiveeringskondisies in 'n gevloeïdiseerde bed vervaardig: 700 – 900°C, 0.0425 – 0.0629g stoom/g gepiroliseerde pitdoppe.min en 30 – 60 min. Die aktiveringskondisies is gevarieer om sodoende die optimale aktiveringskondisies binne die aktiveringsparameterreeks te kry. 'n Geaktiveerde koolstof is as optimaal geklassifiseer as dit 'n goeie mikro- sowel as mesostruktuur getoon het. Die optimaal geaktiveerde koolstowwe is: geaktiveerde koolstof vervaardig van perskepitdoppe by 875°C, 0.0533 g stoom/g gepiroliseerde pitdoppe.min, 60 min en geaktiveerde koolstof vervaardig van appelkoospitdoppe by 850°C, 0.0533 g stoom/g gepiroliseerde pitdoppe.min, 60min.

Die gebruik van die twee optimale geaktiveerde koolstowwe sowel as twee ander geaktiveerde koolstowwe (perskepitdop-geaktiveerde koolstof, 900°C, 0.0425 g stoom/g gepiroliseerde pitdoppe.min, 60 min en appelkoospitdop-geaktiveerde

koolstof, 850°C, 0.0533 g stoom/g gepiroliseerde pitdoppe.min, 60min) is vir goudadsorpsie en watersuiwering ondersoek. Die goudadsorpsie eienskappe van die perske-en appelkoospitdop-geaktiveerde koolstowwe was beter as die van twee kommersiële kokosneutdop-geaktiveerde koolstowwe (Chemquest 650 and GRC 22). Daar kan egter geen definitiewe gevolgtrekkings gemaak word oor die vervanging van kokosneutdop geaktiveerde koolstowwe met dié van perske of appelkoospitdoppe nie, aangesien daar nog toetsresultate oor die slytweerstand en reaktiverings eienskappe van die eksperimentele geaktiveerde koolstowwe uitstaande is.

Die eksperimentele geaktiveerde koolstowwe toon goeie adsorpie ten opsigte van fenol, maar verdere toetswerk is egter nodig.

Contents

List of Figures

List of Tables

Acknowledgements

I would like to express my gratitude towards the National Research Fund of South Africa and the University of Stellenbosch for bursaries during 1999 and 2000.

Sincere thanks to my supervisor Prof. I. Nieuwoudt for his guidance and encouragement during the course of this work.

Loving thanks to my parents, family and friends for their love and support during the course of this work.

1 Introduction

Product development is a group of activities beginning with the perception of a market opportunity and ending with the production, sales and delivery of a product. Successful product development has as end result products that can be sold profitably [Ulrich and Eppinger, 1995].

Waste can be defined as a material that its producer does not want and does not ask for reimbursement for its removal, although it may be of use to someone else. At some stage it will enter a waste handling system, either private or public. Solid waste is seen to be nongaseous and nonliquid waste [Clayton and Huie, 1973]. The disposal of solid waste is a major problem in both underdeveloped and developed countries. The problems arising from solid waste is two-fold: environmental impacts and cost of disposal. No price tag can be put on environmental assets, such as clean air, clean water and so on [Hester and Harrison, 1995].

Peach and Apricot pips are agricultural solid waste products. This research is part of the product development of the products: activated carbon from peach and apricot shells. The aim of this project is therefore not only to find a "waste disposal" method for peach and apricot shells, but also to produce an economically viable product.

1.1 Why Activated Carbon?

There are mainly three reasons why it was decided to produce activated carbon from peach and apricot shells:

- The nature of the raw materials (peach and apricot shells).
- The ease of production.
- The uses of activated carbon.

The nature of the raw materials

Activated carbon can be produced from any cheap material with a high carbon and low inorganic content. The property requirements of an activated carbon and hence the raw materials are also dependent on the application of the activated carbon.

When deciding whether a material will be a good raw material for the production of activated carbon the following factors need to be considered:

- The potential to obtain high quality activated carbon.
- Cost and volume of the raw material.
- Storage life of the raw material.
- Workability of the raw material [Bansal *et al*, 1988].

The quality and yield of an activated carbon is strongly dependent on the composition of the raw material. Table 1.1 provides an approximate analysis of the compositions of peach, apricot and coconut shells. Coconut shells are the raw material of most activated carbons and although it renders a low yield compared to the high carbon content of the raw material, the abundance and low cost associated with it ensures profitability [McDougall, 1991]. Similar results are expected for the peach and apricot shells, due to the nature of these raw materials (table 1.1).

Table 1.1: Proximate analysis of shells, dry basis [Mantell, 1975]

Shell Type	Ash (%)	Silicon in Ash (%)	Nitrogen (%)	Pentosans (%)	Cutin (%)	Lignin (%)	Lignin Corrected, for Cutin (%)	Alpha Cellulose (%)
Apricot	0.7	14.9	0.12	32.8	0.9	31.0	30.1	27.2
Peach	0.4	21.9	0.15	31.1	1.7	38.9	37.2	22.6
Coconut	0.7	2.9	0.12	31.6	0.3	34.2	33.9	24.3

Due to the fact that no major effort is currently being made in South Africa to utilise peach and apricot pips, the assumption can be made that the raw materials would be relatively cheap and abundant. Peach and apricot shells can be stored for long periods without any complications. The preparation of the raw material for the production of activated carbon involves the crushing of the pips, the separation of the kernels and shells, followed by further crushing and classification of the shells. These process steps require no complicated equipment.

The ease of production

It was decided that the activation would be performed using steam according to a simple oxidation reaction between steam and the carbon. Due to the endothermic nature of the reaction, the reaction conditions can be controlled successfully. No complicated equipment or production procedures are therefore required.

Uses of Activated Carbon

The perception of a market opportunity for a product results from the usefulness of a product and it is therefore necessary to investigate the various uses of activated carbon.

Activated carbon has been used for centuries with its use in medicine being mentioned in an Egyptian papyrus from 1550 B.C. In 1773 Scheele described experiments with gases and with that recognised the adsorptive powers of activated carbon. Ostrejeko patented work in 1900 and 1901, which led to the development of modern commercial activated carbon. World War I stimulated the interest and research into granular activated carbon for use in gasmasks. Granular activated carbon made from coconut shells soon became available. An "eat more coconuts" campaign (1917) in the USA resulted, because of the advantages seen in a readily available raw material [Davidson *et al*, 1968].

Present day uses of activated carbon includes solvent recovery, air purification in inhabited spaces like chemical and food processing industries, in the purification of many food and chemical products and in various gas phase applications. It is extensively used to purify, decolourize, dechlorinate and detoxicate domestic and industrial water. It is used for the recovery of gold, silver and other metals in the mining industry. Active carbons are therefore of interest to many industries like wine, paper, pharmaceutical, food, mining, petroleum and petrochemical to mention only a few [Bansal *et al*, 1988].

The single largest consumer of activated carbon in South Africa is the gold mining industry where activated carbon is used to adsorb gold. The activated carbon used is coconut shell based and is imported [McDougall, 1991].

The adsorptive power of activated carbon makes it an attractive product because of the endless number of applications for the product.

1.2 What is Activated Carbon?

"*Activated carbons are unique and versatile adsorbents because of their extended surface area, microporous structure, universal adsorption effect, high adsorption capacity, and high degree of surface reactivity*" [Bansal *et al*, 1988].

or

" . . . *the term activated carbon comprises of a family of substances. None of the members of the family is characterized by a definite structural formula nor can any be separately identified by chemical analysis*" [Hassler, 1974].

Structure and Physical Nature of Activated Carbon

From the above definitions it is clear that activated carbon is famous for its adsorptive powers. But what makes it such a good adsorber? The answer can be found when looking at the physical nature of activated carbon.

Activated carbons are highly porous and therefore, have large surface areas. Within every activated carbon particle, pores of different sizes can be found. These pores can be divided into three groups according to its diameters or slit widths:

- Micropores 8 - 100Å
- Mesopores 100 - 500 Å
- Macropores 500 - 20000 Å

The micropores and mesopores give rise to the internal surface area, while the macropores act like passageways to the internal surface for the adsorbate. The pores within activated carbons generally appear (in cross-section) to be cylindrical or slit-like in shape although a variety of irregular shapes can occur [McDougall, 1991]. The pore size distribution depends on the raw material and the manufacturing method.

The activated carbon structure is made up of flat atomic aromatic sheets that are stacked and cross linked in a random manner [Bansal *et al*, 1988]. The overall structure is disorganized and due to the high level of structural imperfections there are many opportunities for reactions with the carbon atoms at the edges of the sheets.

1.3 Manufacture of Activated Carbon

Any carbon containing substance can be converted into activated carbon. The properties of the produced activated carbon will, however, differ depending on the nature of the raw material, the activating agent and the activation conditions [Bansal *et al*, 1988]. Although an activated carbon must have a large surface area for 'good' adsorption, it is also important that the adsorption is rapid. The surface area should therefore be easily accessible so that migration of the adsorbed molecule from the exterior of the particle to the interior can proceed fast [Davidson *et al*, 1968]. The production of activated carbon is a two-step process namely carbonization and activation.

Carbonization

Carbonization involves the thermal decomposition of the carbonaceous raw material in an inert atmosphere. The non-carbon elements such as oxygen and hydrogen are removed as gaseous volatile products. A poor pore structure develops when the residual carbon atoms group themselves into sheets of condensed aromatic rings. The aromatic rings arrange themselves randomly leaving free interstices between them. These interstices give rise to pores, but become filled with the products of decomposition or are partially blocked by disorganized carbon. During physical activation this pore structure is enhanced and fully developed [Bansal *et al*, 1988].

Activation

Commercially there are two methods of activation, physical and chemical activation. During chemical activation, chemical activating agents act as dehydrating agents as well as oxidants and the carbonization and activation steps are carried out simultaneously. Physical activation is an oxidation reaction at elevated temperatures between the oxidizing agents usually carbon dioxide, steam or air and the carbon atoms of the carbonization product [Bansal *et al*, 1988].

Chemical Activation

Chemically activated carbons are formed when the raw material is mixed with an activating agent and then carbonized at a relatively low temperature (200°C-600°C). During carbonization the impregnated chemicals dehydrate the raw material, resulting in charing and aromatization of the carbon skeleton. The result is a very porous carbon structure, filled with activating agent. The latter is removed and usually recycled. Activating agents like phosphoric acid, zinc chloride and sulfuric acid are widely used. Other chemicals such as sodium carbonate, sodium and calcium hydroxide and the chloride salts of calcium, ferric iron, magnesium and aluminium have also been suggested. A common feature of these chemicals is that they are dehydrating agents [McDougall, 1991].

Physical Activation

During physical activation the carbonized product develops an extended surface area and a microporous structure. Two stages can be distinguished. During the first stage blocked pores are opened when the disorganized carbon is burned out. The burning of the aromatic ring system, which produces active sites and wider pores, follows. Physical activation is generally done at temperatures between 800°C and 1100°C in the presence of a suitable oxidizing gas or mixture thereof [Bansal *et al*, 1988]. Oxidizing gases like steam and carbon dioxide are normally used although activation can also be done with air.

Gasification of the carbonization product by carbon dioxide and steam occurs according to the following endothermic reactions:

$$C + CO_2 \rightarrow 2CO \qquad (\Delta H = 121 \text{ kJ/mol}) \qquad (1.1)$$

$$H_2O \rightarrow CO + H_2 \qquad (\Delta H = 163 \text{ kJ/mol}) \qquad (1.2)$$

A secondary reaction of water-gas formation, which is catalysed by the carbon surface, occurs during the reaction of water vapour with carbon:

$$CO + H_2O \rightarrow CO_2 + H_2 \qquad (\Delta H = -42 \text{ kJ/mol}) \qquad (1.3)$$

Because the reactions of carbon with steam and carbon dioxide are endothermic, external heating is required making control of the reactions easy. These two methods

of physical activation are therefore preferred in the industry. Air can also be used as an activating gas, but the reaction between carbon and air (oxygen) is extremely exothermic making control impossible [McDougall, 1991].

$$C + O_2 \Leftrightarrow CO_2 \qquad (\Delta H = -406 \text{ kJ/mol}) \qquad (1.4)$$

Adsorptive powers developed during physical activation are determined by:

- The concentration and chemical nature of the oxidizing gas.
- The reaction temperature.
- The extent to which the activation is conducted (activation time).
- The amount and kind of mineral ingredients in the carbonized precursor.

The optimum activation conditions will be determined by the application of the final product [Hassler, 1974].

1.4 Peach and Apricot Production in South Africa

Peaches (*prunus persica (L) Batcarm*) and Apricots (*prunus armeniaca*) are grown in South Africa mainly for the following uses: fresh fruit, dry fruit, canned fruit, juices, jams and pulps. Table 1.2 gives the annual production figures of peaches and apricots, with the exception of fresh fruit figures, because the pips of fresh fruit are lost for the production of activated carbon. The figures (in tonnes) were obtained from the Canning Producers Association of South Africa.

Table 1.2 Peach and apricot annual production figures (excluding fresh fruit)

FRUIT TYPE	1995/96	1996/97	1997/98	1998/99	1999/2000
ROYAL TYPE APRICOTS					
Moes, Jam and Juice	4894	2828	1242	812	450
Dried	7500	8500	8000	8500	6500
TOTAL	**12394**	**11328**	**9312**	**9312**	**6950**
BULIDA TYPE APRICOTS					
Canned, Juice and Pulp	46738	47591	44650	47232	38708
Dried	800	450	450	600	480
TOTAL	**47538**	**48041**	**45100**	**47832**	**39188**
CLINGSTONE PEACHES					
Canned, Juice and Pulp	117238	124738	99060	116533	107026
Dried	5500	5800	6500	6890	7830
TOTAL	**122738**	**130538**	**105560**	**123423**	**114856**

If it is assumed that the flesh of peaches and apricots consists 90% and 80% of the fruits respectively, then the annual mass of stones and shells generated by the above mentioned processing processes can be calculated [Salunkhe and Kadam, 1995]. The percentage of shell contained by the stones was determined experimentally and are 94% (peach) and 82% (apricot). The values in table 1.3 are in tonnes.

Table 1.3 Approximate annual peach and apricot stone/shell generation

Stone Type	**1995/96**	**1996/97**	**1997/98**	**1998/99**	**1999/2000**
Apricot	11986	11874	10882	11429	9228
Peach	12274	13054	10556	12342	11486
Shell Type					
Apricot	9829	9737	8924	9372	7567
Peach	11550	12284	9933	11614	10808

1.5 Objectives of the Study

This study is the first part of the product development of activated carbon from peach and apricot pip shells. The main objectives of this study are:

1. To produce activated carbon from peach and apricot shells with good adsorption capacity.
2. To find the optimum activation conditions to achieve the first objective by investigating the influence of activation time, the activation temperature and the amount of oxidizing agent used during the activation reaction.
3. To investigate the use of peach and apricot shell activated carbon for gold adsorption.
4. To investigate the use of peach and apricot shell activated carbon for water purification.

2 Activated Carbon Production from Peach and Apricot Shells

2.1 Introduction

The most frequently used raw materials for the production of activated carbon are coal, coconut shells, lignite, wood and some polymers. This chapter looks at the production of granular activated carbon (GAC) from peach and apricot shells, present research as well as research done in the past.

Previous Research

Activated Carbon from Peach Shells

MacDonald and Quinn (1996) produced chemical activated peach shell carbon for methane adsorption by impregnation of peach shells with various concentrations of phosphoric acid and subsequent heating between 350°C and 900°C. Activated carbon with high Brunauer-Emmet-Teller (BET) surface area (N_2, 77K) and micropore volume was produced. Its methane adsorption was, however, less than that of truly carbonaceous materials.

Research done at the University of Cincinnati (Cincinnati, Ohio) indicates that peach shells can be used for the production of specialty carbon for use as molecular sieves and catalyst support. According to Professor Robert Jenkins it isn't practical to try to compete with mass-produced activated carbon and therefore, high value products need to be developed. The peach shells were pyrolyzed in a nitrogen atmosphere (950°C), followed by carbon dioxide activation (800°C). By heating this product at 1000°C in a nitrogen atmosphere, the pores shrink and a specialty carbon is produced [Chementator, 1998].

Arriagada did research on the effect of steam activation on the porosity and chemical nature of activated carbons obtained from eucalyptus globulus and peach stones. Peach stones washed in a diluted solution of sulphuric acid were pyrolyzed at 930°C under nitrogen flow (200mℓ/min) and activated with steam (140mℓ/min) at 825°C [Arriagada *et al*, 1997]. Results that were obtained are summarised can be seen in

table 2.1. It must be mentioned that the authors failed to give the activation sample size and therefore the steam concentration per gram of sample is unknown.

Table 2.1 Peach stone activated carbon characteristics [Arriagada *et al*, 1997]

Activation Time [min]	Burn-off during Activation [%]	BET Surface Area [m^2/g]
0		10
360	28	785
600	47	1029
960	59	1247

Activated Carbons from Apricot Shells

Gergova and Eser (1996) investigated the differences in the porous structure of activated carbons produced from apricot stones using two different activation methods, a one-step pyrolysis/activation and a two-step physical activation. The one–step carbons were prepared by the pyrolysis and partial gasification of the raw material at 600-800°C for 2 – 3 hours in a steam atmosphere. The two-step carbons were prepared by carbonization of the raw material in nitrogen at 750-850°C for 2-4 hours followed by steam activation at 750-950°C for 2-4 hours. The experiments were done in a vertical reactor placed in a tube furnace at a heating rate of 20°C/min and a steam flow of 0.2g steam/min.g precursor.

The conclusions drawn from the experiments can be summarised as follows: In order to achieve high surface area and good porosity development, relatively low temperature and long reaction time need to be applied to one-step carbons and high temperatures and shorter activation times for two-step carbons. The activated carbons produced by the apricot shell, whether one or two-step method is used, displayed a wide pore size distribution with well-developed microporosity. The microstructure of the two-step carbons suggests layer by layer activation with the presence of macropores on the surface of the carbons. These macropores are connected to a network of meso- and micropores running to the interior of the activated carbon. The one-step pyrolysis/activation leads to the preservation of the original cell structure of

the apricot shell. The pores of the one step carbons are mainly round and bottle shaped while two-step carbon's pores appear to be conical shaped [Gergova and Eser, 1996].

Research on the production of activated carbon from apricot shells has been conducted at the Department of Physical Chemistry, Technical University of Budapest, Hungary since 1982. Bóta and László (1997) produced activated carbon from apricot shells by steam activation in a rotary kiln and steam/carbon dioxide activation in a fluidized bed reactor. The raw material was pyrolyzed at 700°C and 80dm^3/h nitrogen flow for 30min. After pyrolysis the yield of the carbonized product was 25%. 10g char was activated in a quartz-rotating reactor at 900°C. A 50g sample of char was activated in a fluidized bed reactor with the combustion gases of butane, with the addition of more steam in some experiments. The results obtained from these experiments can be seen in table 2.2.

Table 2.2 Parameters of activation and adsorptive properties of activated apricot pips [Bóta and László, 1997]

Reactor	Activation Agent	Temperature [°C]	Activation Time [min]	Yield After Activation [%]	Iodine Number [mg/g]	Methylene blue [g/100g]
Rotating	H_2O	900	30	78	750	4.0
Rotating	H_2O	900	60	61	1050	14.5
Fluid	H_2O/CO_2	900	10	76	610	6.4
Fluid	H_2O/CO_2	900	20	54	980	17.0
Fluid	H_2O/CO_2	900	30	45	1120	25.5
Fluid	H_2O/CO_2	900	60	21	1620	30.0
Fluid	$H_2O/CO_2 + H_2O$	880	20	45	1270	23.5
Fluid	$H_2O/CO_2 + 2H_2O$	880	25	31	1340	29.0

Activation done in the rotating quartz reactor was gentle with no significant changes in grain size during activation. In the fluidized bed the activation caused significant

changes in the mechanical strength of the particles and grain sizes. At 900°C the conversion rate in the fluidized bed reactor was twice that of the conversion rate in the quartz reactor, the ratio of the specific surface area compared to the weight loss was, however, less favourable for the fluidized bed reactor. The higher conversion rate occurred in parallel with the formation of larger pores [Bóta and László, 1997].

2.2 Experimental Setup

In this study the carbonization and activation of peach and apricot shells were done in a fluidized bed reactor. The shells were activated with steam.

Reasons for Choice of Experimental Reactor

Most producers of activated carbon use rotary kilns for the carbonization and activation of the precursor. These furnaces offer poor gas/solid contact and are energy intensive. Other industrial equipment that have been used for the production of activated carbon includes, multiple hearth furnaces, pile furnaces, vertically stacked and connected crucibles, moving grate strokers, spaced perforated plates, dual pulse jet combustion systems and fluidized beds [Sai *et al*, 1997].

The fluidized bed reactor is said to be the most efficient reactor for activation because it offers good gas/solid contact and has high heat transfer. The waste gaseous products are also quickly removed from the solid, exposing it to fresh activating gas [Kirubakaran *et al*, 1991]. It was therefore, decided to design and construct a fluidized bed reactor for the production of the activated carbon samples. Figure 2.1 is an illustration of the fluidized bed reactor.

Description of the Fluidized Bed Reactor

The fluidized bed reactor (figure 2.1) is made from 316 stainless steel. It consists of two parts, the reactor bed and the reactor lid, which is bolted unto the reactor bed.

The wall of the bed tube, OD 80mm, is 10mm thick and a ¼" stainless steel tube is fitted within the wall. This ¼" tube is connected to the bottom of the bed and acts as a feeding point for the fluidization gas. A 150μm stainless steel perforated sheet at the bottom, within the bed tube, acts as a gas distributor. An inconel 600 sheet is

wrapped around the bed wall and an electrical element fitted around it. The reason for the gas tube within the bed tube wall is to allow simultaneous heating of the bed and the fluidization gas. No preheating of the fluidization gas is therefore required. A thermocouple fitted at the outside of the reactor tube wall measures the temperature on the outside of the reactor in order to control the heat on the element. The reactor is isolated to prevent any heat losses to the environment.

The reactor lid consists of an exhaust pipe, a feeding point with lid and an opening for the internal thermocouple. To unload the sample the lid is removed and the reactor rotated around its axis.

Figure 2.2 is a schematic diagram of the experimental setup. The experimental equipment is mounted on a trolley to allow easy movement of the experimental setup. It consists of an electric control box, a type K thermocouple, a rotameter, a peristaltic pump and the fluidized bed reactor.

The internal temperature of the fluidized bed is measured by placing the thermocouple in the reactor through the hole in the reactor lid. A PID controller controls the temperature within the reactor. In order to prevent overheating of the electric element the external thermocouple is connected to an on-off controller. When the temperature on the element is too high this controller cuts the power to the element.

During carbonization and activation nitrogen is supplied to the fluidized bed reactor from a gas cylinder. The nitrogen flowrate is measured by the rotameter and controlled manually. The water and nitrogen are fed simultaneously through the reactor gas pipe during activation. The water moves through the bed gas pipe, evaporates and enters the fluidized bed as steam. It is fed to the reactor with a peristaltic pump.

Before each activation or carbonization the reactor was first purged with nitrogen to ensure that no air was locked within the reactor.

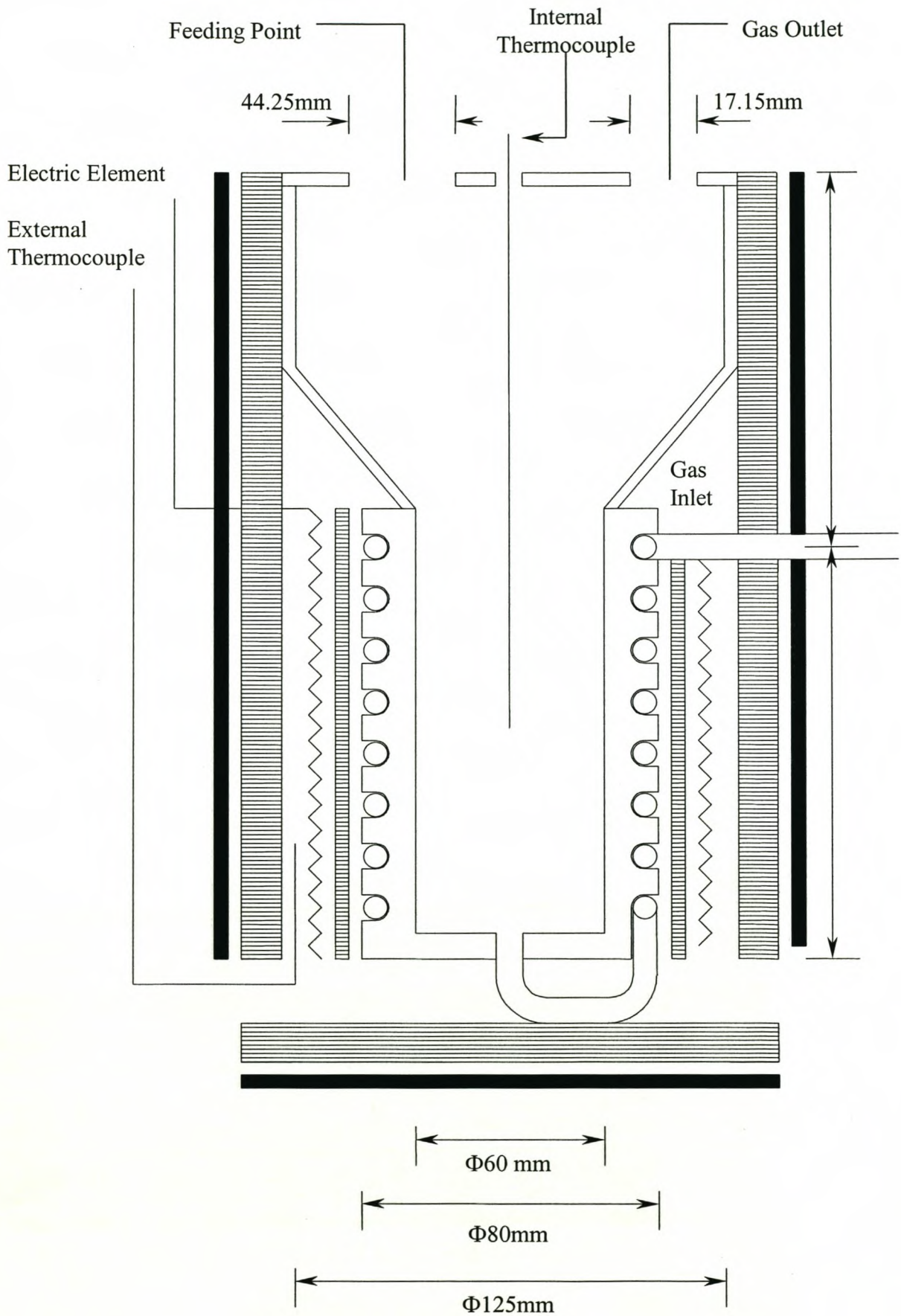

Figure 2.1 Fluidized Bed Reactor

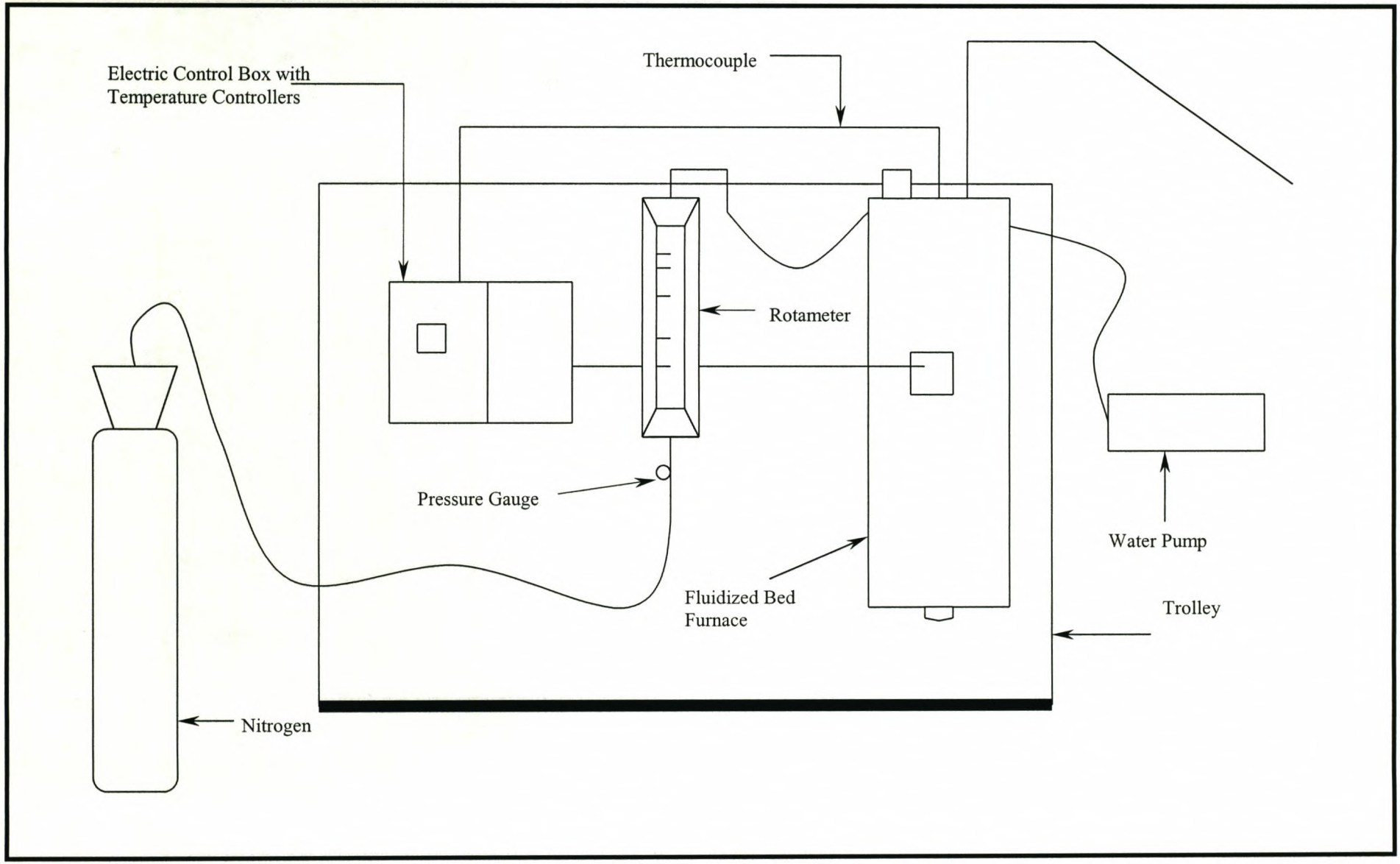

Figure 2.2 Experimental Setup: Batch Production of Activated Carbon

2.3 Batch Production of Peach and Apricot Shell Granular Activated Carbon (GAC)

Figure 2.3 summarises the batch production process used to produce the activated carbon samples.

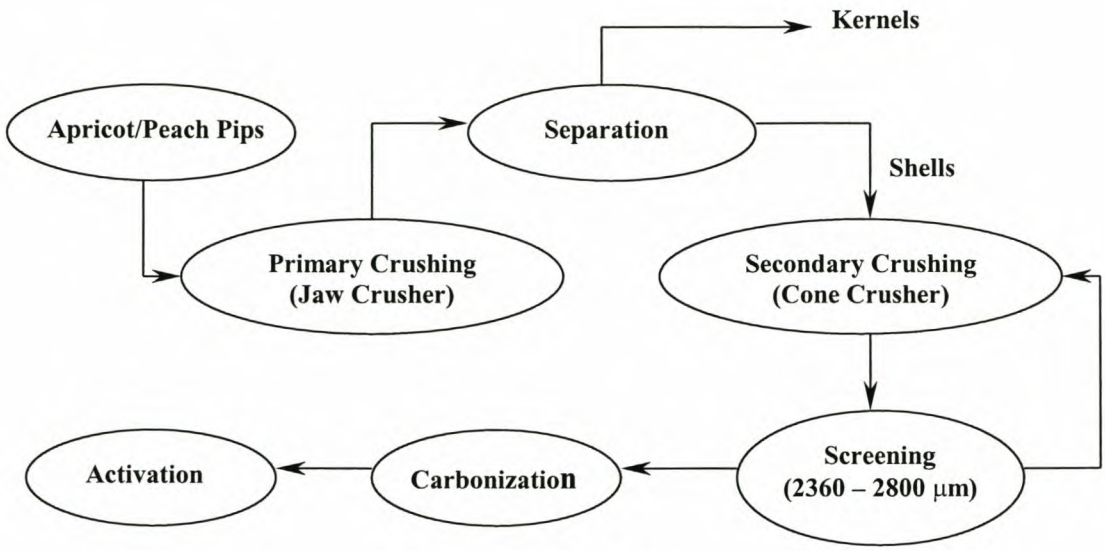

Figure 2.3 Batch production of peach and apricot shell GAC

Peach and apricot pips were first "cracked" with a jaw crusher and the kernels and shells separated. Further crushing was done with a cone crusher to obtain shell particles with sizes between 2360 and 2800 μm.

Batches of 200g of the peach/apricot shell were carbonized in an inert nitrogen atmosphere. The carbonization temperatures were obtained from previous research done by van Dyk (1998) and Botha (1998). The shells were carbonized at 345°C (peach) and 350°C (apricot) for 30 minutes. As the carbonization progressed and the densities of the shells decreased, the nitrogen flowrate was adjusted from 32.4 to 16.35 (ℓ/min @ 20°C, 1 atm). After 30 minutes, the carbonized samples were removed, cooled with nitrogen and the mass recorded.

Batches of 100g of the peach/apricot shell char were activated at different activation conditions. Activation parameters that were varied are the steam flowrate, the

activation temperature and activation time. The steam flowrates were insufficient to achieve fluidization of the char and consequently nitrogen was added at a flowrate of 14 (ℓ/min @ 20°C, 1 atm) to obtain fluidization. After activation the sample were left in the fluidized bed to cool under nitrogen flow until the temperature in the reactor equalled the carbonization temperature. The sample was unloaded and further cooled with nitrogen to room temperature. The mass of the sample was recorded and the total yield calculated.

2.4 Characterization of Peach and Apricot Shell GAC

In order to compare the different activated carbon samples it is important to obtain information about the physical nature of the activated carbon.

Total Yield

The value of the total yield of the activated carbon sample enables the producer to determine the amount of activated carbon that can be obtained from the raw material. The following formulas were used to determined the total yield:

$$Y_C = \frac{M_{CA}}{M_{RM}} \tag{2.1}$$

Y_C : Yield after Carbonization

M_{CA} : Mass of sample after Carbonization

M_{RM}: Mass of Raw material before Carbonization

$$Y_T = \frac{Y_C \times M_{GAC}}{M_{CS}} \times 100 \tag{2.2}$$

Y_T : Total yield % of activated carbon (Raw material to GAC)

M_{GAC}: Mass of sample after Activation

M_{CS}: Mass of char before Activation

Iodine Adsorption Isotherms

The iodine number is a value that is used to indicate the porosity of an activated carbon and is generally used as an indication of pores bigger than 10Å. The

American Standard Test Method no.D4607-94 (1994) was used to determine the iodine number.

An iodine adsorption isotherm is determined when three different activated carbon weights are brought into contact with a 0.1N iodine solution. The carbon and iodine are separated through filtration and the residual concentration of the iodine is determined by titration with a 0.1N sodium thiosulfate solution.

The stiochiometric equation for this reaction is:

$$I_3^- + 2S_2O_3^{2-} \Leftrightarrow 3I^- + S_4O_6^{2-} \qquad (2.3)$$

Yellow-brown Colourless

From the adsorption isotherm the amount of iodine adsorbed per gram of activated carbon, at residual iodine concentration of 0.02N is determined. This value is called the iodine number. A summary of the test method can be found in appendix A4.

Nitrogen adsorption isotherm

Nitrogen adsorption isotherms (77K) were determined through analysis of the activated carbon samples with a Micromeritics ASAP 2010 (Accelerated Surface Area and Porosimetry System) analytical instrument.

BET Surface area and External/ Mesoporous Surface Area

The nitrogen adsorption isotherm was used by Micromeritics software to determine the BET surface area and the mesoporous surface area of the activated carbon.

The Brunauer-Emmet-Teller (BET) equation is the most widely used equation to analyse adsorption isotherms and obtain the surface areas of adsorbents. Industrial carbons are characterized by their BET values. This equation does, however, have limitations for microporous carbon. It is assumed that the adsorption in micropores takes place by a successive build up of molecular layers, instead the enhanced adsorption potential causes micropore filling. The BET surface will, however, continue to be used for microporous carbons because of its wide spread use for other adsorbents [McEnaney, 1988]. The BET surface area is determined by plotting

$(P/P_0)/[V(1 - P/P_0)]$ versus P/P_0 and using the values of the slope and intercept in the following equation:

$$S_{BET} = \frac{4.353}{slope + \text{int}\,ercept} \tag{2.4}$$

The mesoporous surface areas of the activated carbon were determined by using t-plot calculation data [Micromeritics ASAP 2010 Operator's Manual, 1998]. Pores with diameters or slits with width of less than 20Å are referred to as micropores and pores with diameters or slits with width of between 20 and 500Å are referred to as mesopores. The t-plot is one of the most popular methods used for assessing micro/mesoporosity. It is based on the comparison of the isotherm with that of a nonporous reference solid. The amount absorbed on the porous solid is plotted against the statistical film thickness, t_l, of a nonporous reference adsorbent [Webb and Orr, 1997].

The film thickness for each point designated for t-plot calculations is determined with the Harkins and Jura equation:

$$t_l = \left(\frac{13.99}{0.0340 - \log(P/P_0)} \right)^{0.5} \tag{2.5}$$

A least square analysis fit is performed on the film thickness values at each point (independent variable) and the amount adsorbed (dependant variable) at that point. The slope (S) is used for the determination of the external/ mesoporous surface area of the activated carbon. Only t_l values between the minimum and maximum thickness are used.

External Surface Area/ Mesoporous Surface Area (m^2/g) [Micromeritics ASAP 2010 Operator's Manual, 1998]:

$$SA_{EXT} = \frac{S[cm^3/g - A\ STD] \times [10^{10}\ A/m] \times D[cm^3 liquid/cm^3 STD]}{F \times [10^6 cm^3/m^3]} \tag{2.6}$$

D : density conversion factor

F : surface area correction factor

Determination of the Pore Area Distribution

The pore area distribution of the A900_0.0425_60, A850_0.0533_60, P900_0.0425_60, P875_0.0533_60, Chemquest 650 and GRC 22 activated carbon samples were determined for further characterization of the activated carbons. The

BET and mesoporous surface area values do not say anything about the individual pores. It may be that some pores are inaccessible to a solute due to the molecular size of the solute making the area associated with those pores useless for adsorption. The pore size distribution of each activated carbon was used to see whether differences in the pore size distributions have any effect on the adsorption of gold. The pore area size distribution of the activated carbon samples can be found in appendix B4.
The pore area distributions of the activated carbon samples were determined with DFT Plus Software from the Micromeritics Instrument Corporation using the nitrogen adsorption data obtained from the Micromeritics Instrument.

The adsorption isotherm is known to contain a lot of information about the energetic heterogeneity and geometric topology of the activated carbon sample. Activated carbon exhibits a wide distribution of pore sizes and the adsorption isotherm for a typical material is therefore a convolution of an adsorption process with the distribution of one or more properties, which affect that process. Ross and Olivier [Micromeritics DFT Plus Models Library, 1997] stated this mathematically with the integral equation of adsorption and for its application to pore size distribution the form is as follows:

$$Q(p) = \int dH q(p,H) f(H) \tag{2.7}$$

$Q(p)$ = experimental quantity adsorbed at pressure p,

$q(p,H)$ = quantity adsorbed per unit area at the same pressure, p, in an ideal pore size of H

and $f(H)$ = the total area of pores of size H in the sample

The assumption was made that each pore acts independently and therefore each pore size present contributes to the total adsorption isotherm in proportion to the total area of the sample that is present. Modern statistical mechanics such as density functional theory or molar simulations can be used to find numerical values for $q(p,H)$ in the form of model isotherms. It can also be calculated from one of various classical theories based on the Kelvin equation.

These model isotherms are contained within the DFT models library. Because of the difficulty in solving equation (2.7), a descrete form is used:

$$Q(p) = \sum_i q(p, H_i) f(H_i) \tag{2.8}$$

For a set of model isotherms, $q(p,H)$ and an experimental isotherm, $Q(p)$, contained in the sample information file, the DFT Plus software determines the set of positive values for $f(H)$ that provides the best solution for equation (2.8).

The model used for the determination of the pore area distribution of the activated carbon samples is the Non Local Density Functional Theory with density independent weights. The models used for calculations assume slit-like pore geometry and model isotherms are derived from the density functional theory.

But what is this density functional theory? The system being modelled consists of a pore with parallel walls a distance H from each other that is open and immersed in an adsorbate at constant temperature and pressure. The fluid responds to the walls and reaches equilibrium. At equilibrium the chemical potential at every point in the fluid is equal to the chemical potential of the bulk fluid. The chemical potential of the bulk fluid in a homogeneous system at constant pressure can be determined by known equations. The density of the fluid near the walls is not constant and the chemical potential thereof is a combination of position dependent contributions that must equal the chemical potential of the bulk fluid at every point. At equilibrium the free energy (Helmholtz) of the system referred to, as the grand potential energy is a minimum.

The density functional theory describes the thermodynamic grand potential energy as a function of the single particle density distribution. It calculates the density profile that minimizes the grand potential energy and yields an equilibrium density profile. The amount adsorbed at the specific pressure can then be obtained by determining the integral of the profile. Repeating this calculation over a range of pressures gives rise to the adsorption isotherm for the model. If H is large, the obtained isotherm corresponds to that of a free, or external surface. If H is smaller, two minima exist for the grand potential energy indicating that two meta-stable phases with different density distributions exist, but with the same chemical potential. The phase with the

lower grand potential energy is the stable one. With an increase in pressure a point is reached where the other phase becomes the stable one. This phase change indicates condensation of the adsorbate in the pore and the pressure at which this happens is called the critical pore-filling pressure. A critical pore-filling pressure can therefore, uniquely characterize the pore size [Micromeritics DFT Plus Models Library, 1997].

2.5 Results and Discussion

Carbonization

Before discussing the pyrolysis results it is important to explain how the previous researchers, Van Dyk (1998) and Botha (1998), obtained the carbonization temperatures. For each shell type a thermogravimetric analysis was done. The precursor was heated at a constant heating rate in an inert nitrogen atmosphere and the mass loss at different temperatures recorded. The temperature where the highest rate of mass loss occurred was defined as the carbonization temperature. It is clear from this definition of the carbonization temperature that some volatile matter that only decomposes at higher temperatures than the carbonization temperature might still be trapped within the carbon matrix. The carbonizations were done in an inert nitrogen atmosphere at 345°C for peach shells and 350°C for apricot shells.

The yields obtained for the chars after pyrolysis were 28.90% for apricot shells and 31.76% for peach shells

Activation

Activated carbon was produced by steam activation of the carbonization product. Activation parameters that were identified to influence the physical and adsorption properties of the produced activated carbons were the activation temperature, the activation time and the amount of steam used during activation. In order to determine the influences of these activation parameters on the properties of the activated carbon samples produced from peach and apricot shells, activated carbon samples were produced at different activation conditions.

The range of activation parameters was:

- Steam Flowrate: 0.0425 – 0.0629 [g steam/g char.min]

- Activation Temperature: 700 – 900 [°C]
- Activation Time: 30 – 60 [min]

Optimal Activation Conditions

The statistical software package Statistica was used to develop an experimental design for the determination of the optimal activation conditions. A full 2^3 factorial experimental procedure was generated and the same experimental design was used for both shell types. The experimental design is as follows:

Table 2.3 Experimental design (2^3 factorial design)

Order of Experiments	Temperature [°C]	Time [min]	Steam Flow Rate [g steam /g char.min]
2	900	30	0.0425
4	900	60	0.0425
7	700	60	0.0629
3	700	60	0.0425
6	900	30	0.0629
8	900	60	0.0629
5	700	30	0.0629
1	700	30	0.0425

Eight activated carbon samples were prepared from each precursor. The iodine number and nitrogen adsorption isotherm of each activated carbon sample were determined and the results obtained are summarised in table 2.4.

Statistica was further used to analyze the activation results. The aim was to see whether a relatively simple model could be fitted to the data in order to make a rough estimate of the "optimal" activation conditions (within the activation parameter range). The "optimal activated carbon" refers to an activated carbon with a good yield×iodine number and yield×mesoporous surface area ratio.

Table 2.4 Activation parameters and adsorption properties of peach and apricot shell activated carbon

Sample ID*	Total Yield (Y_T) [%]	Iodine Number [mg/g]	BET Surface Area [m^2/g]	Mesoporous Surface Area [m^2/g]
A700_0.0425_30	19.19	492	471	59
A700_0.0425_60	17.84	662	543	79
A700_0.0629_30	19.05	562	492	66
A700_0.0629_60	17.04	746	608	117
A900_0.0425_30	14.60	904	742	208
A900_0.0425_60	9.20	1301	1103	458
A900_0.0629_30	13.16	1004	865	305
A900_0.0629_60	4.87	1569	1508	821
P700_0.0425_30	20.39	490	457	53
P700_0.0425_60	19.62	625	527	68
P700_0.0629_30	20.22	551	477	56
P700_0.0629_60	18.73	727	586	88
P900_0.0425_30	16.23	883	716	165
P900_0.0425_60	12.80	1127	936	294
P900_0.0629_30	15.91	930	750	182
P900_0.0629_60	6.17	1557	1442	653

** The first letter indicates whether the precursor is peach shell (P) or apricot shell (A). The next part indicates the activation temperature followed by the steam flow rate and the activation time. For example, the sample ID A900_0.0425_60 would refer to the activated carbon made from apricot shell, activated at 900°C, 0.0425 g steam/g char.min steam flow at an activation time of 60 minutes.*

Linear models (appendix A5), with three-way interaction between the activation variables, were fitted to the data. The models showed good estimations for the iodine numbers and yields of apricot shell activated carbon samples produced at 800°C, 0.0425 g steam/g char.min, 30/90 min, refer to figures 2.4 and 2.6, and it was therefore decided to use the model.

Equations were obtained for the yield, iodine number and mesoporous surface area in terms of the activation time, activation temperature and the steam flow rate. These equations were used to determine yield×iodine number and yield×mesoporous surface area values. By changing the temperature and time values while keeping the steam flowrate constant the optimal values were found. The reason why the steam flowrate was kept constant is that the pump could only supply water at certain rates. Optimal activation conditions obtained were: peach shell 875°C, 0.0533 g steam/g char.min, 60 min and apricot shell 850°C, 0.0533 g steam/g char.min, 60 min. Figures 2.4 to 2.13 represents the correlations between the fitted model values and the observed values for the different activation parameters.

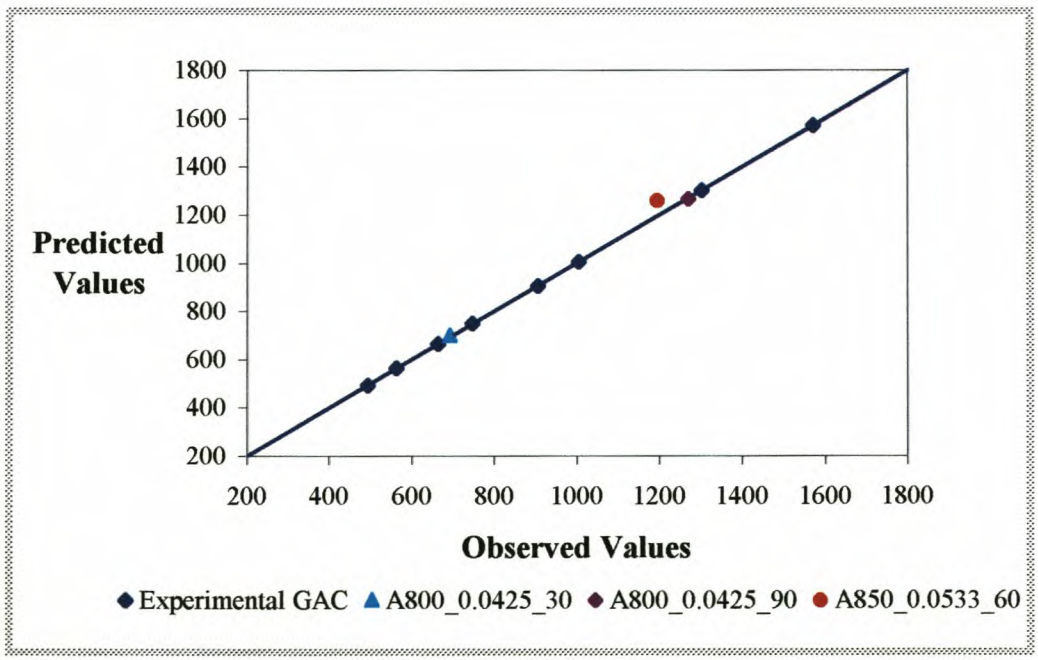

Figure 2.4 Model predicted values for iodine numbers [mg/g] versus experimental observed values (Apricot shell activated carbon)

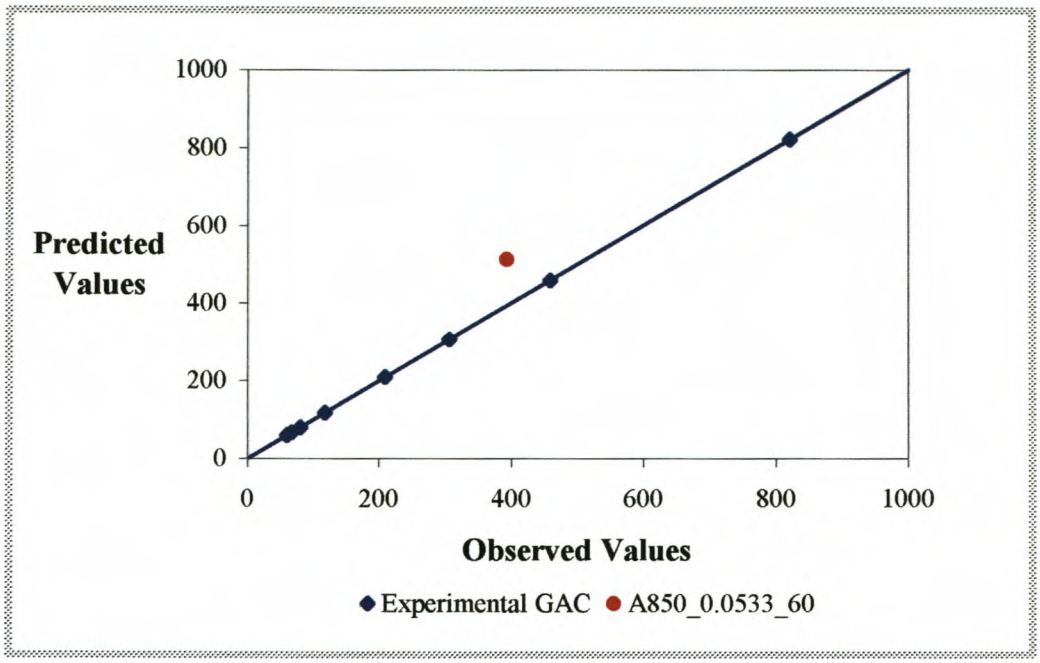

Figure 2.5 Model predicted values for mesoporous surface areas [m^2/g] versus experimental observed values (Apricot shell activated carbon)

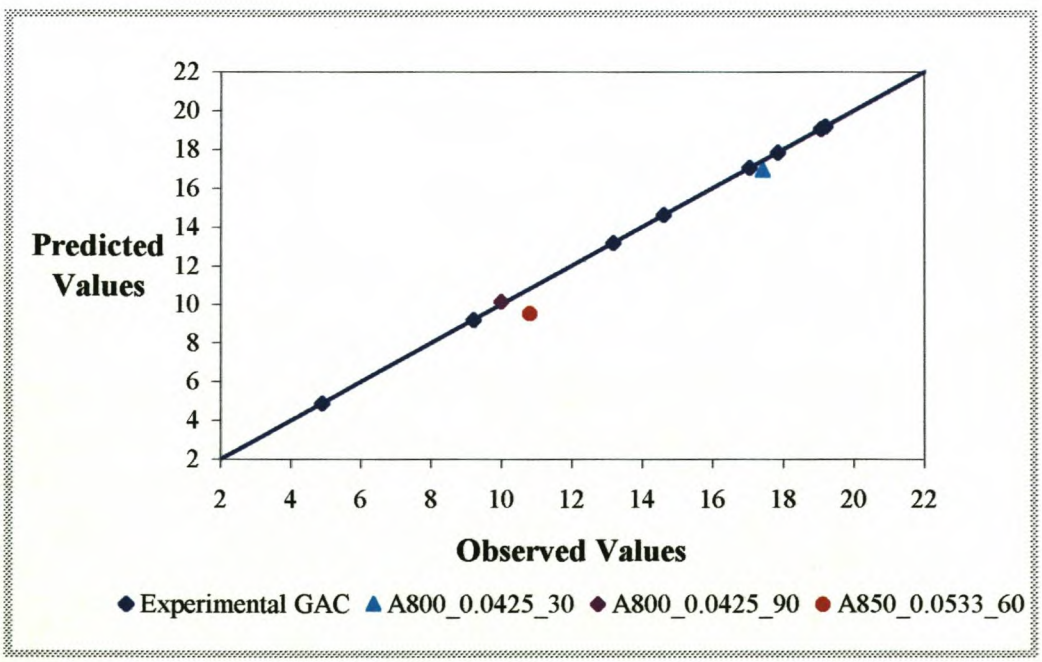

Figure 2.6 Model predicted values for yields [%] versus experimental observed values (Apricot shell activated carbon)

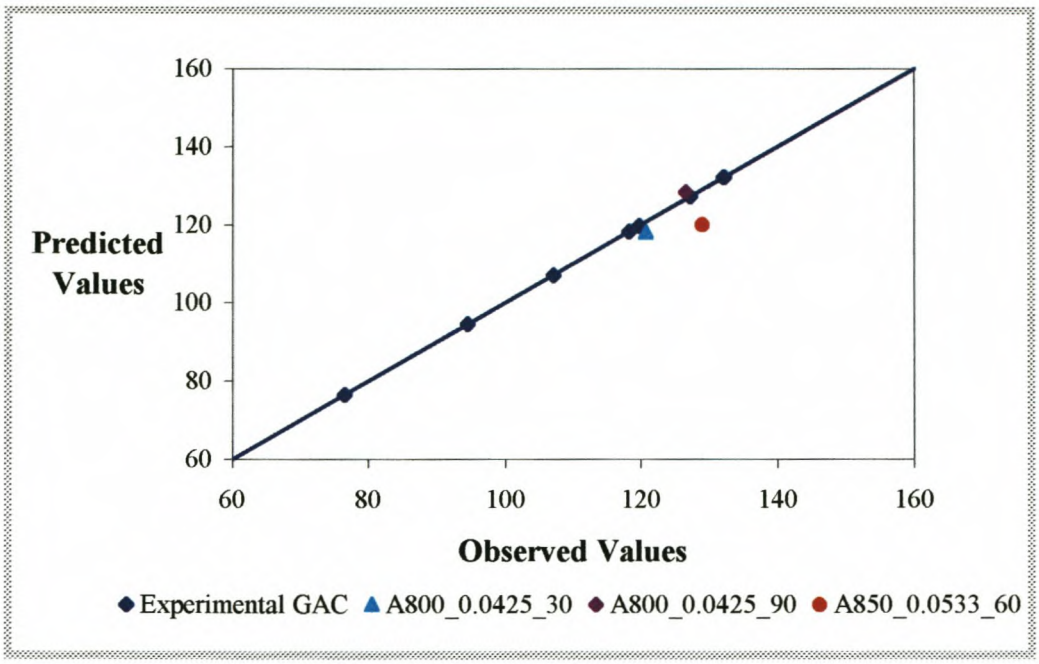

Figure 2.7 **Model predicted values for yield×iodine number values versus experimental observed values (Apricot shell activated carbon)**

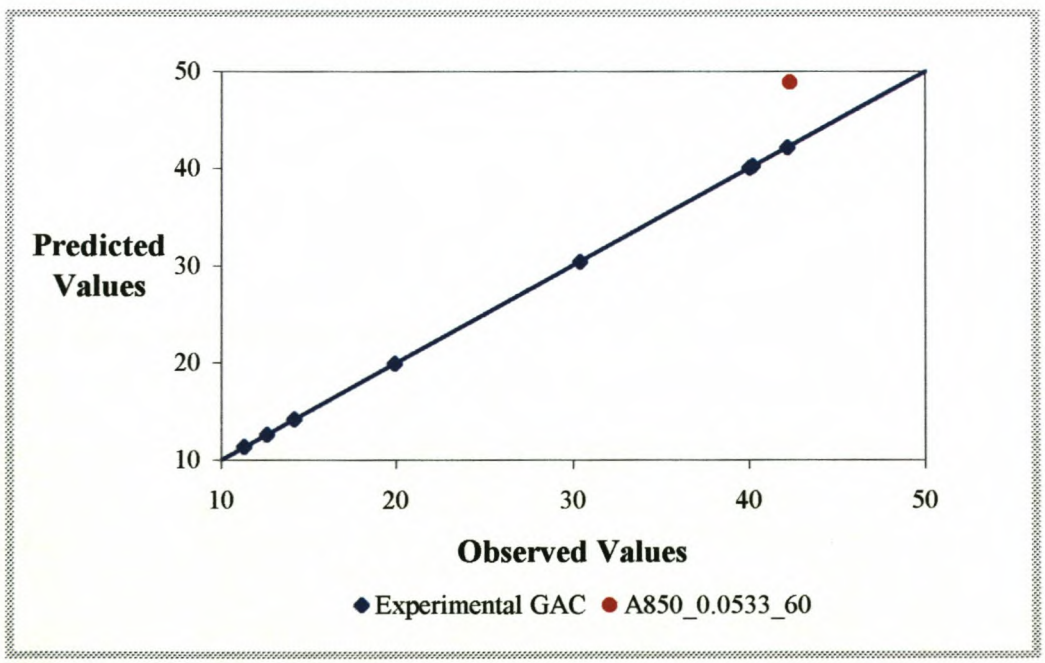

Figure 2.8 **Model predicted values for yield×mesoporous surface area values versus experimental observed values (Apricot shell activated carbon)**

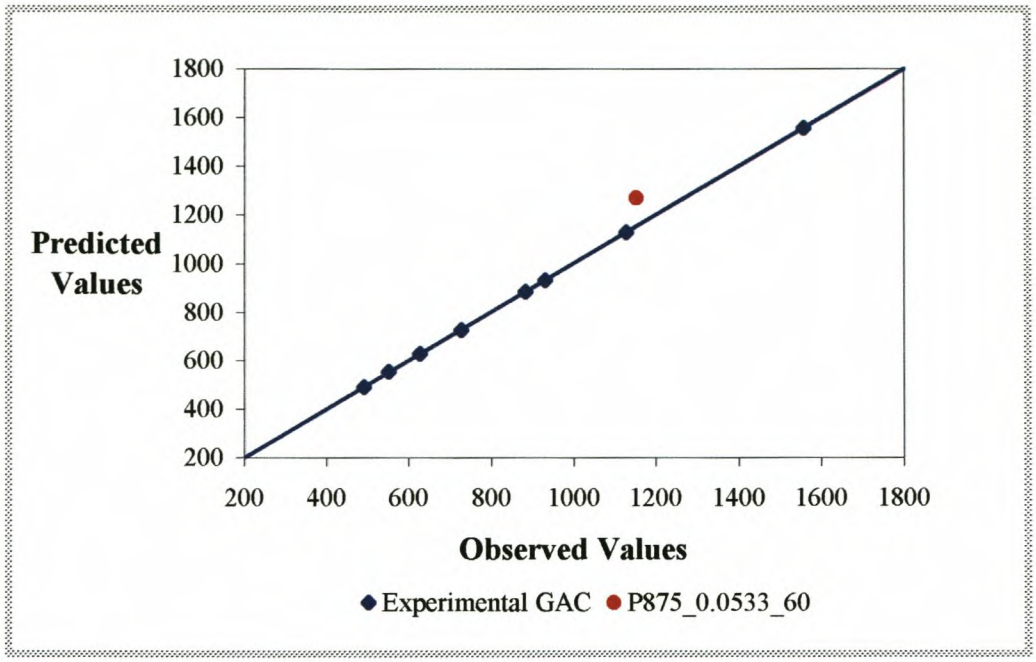

Figure 2.9 Model predicted values for iodine numbers [mg/g] versus experimental observed values (Peach shell activated carbon)

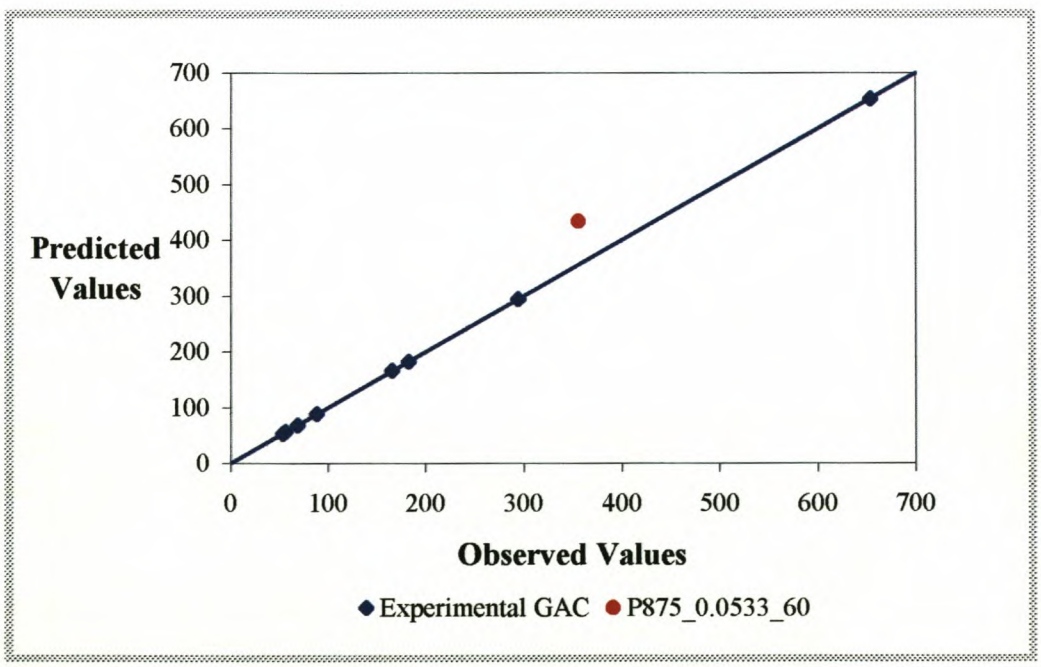

Figure 2.10 Model predicted values for mesoporous surface areas [m^2/g] versus experimental observed values (Peach shell activated carbon)

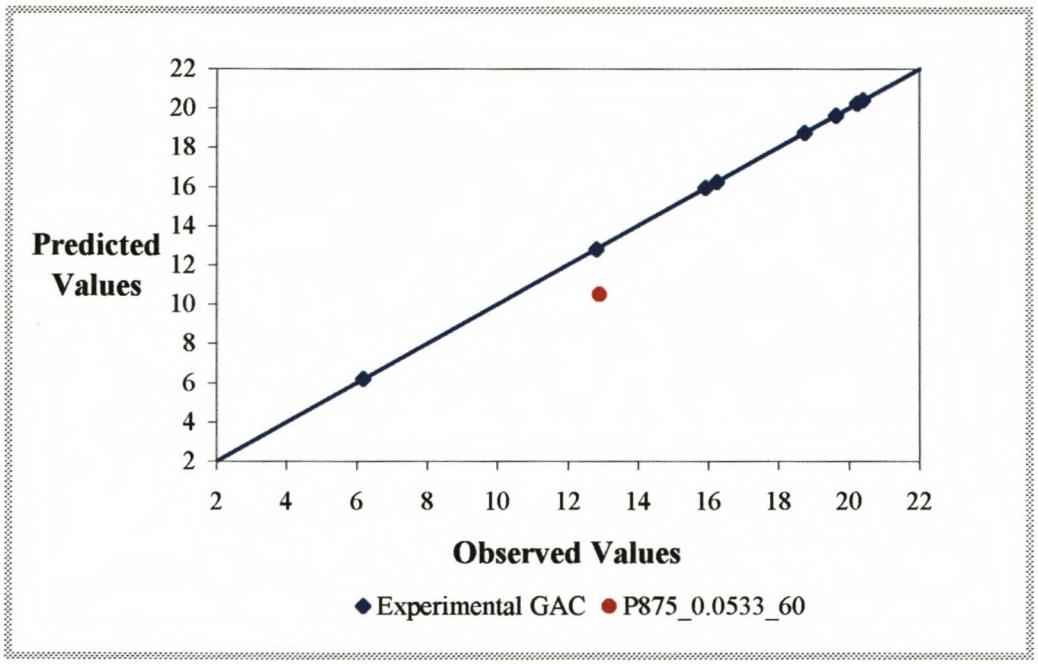

Figure 2.11 Model predicted values for yields [%] versus experimental observed values (Peach shell activated carbon)

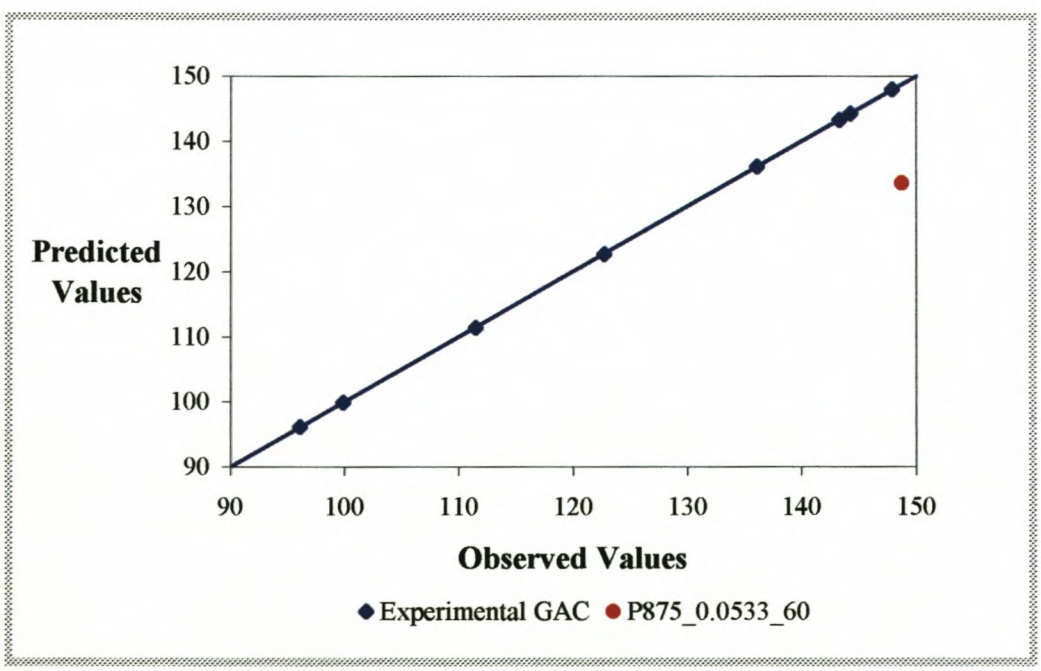

Figure 2.12 Model predicted values for yield×iodine number values versus experimental observed values (Peach shell activated carbon)

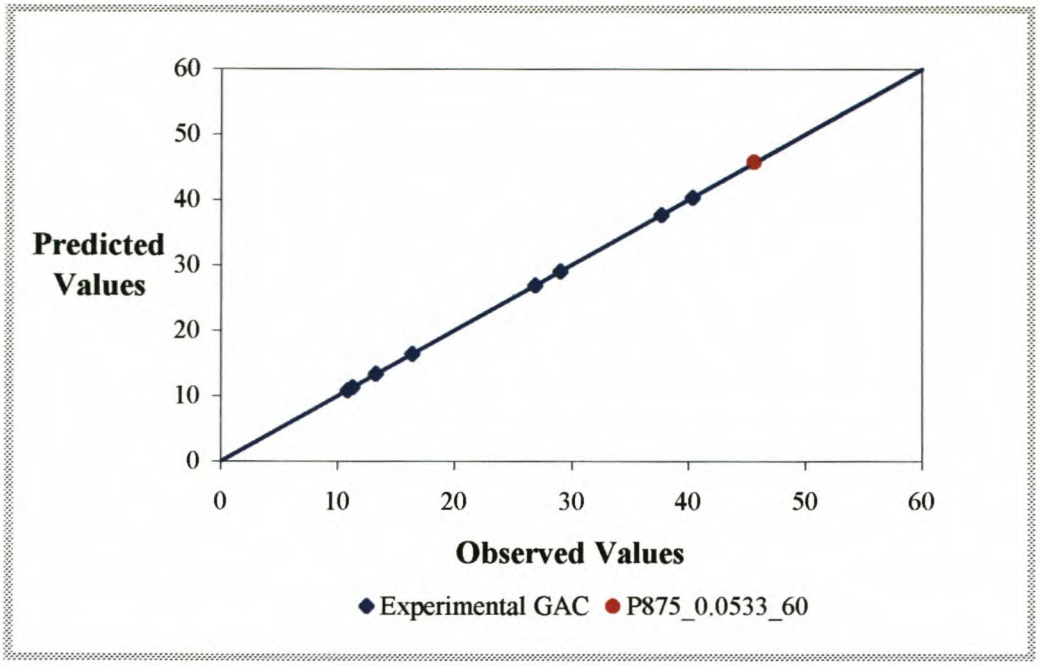

Figure 2.13 Model predicted values for yield×mesoporous surface area values versus experimental observed values (Peach shell activated carbon)

The properties of the optimum carbons can be seen in table 2.5. Although the model over and under predicts the individual values for the yield, iodine number and mesoporous surface area it seems as though this effect is cancelled out when the yield×iodine number and yield×mesoporous surface area values are determined (figures 2.4 to 2.13). The range of accuracy that these values lay in is less than 12%. As a rough estimation method the model therefore proved to be adequate.

Table 2.5 Characteristics of "optimal" activated carbons and coconut shell based commercial activated carbons

Sample ID	Total Yield (Y_T) [%]	Iodine Number [mg/g]	BET Surface Area [m^2/g]	Mesoporous Surface Area [m^2/g]
A850_0.0533_60	10.80	1194	1003	392
P875_0.0533_60	12.91	1152	1005	355
CHEMQUEST 650		1262	1200	284
GRC 22		1086	890	126

Influence of activation conditions on the characteristics of activated carbon samples.

In chapter 1 it was mentioned that the adsorptive powers developed during physical activation are determined by four factors. These four factors were investigated for activated carbon from peach and apricot shells by varying the steam flowrate, the activation time and the activation temperature. But what is the significance of these parameters towards the activation reaction?

Steam is one of the reactants of the activation reaction and the flowrate would therefore, represent the concentration of steam in the system. The higher the flowrate the more exposure between the solid and the oxidizing gas. The extent to which the activation reaction takes place is represented by the activation time. The activation reaction is an endothermic reaction and consequently heat needs to be added to the system in order for the reaction to take place. The activation temperature is an indication of the amount of heat energy transferred to the char during activation. The reaction temperature also controls the reaction rate constant.

The value of the total yield is an indication of the amount of volatile matter removed from the structure and the amount of carbon that reacted during the activation reaction. What the separate contribution of the two processes on the burn-off is one cannot determine by just looking at the yield after carbonization and yield after activation values, because there is still removal of volatile matter during the activation reaction. The activation temperatures at which the activated carbon samples were prepared are, however, higher than that temperature where no removal of volatile matter takes place according to the TGA analysis. If the total yields of two carbon samples made at different activation conditions are therefore compared, the difference in these values would only be due to the difference in the amount of carbon that reacted during activation.

From the yield values for the different activated carbons listed in table 2.4 the following conclusions can be drawn for peach and apricot shell activated carbon. Two regions can be observed, i.e. a low temperature (700°C) region, where the reaction rate is low and a high temperature region (900°C), where the reaction rate is high. For example if one compares the amount of yield obtained for activated carbon

sample A700_0.0425_60 with that of A900_0.0425_60 the difference in the yield values are quite large indicating that more carbon reacted during activation at 900°C, although the steam flowrate and activation time where the same as at 700°C.

The influence of the steam flowrate on the yields are low at 700°C, even when the activation times are 60 minutes the influence of the steam flowrate is not substantial. At 900°C the picture is, however, different, where the activation time and steam flowrate have significant influences on the burn-off. The faster rate of reaction allows faster consumption of the reactant and this combined with longer activation times leads to excessive burn-off. This can be seen in the differences of the yield values of activated carbons produced from peach and apricot shells at 900°C, 0.0629 g steam/g char.min and 30/60 min. In general the yields of the peach shell activated carbons are higher than that of the apricot shells. The difference in the yield values from one activation condition to another does, however, compare with the values obtained for apricot shells. It does therefore, appear that apricot shells contain more volatile matter than peach shells.

During the research various other activated carbons were produced from apricot shell and the results obtained for these carbons can be used to determine the influence of the steam flowrate, the activation time and activation temperature on the activation reaction of apricot shell more clearly. Figure 2.14 depicts the influence of the activation time on the yield with change in temperature. The fact that the rate of reaction increases with an increase in activation temperature is confirmed from figure 2.15 if the differences in the yield values are compared at the same steam flowrates.
It is also clear from figure 2.15 that at 700°C the reaction is controlled by the rate, because with higher steam flowrates the differences in the yields from one steam flowrate to another are low. At 900°C the decline in yields are high from one steam flow rate to another, which indicates that the reaction is controlled by the amount of steam that can be fed to it. The increase in reaction rate with increase in activation temperature is typical of an endothermic reaction.

It also seems as though there is a linear relationship between the yield and the steam flowrate at these activation conditions. When the apricot char was activated at 900°C, 0.1 g steam/g char.min, 60 min the product was almost nothing but black dust.

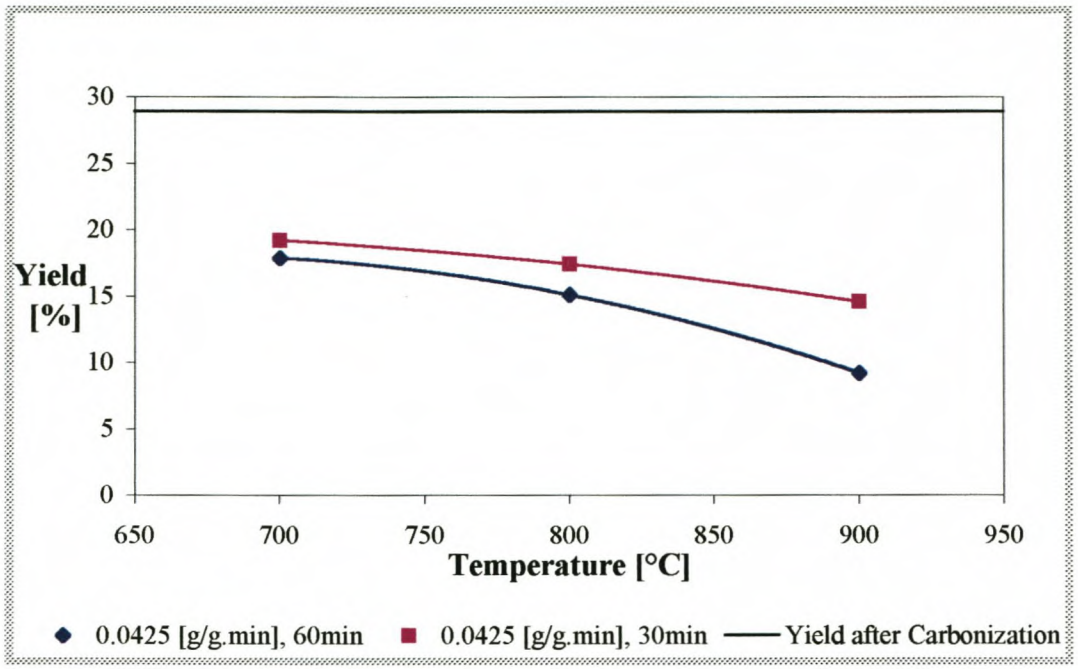

Figure 2.14 The influence of the activation time on the activation of apricot shell char

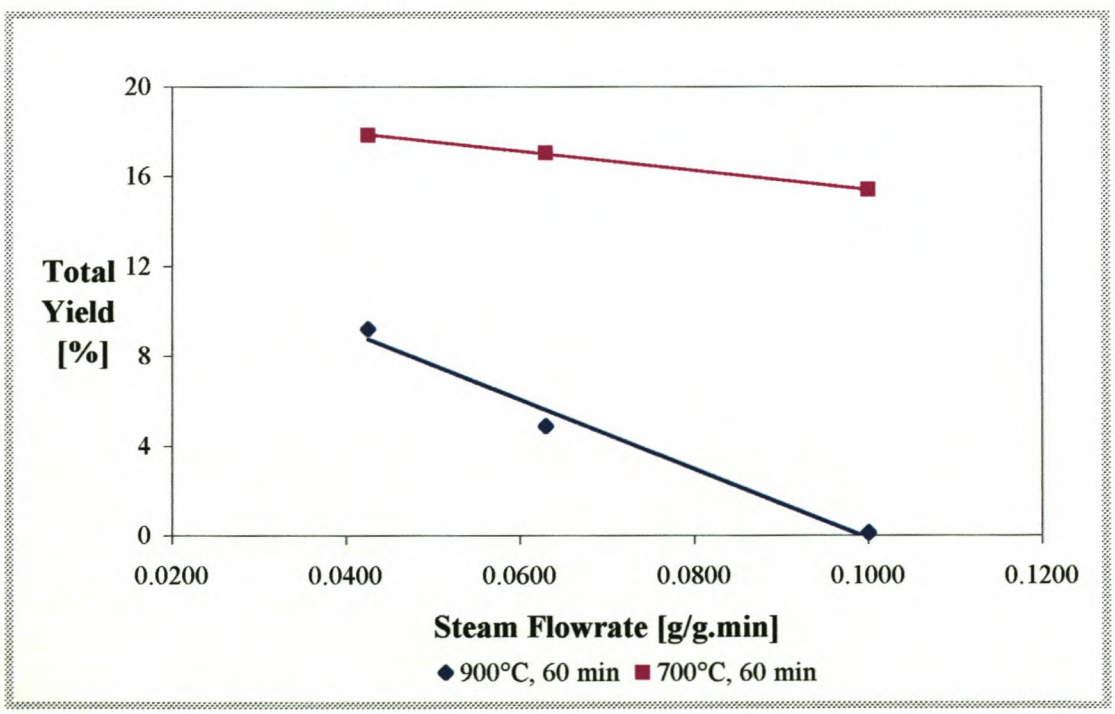

Figure 2.15 The influence of the steam flowrate on the yield of apricot shell activated carbon

Influence of the activation parameters on the physical characteristics of activated carbon

Activated carbons are generally classified according to their physical properties. The physical characteristics of an activated carbon can, however, only be used as a relative indication of adsorption properties, because the only way to investigate adsorption for a substance is by doing adsorption experiments.

Activated carbon samples were classified according to iodine number, BET surface area and a mesoporous surface area. During carbonization the interstices that are formed when the aromatic rings arrange themselves randomly, as explained in chapter 1, become filled with the products of carbonization or are partially blocked by disorganized carbon. The first stage of activation is characterized by the opening of blocked pores. This is followed by the burning of the aromatic rings and the formation of active sites and wider pores [Bansal *et al*, 1988].

At 700°C the mesopore areas are small compared to the mesopore areas at 900°C. Even when the activation time is 60minutes there isn't a substantial increase in the mesoporous area. From this it seems as though at 700°C for the activation times and steam flowrates the initial blocked pores become unblocked and that the initial pore structure is preserved. At 900°C with the higher reaction rates the pores formed from the unblocking, burns and the pores widen. Some pore walls may even collapse and even bigger pores are formed. Activation at 700°C is therefore a gentle process while activation at 900°C is aggressive and excessive.

The fact that the iodine numbers of apricot shell granular activated carbon (GAC) are higher than the peach shell GAC can indicate two things. The first would be that the amount of pores bigger than 10Å is higher for apricot shell GAC than peach shell GAC. Another explanation refers to the way the iodine number is determined. The adsorption isotherms for iodine are determined by shaking the carbon and iodine for 30 seconds, separating the two and determining the adsorption. If it is assumed that the meso- and macropores are the passageways to the micropores, the higher mesopore area of the apricot shell GAC will allow faster transport of iodine.

The advantages of higher mesopore area are accompanied by lower yields. It is therefore necessary to look at the total mesoporous and BET surface area per gram of precursor obtained for an activated carbon sample instead of just the values per gram of GAC. Activated carbons were also prepared at 800°C, 0.0425 g steam/g char.min, 60 min from peach and apricot shell. Figures 2.16 and 2.17 show the influence of the activation temperature on the total BET surface areas and total mesoporous areas per gram of precursor obtained for activated carbons produced at a steam flowrate of 0.0425 g steam/g char.min and an activation time of 60 minutes.

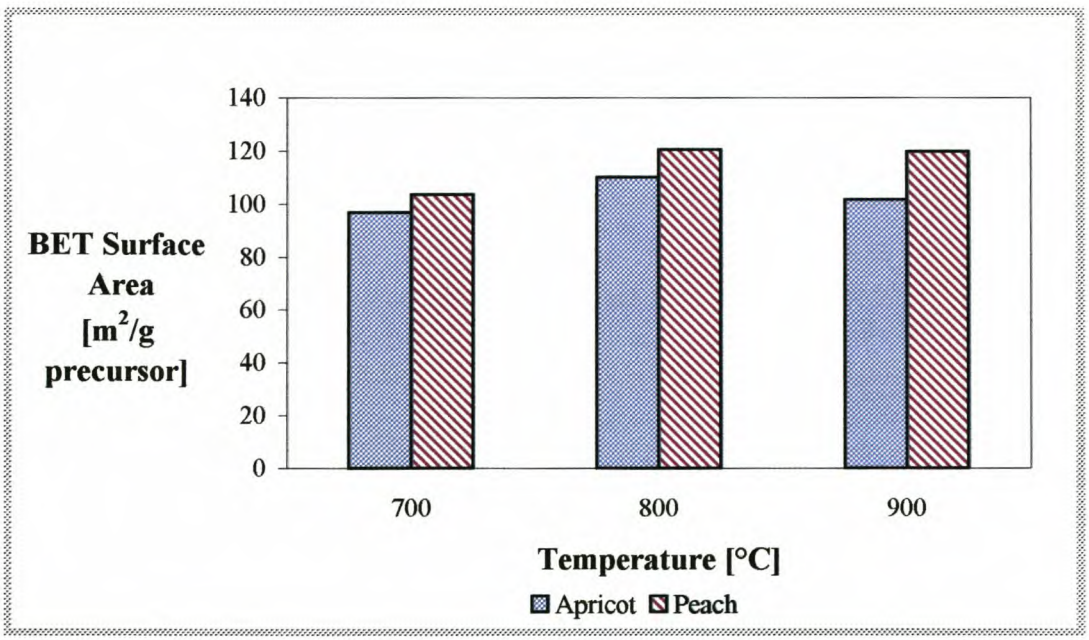

Figure 2.16 The influence of activation temperature on the total BET area/g of precursor

From table 2.4 and figure 2.16 it can be seen that although the BET surface area values of apricot shell GAC are higher than those of peach shell GAC, the total BET surface area/gram of precursor of the peach shell GAC is, however, higher than those of apricot shell GAC. This means that when activated carbon is produced from apricot shells the BET surface values may be higher, but looking at it from the producer's side this may perhaps not be an advantage. More raw material needs to be used to obtain the same total surface area leading to higher production costs.

The following conclusions can be drawn about the change of total BET surface area/gram of precursor with a change in activation temperature: For apricot shell GAC it seems as though a maximum total BET surface area per gram of precursor exists somewhere between 750 – 850°C while a maximum total BET surface area per gram of precursor for peach shell GAC is somewhere between 800 - 900°C at the same steam flowrates and activation times (0.0425 g steam/g char.min and 60 min).

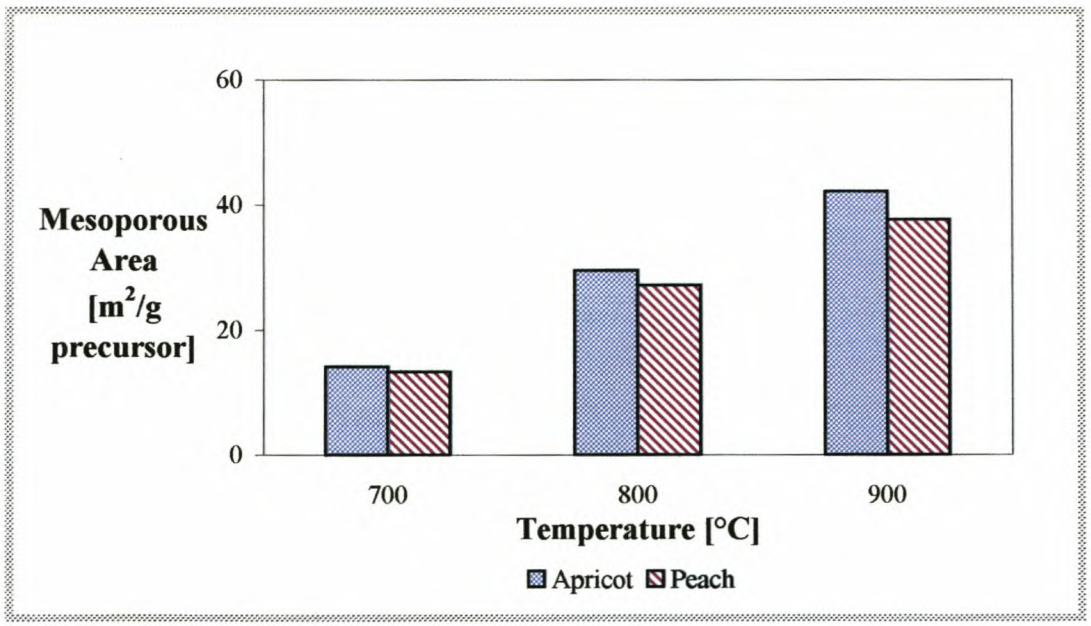

Figure 2.17 The influence of activation temperature on the total mesoporous area/g of precursor

The total mesoporous area per gram of precursor of apricot shell GAC is still higher than that of peach shell GAC despite the higher yields for peach shell GAC. If the producer's objective were to produce mesoporous activated carbons, apricot shells would be the better choice of precursor.

2.6 Conclusions

- Activated carbons with high microporous areas can be prepared at low activation temperatures and long activation times. In order to achieve the same results at higher temperatures short activation times are required.

- The activation at 700°C seems to be controlled by the reaction rate, while activation at 900°C is controlled by the rate at which the reaction can be fed with steam.

- Optimal activation conditions for the production of peach and apricot shell activated carbon within the activation parameter range were found to be: 875°C, 0.0533 g steam/g char.min and 60 min for peach shells and 850°C, 0.0533 g steam/g char.min and 60 min for apricot shells.

- Activated carbons produced from apricot shells display better mesoporous character than peach shell activated carbons produced at the same activation conditions.

3 Application of Peach and Apricot Shell Activated Carbon

When producing a product, the product is of no value unless a profitable application can be found for it. This chapter deals with the use of peach and apricot shell activated carbon for gold adsorption and water purification.

3.1 Gold Adsorption

3.1.1 Introduction

The present day gold recovery system started in 1890 when the MacArthur and Forrest brothers realized that gold and silver could be leached by cyanide solutions and consequently precipitated by zinc. It was already known by 1880 that activated carbon could adsorb or precipitate gold from gold solutions obtained by gold chlorination. When the cyanide process became known, it was also realized that activated carbon could be used for adsorption of gold from these solutions. The development of the use of activated carbon over zinc was, however, retarded by the fact that no elution or recycling method for the activated carbon existed and that the Crowe-Merrill method by which gold was precipitated by zinc dust was believed to be adequate.

At the end of World War II very hard activated carbon produced by fruit pips was used experimentally for the recovery of gold from slime at the Getchell Mines in Nevada. Still no elution method was known and the carbon had to be burned to recover the gold, which was a costly and wasteful procedure. On a request from the Getchell Mine, Zadra at the United States Bureau of Mines developed a procedure to elute the gold with hot caustic soda from the loaded granular carbon. Zadra [Laxen *et al*, 1979] also developed an electrolytic cell to recover the gold from this eluate.

By 1961 a flowsheet was developed in which granular activated carbon flowed counter-current to the cyanide pulp in adsorption contactors to recover the gold. This means that virgin carbon comes into contact with the tailings of the adsorption circuit

and loaded carbon into contact with high gold values. The maximum amount of gold is therefore adsorbed from the cyanide pulp and this process is known as the carbon-in-pulp process (CIP). In this flowsheet the loaded carbon is eluted by the Zadra process and gold recovered electrolytically. In addition the flowsheet suggested the thermal reactivation of the spent activated carbon.

In 1973 the carbon-in-pulp process was introduced for the first time at the Homestake Mine, which was the biggest and most important development for the carbon-in-pulp process. In South Africa the first major effort to test the potential of activated carbon for the recovery of gold was made by Rand Mines in the mid-1960s [Laxen *et al*, 1979]. Today the CIP process is still in use at many South African mines. A further development on the CIP process is the carbon-in-leach (CIL) process where carbon is directly added to the gold leaching circuit and leaching and adsorption proceed simultaneously [Stanley, 1987].

Despite the extensive industrial use of activated carbon the mechanism of the adsorption of the goldcyano complex on activated carbon is still not fully understood. Extensive research has been done in the past decades on the adsorption of aurocyanide species on activated carbon [Jia *et al*, 1998].

Mechanism of Adsorption of Gold on Activated Carbon

The present state of proposed adsorption mechanisms of aurocyanide on activated carbon can be divided into three categories:

- Those proposing that gold is present as an aurocyanide ion.
- Those proposing that gold is present as a compound other than aurocyanide (e.g. precipitated AuCN).
- Those suggesting that the aurocyanide is reduced to metallic gold.

The controversy surrounding the adsorption mechanism is due to the fact that activated carbon is not responsive to physical investigation by techniques such as infrared spectroscopy. Consequently little information about the nature of the adsorbed gold cyanide species and the surface functional groups present on the carbon is available.

Two facts that have, however, been confirmed by various researchers regarding the adsorption of gold on activated carbon are:

- Extraction of $Au(CN_2)^-$ by activated carbon is strongly enhanced by the presence of electrolytes, KCl or $CaCl_2$, in the adsorption medium.
- Adsorption is strongly enhanced by the increase in acidity of the adsorption medium.

Any adsorption mechanism therefore has to account for these two effects [McDougall *et al*, 1980]. A discussion of a few of the adsorption mechanism models will now follow.

Early researchers postulated a reduction mechanism for the adsorption of gold where the reducing agent was assumed to be carbon monoxide occulated by the carbon. Allen advanced the hypothesis that gold cyanide was adsorbed without chemical charge as $Na[Au(CN)_2]$, but Williams found that the sodium content of the activated carbon loaded with $Na[Au(CN)_2]$ was not enough to explain the amount of gold present on the activated carbon [McDougall *et al*, 1980].

Garten and Weiss [McDougall *et al*, 1980] proposed that there is electrostatic attraction between $Au(CN)_2^-$ anions and positively charged carbonium ion sites which amounts to the unlikely oxidation of Au(I) to Au(III). A representation of this mechanism is as follows:

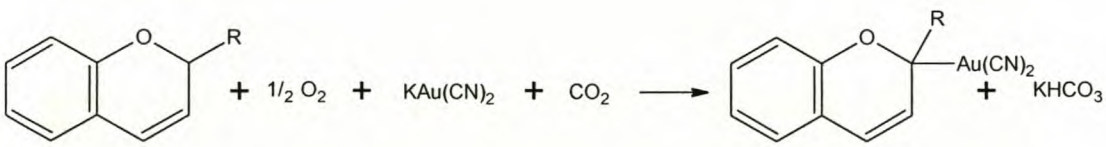

In his investigation of the factors that influence the adsorption of gold on coconut shell activated carbon Davidson [McDougall *et al*, 1980] found that the degree of gold adsorption is strongly dependent on the "spectator electrolytes" present in the adsorption medium. It was further found that adsorption could not take place without the presence of stabilizing cations like Ca^{2+} and Na^+. The mechanism suggested by him involves the adsorption of gold as a metal dicyanoaurate complex: $M^{n+}[Au(CN_2)]_n$. He claimed that when the cation of the complex M^{n+} is an alkaline

earth metal, the complex is bound more firmly to the carbon than when the cation M^{n+} is an alkali metal. The strength of the adsorption of the $M^{n+}[Au(CN_2)]_n$ adsorbate is believed to follow the following sequence: $Ca^{2+} > Mg^{2+} > H^+ > Li^+ > Na^+ > K^+$ [McDougall *et al*, 1980].

Fourier transform infrared spectroscopy, X-ray photoelectron spectroscopy and Mössbauer spectroscopy were used to investigate the adsorption of aurocyanide species on activated carbon and it was suggested that the adsorption of the ion pair $M^{n+}[Au(CN)_2]$, was followed by the partial reduction of $Au(CN)_2^-$ to $Au(CN)_x^-$. However, although it was proposed that AuCN formed during the adsorption of $Au(CN)_2^-$, other studies clearly indicated that $Au(CN)_2^-$ adsorbs without any chemical change [Jia *et al*, 1998].

Requirements of activated carbon to be used for gold adsorption

When an activated carbon is used in the CIP and CIL gold recovery processes it has to comply with certain standards:

- It must have good gold adsorption characteristics.
- It must have good abrasion resistance in order to prevent any gold loss due to adsorption on activated carbon fines.
- The thermal reactivation properties of the activated carbon must be good to ensure the reuse of the activated carbon [Stanley, 1987].

3.1.2 Experimental

Gold adsorption tests were done on activated carbon samples A900_0.0425_60, A850_0.0533_60, P900_0.0425_60, P875_0.0533_60 and two commercial coconut shell carbon samples, Chemquest 650 and GRC 22. The virgin coconut shell activated carbons were obtained from Doornkop Gold Extraction Plant, Gauteng.

Preparation of Activated Carbon

The activated carbon samples were sieved to obtain particles within the particle size range 1400 - 1700 μm. After the samples were sieved compressed pressure air was blown over it to remove dust and ashes. No water washing was done, because even if some dust particles were present in the sample it would not have affected the outcome

of the gold adsorption tests. The samples were dried at 110°C for two hours and then placed in a dissacater prior to the gold adsorption tests.

Batch Kinetic Gold Adsorption

Batch kinetic gold adsorption tests were done to obtain a relative indication of the rates at which the activated carbons produced in this study and commercial activated carbons adsorbed gold. Experiments were done in two 2.5ℓ stainless steel reactors equipped with overhead stirrers connected to a single motor.

Solutions containing ±10 ppm Au^+ and 100 ppm CN^- were used for all the experiments. The pH of the solution was kept between 10.5 to 11 with a 0.1N KOH solution. 2ℓ of the $KAu(CN)_2$ solution was brought into contact with 0.25g/ℓ activated carbon. For the first two hours 2mℓ samples were taken after 0, 5, 10, 15, 30, 45, 60, 90,120 minutes and thereafter samples were taken at random time intervals.

The samples were analysed for its gold content with a Varian SpectrAA – 250Plus Atomic Absorption Spectrometer

Gold Adsorption Isotherms

Gold adsorption isotherms for each activated carbon sample were determined by equilibrium gold adsorption tests done in rolling bottles. 500mℓ of a 100ppm Au^+ and 100ppm CN^- solution was brought into contact with a known mass of activated carbon and left for four weeks to reach equilibrium. For each carbon sample five bottles were filled with the carbon/gold solution. Four bottles contained activated carbon while the fifth one rolled without any carbon to monitor the background gold levels of the solutions. The bottles were opened and shaken regularly to allow air into the system.

After the four weeks the solutions were filtered and the gold concentration determined with a Varian SpectrAA – 250Plus Atomic Absorption Spectrometer.

3.1.3 Results and Discussion

Equilibrium Gold Adsorption Tests

Data obtained from the bottle roll equilibrium tests were used to obtain the Freundlich Isotherm for each activated carbon sample.

Freundlich Isotherm $$q_s = AC_s^n \quad (3.1)$$

Where: q_s is the gold loading [mg gold adsorbed/ g activated carbon]

and C_s is the equilibrium gold concentration [mg gold/dm^3 solution]

The values of A and n, the Freundlich isotherm parameters, obtained for the various activated carbon samples are summerized in table 3.1.

Table 3.1 Freundlich isotherm parameters

Activated Carbon Sample	A	n	R^2
Chemquest 650	21.019	0.2327	0.998
GRC 22	23.516	0.2126	0.999
A850_0.0533_60	23.656	0.2231	0.986
P875_0.0533_60	23.494	0.2226	0.992
A900_0.0425_60	22.299	0.2219	0.981
P900_0.0425_60	23.647	0.2180	0.987

The graphic representations of the various isotherms can be seen in appendix B3. No vast differences in the equilibrium loadings of the activated carbons exist making it difficult to decide which activated carbon would be best suited for gold adsorption. The mean residence time of the activated carbon per adsorption stage in an operating plant seldom exceeds 48 hours, so that equilibrium is never achieved. It is therefore, necessary to obtain data about the kinetics of the adsorption reaction [Nicol *et al*, 1984].

Batch Kinetic Adsorption of Gold

The results of the individual batch kinetic gold adsorption tests can be seen in the modelling section of this chapter. Figures 3.1 to 3.3 are used to illustrate the differences in adsorption rates from one carbon sample to the other. Ci is the concentration of the gold in solution at a certain time, while Co represents the initial gold concentration of the solution.

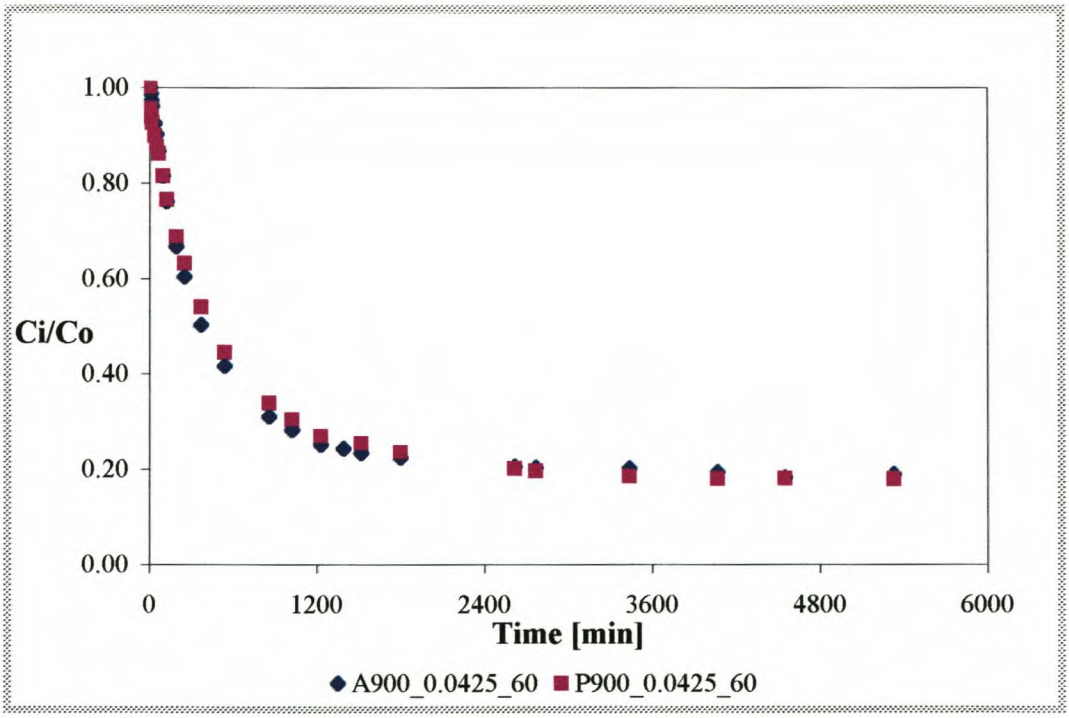

Figure 3.1 Batch kinetic gold adsorption: Peach versus apricot shell activated carbon gold adsorption

Figure 3.1 illustrates the difference in the adsorption of gold onto activated carbon produced from peach and apricot shells at similar activation conditions (900°C, 0.0425 g steam/g char.min, 60 min). It can be seen that the initial gold adsorption rate is similar for the two carbons, followed by a region where adsorption is faster on the apricot shell GAC and then the adsorption rates seem to be equal again. The faster uptake of gold by the apricot shell activated carbon can be due its higher mesoporosity.

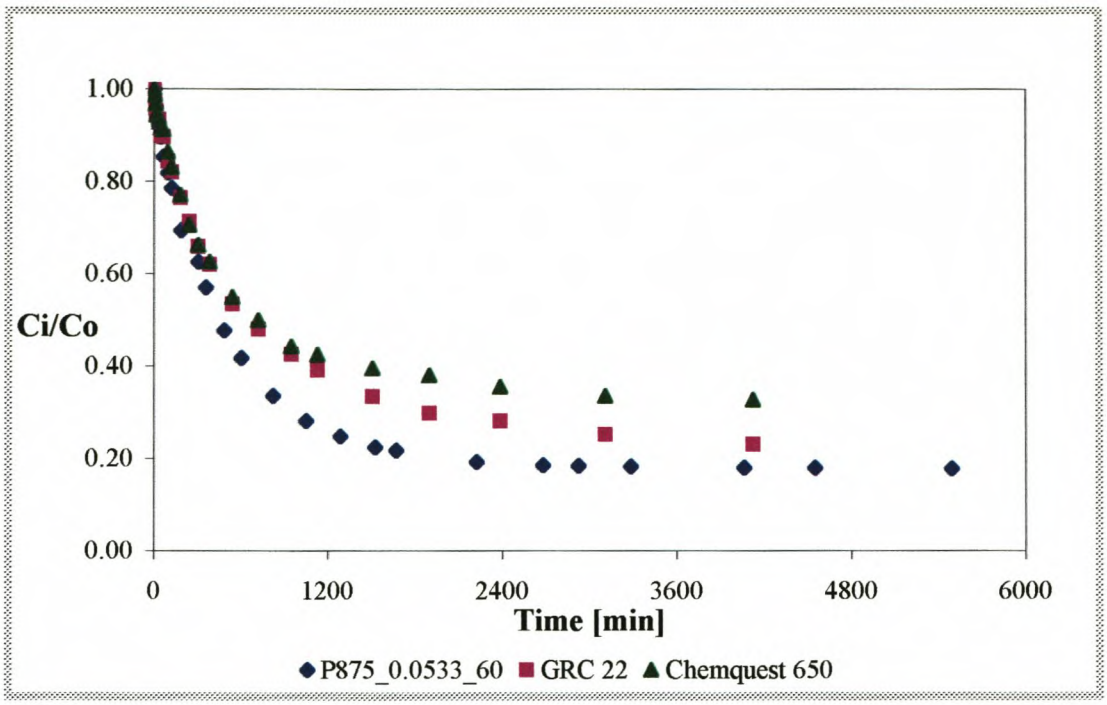

Figure 3.2 Batch kinetic gold adsorption: Peach versus coconut shell activated carbon gold adsorption

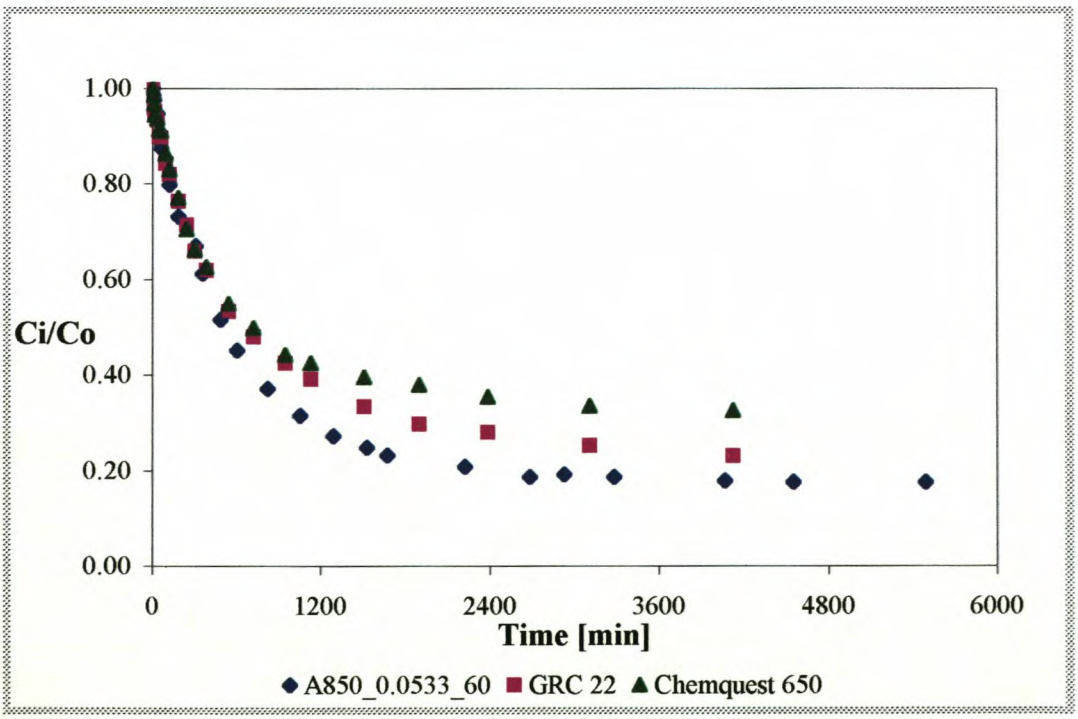

Figure 3.3 Batch kinetic gold adsorption: Apricot versus coconut shell activated carbon gold adsorption

From figures 3.2 and 3.3 it is clear that the adsorption kinetics of gold onto peach and apricot shell activated carbon are faster than gold uptake onto commercial activated carbon. If one compares the pore area distribution curves for the various activated carbon samples (appendix B4) it can be seen that activated carbons prepared from peach and apricot shells have a broader pore area distribution than commercial activated carbons.

If it is assumed that the mesopores are the corridors to the micropores, then a larger distribution of meso/micropores would lead to faster gold adsorption.

3.1.4 Gold Adsorption Modelling

Information obtained from the batch kinetic and equilibrium gold adsorption tests were used in a kinetic model for the adsorption of gold cyanide on activated carbon postulated by van Deventer(1984).

Model Description

The activated carbon particle is divided into two distinct regions: a fraction of mesopores (α) and a fraction of micropores (1 - α). The mesopores are believed to be large relative to the molecular size of the solute making access easy. Diffusion in the mesopores is unhindered and the mass transfer proceeds fast. The micropores are similar in size to the solute molecule and diffusion in these pores may be retarded due to steric interactions. The fraction of activated carbon available as mesopores, α, can only be evaluated from experimental adsorption data.

The assumptions made for the development of the model are as follows:

- Activated carbon particles are treated as equivalent spheres.
- Micro and mesopores are distributed homogeneously through the carbon particle.
- Only the mesopores mouth on the carbon surface and the micropores mouth into the mesopores.

- The radial transport of gold cyanide in the mesopores can be described by a surface diffusion mechanism and therefore pore diffusion is negligible.
- The rate of diffusion from the meso - to the micropores can be described by a linear driving force expression.
- Local equilibrium exists at the solid-liquid interface, because transfer of metal cyanides from the dissolved to the adsorbed state is not rate controlling.
- Adsorption of gold cyanide onto activated carbon is reversible.

Material balance Equations

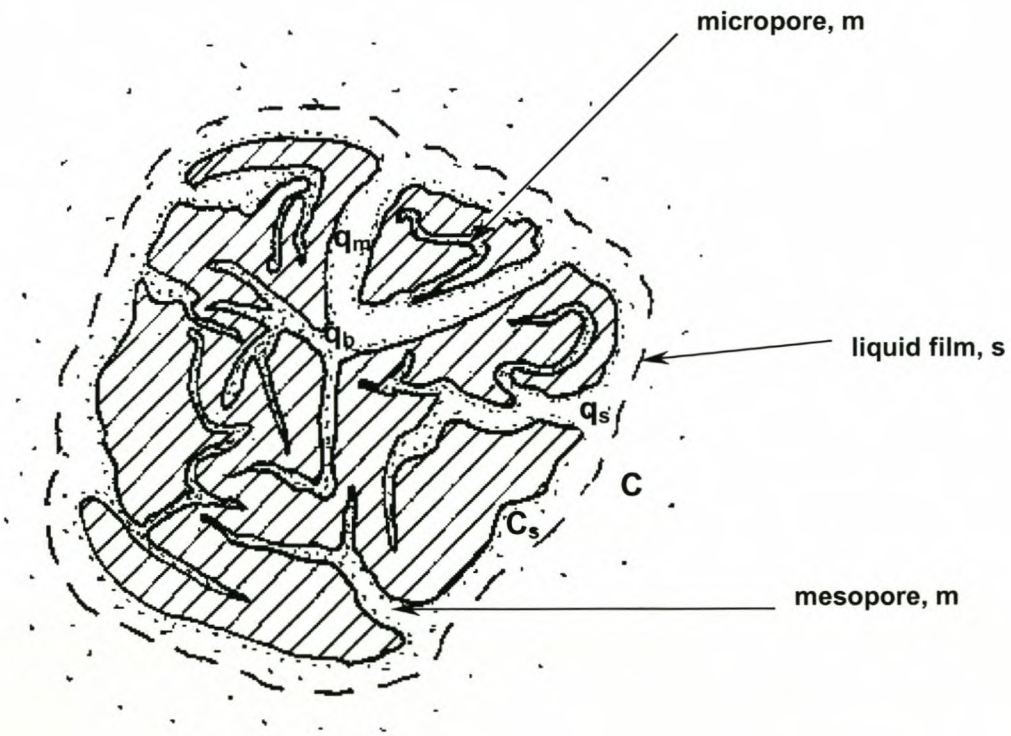

Figure 3.4 Conceptual representation of meso- and micropore structure of activated carbon [van Deventer, 1984]

The adsorption of gold onto the activated carbon is described by a four step process. During the first stage gold is transferred through the liquid film surrounding the carbon particle to the carbon surface. The linear driving force expression for the flux of solute through the external boundary layer is:

$$\frac{dC}{dt} = \frac{6k_f M_c}{\rho_c V d_p}(C_s - C) \tag{3.2}$$

The second stage is the adsorption at the carbon/ fluid interface and the local equilibrium at the solid liquid interface is described by a Freundlich isotherm.

$$q_s = AC_s^n \tag{3.1}$$

The gold cyanide then diffuses into the mesopores. The partial differential equation for the loading in the mesopores converted to an ordinary differential equation by assuming a quadratic dependence of concentration on position.

Mesopore Mass Balance:

$$\alpha \frac{d\,q_m}{dt} = \frac{60\alpha\,\bar{D}_s}{d_p^2}\left(\frac{q_s^2 - q_m^2}{2q_m}\right) - k_b(q_m - q_b) \tag{3.3}$$

The surface diffusion coefficient D_s is used as a measure of the rate of diffusion of the solute into the mesopores. The last step is the transport of the gold cyanide from the mesopores to the micropores. A linear driving force approximation was used to convert the partial differential equation to an ordinary differential equation.

Micropore Mass Balance:

$$(1-\alpha)\frac{dq_b}{dt} = k_b(q_m - q_b) \tag{3.4}$$

k_b is the rate coefficient for transport from the meso to the micropores.

If it is assumed that there is no accumulation of gold cyanide at the external surface then a total mass balance can be done over the external particle surface.

Kilogram of solute through the boundary layer per second

=

Kilogram of solute to the mesopores per second

Total mass balance:

$$k_f(C - C_s) = \frac{10\alpha\rho_c \bar{D}_s}{d_p}\left(\frac{q_s^2 - q_m^2}{2q_m}\right) \tag{3.5}$$

Data Modelling

By solving equations (3.1) to (3.4) one can get a relative indication of the rate at which the gold cyanide is adsorbed onto the activated carbon. The three differential equations, equations (3.2) to (3.4), can only be solved numerically. When modelling was performed a fourth order Runge-Kutta routine was used to solve the liquid phase, meso- and micropore mass balance equations. This was done by guessing the future values of the liquid phase and solid phase concentrations at the solid – liquid, interface and using it in the Runge-Kutta routine to solve the mass balance equations. From these initial estimates of the liquid concentration, meso- and micropore loadings were obtained. These values were used in equation (3.5) to obtain improved estimates of the future interface concentrations.

The optimum values of $\bar{D}_s$, k_b and α for each activated carbon sample were calculated using a Marquardt non-linear squares curve-fitting algorithm on the batch kinetic gold adsorption data [Nieuwoudt, 1989].

The film transfer coefficient k_f, was determined from the initial rate data. During the initial stages of adsorption C_s is much smaller than C and equation (3.2) can reduce to:

$$\frac{dC}{dt} = \frac{-6k_f M_c}{V\rho_c d_p} C \tag{3.6}$$

When integrated:

$$\ln\left(\frac{C_0}{C_i}\right) = \frac{6k_f M_c}{V\rho_c d_p} t \tag{3.7}$$

Therefore, the slope of $\ln\left(\frac{C_0}{C_i}\right)$ vs. t can be used to calculate k_f.

The parameters A and n of the Freundlich adsorption isotherm were determined with the data obtained from the equilibrium gold adsorption tests.

In the kinetic model it was assumed that all the activated carbon particles have spherical shapes. The apparent density was determined by counting the total number

of particles used in a size analysis and using this value and the mass of the carbon in the following equation [Van Deventer, 1984]:

$$\rho_c = \frac{M_c}{n_I\left(\frac{\pi \times d_p^3}{6}\right)} \tag{3.8}$$

Modelling Results

In the gold recovery process one of the most important operations is that of the adsorption circuit, since the efficiency of the gold recovery of activated carbon determines the overall efficiency of the plant, as well as the size of the elution, reactivation and electrowining circuits [Nicol *et al*, 1984]. It is therefore, clear that if a relatively simple model can be used to model gold adsorption in the adsorption circuit, optimization of this circuit can be achieved, leading to better plant design as well as bigger profits. The kinetic gold adsorption model of van Deventer (1984) was fitted on the gold adsorption data of each activated carbon sample.

The values of the film transfer coefficients and apparent densities of the activated carbon samples used in the modelling are tabulated in table 3.2. The values of activated carbon mass, volume of gold solution and average particle size are equal for all the samples and are: $M_c = 0.0005$ [kg], $V = 0.002$ [m^3] and $d_p = 0.00155$ [m]. The Freundlich Isotherm constants were given in table 3.1.

Table 3.2 Gold adsorption model parameters

Activated Carbon Sample	Film transfer coefficient k_f [s^{-1}]	Apparent Density ρ_c [m^3/kg]
Chemquest	2.977 E-05	1015
GRC 22	3.409 E-05	1162
A850_0.0533_60	2.364 E-0.5	820
P875_0.0533_60	2.658 E-05	789
A900_0.0425_60	3.728 E-05	934
P900_0.0425_60	3.266 E-05	843

The model parameters fitted to the batch kinetic gold adsorption data can be seen in table 3.3.

Table 3.3 Model parameters fitted for gold adsorption data

Activated Carbon Sample	α	$\bar{D}_s$ [m^2/s]	k_b [s^{-1}]
GRC 22	0.389	980E-12	12.0E-6
Chemquest 650	0.350	980E-12	12.9E-6
A900_0.0425_60	0.624	924E-12	15.5E-6
P900_0.0425_60	0.555	910E-12	15.0E-6
A850_0.0533_60	0.568	1006E-12	16.1E-6
P875_0.0533_60	0.500	805E-12	17.4E-6

The values of α, the fraction of gold loading capacity available as mesopores, indicates that the apricot shell activated carbon displays the biggest mesoporous character. The α values for the GRC 22 and Chemquest 650 are smaller than the α values of the peach and apricot shell activated carbon, which can be expected seeing that a slower gold uptake is observed for these two carbons.

The mass transfer rates of the adsorbed gold species from the meso- to the micropores are also slower for the coconut shell activated carbons, although the surface diffusivity values are comparable and sometimes higher than values obtained for peach and apricot shell activated carbons.

The model fitted to the experimental batch kinetic gold adsorption data can be seen in figures 3.5 to 3.10.

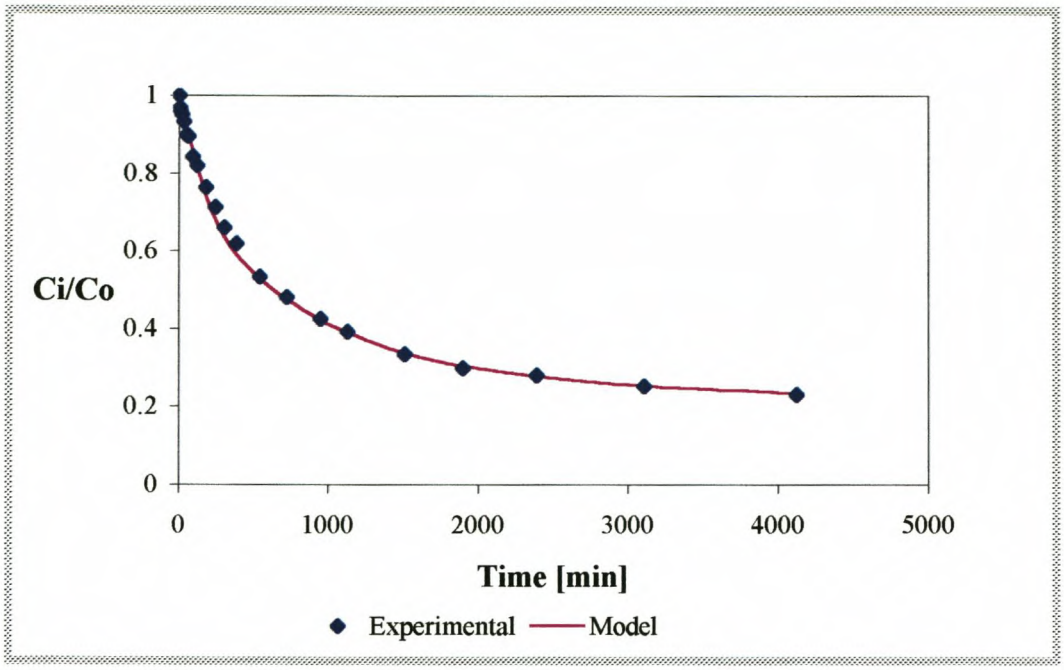

Figure 3.5 Batch kinetic gold adsorption modelling: GRC 22
(Co = 10.03 ppm, 0.25 g GAC/ℓ, 1400 < d_p < 1700 μm)

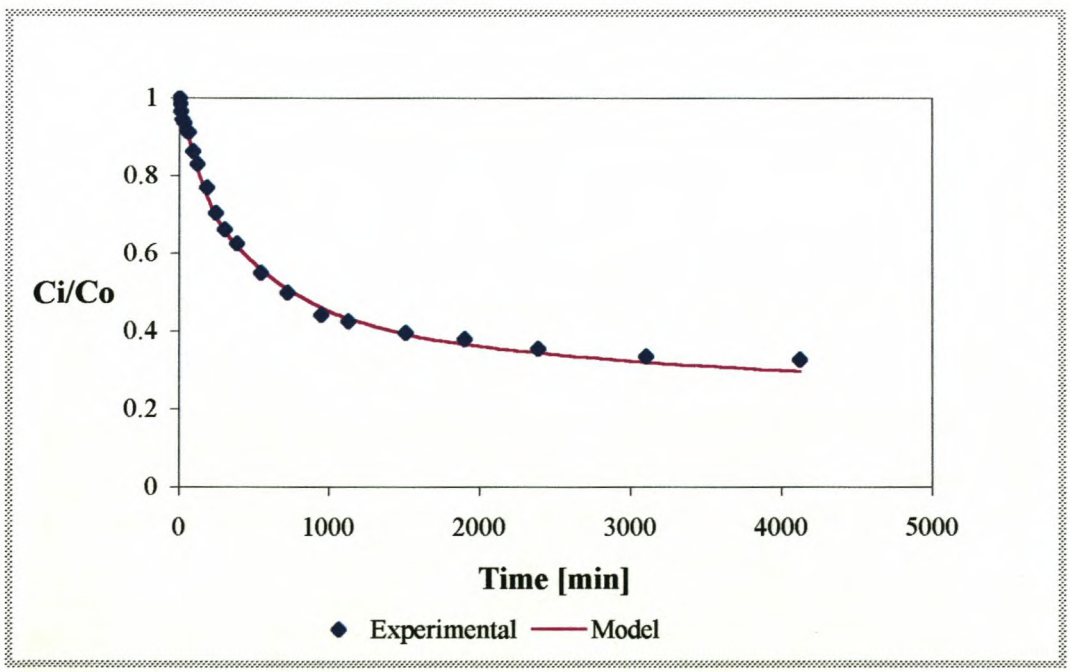

Figure 3.6 Batch kinetic gold adsorption modelling: Chemquest 650
(Co = 9.76 ppm, 0.25 g GAC/ℓ, 1400 < d_p < 1700 μm)

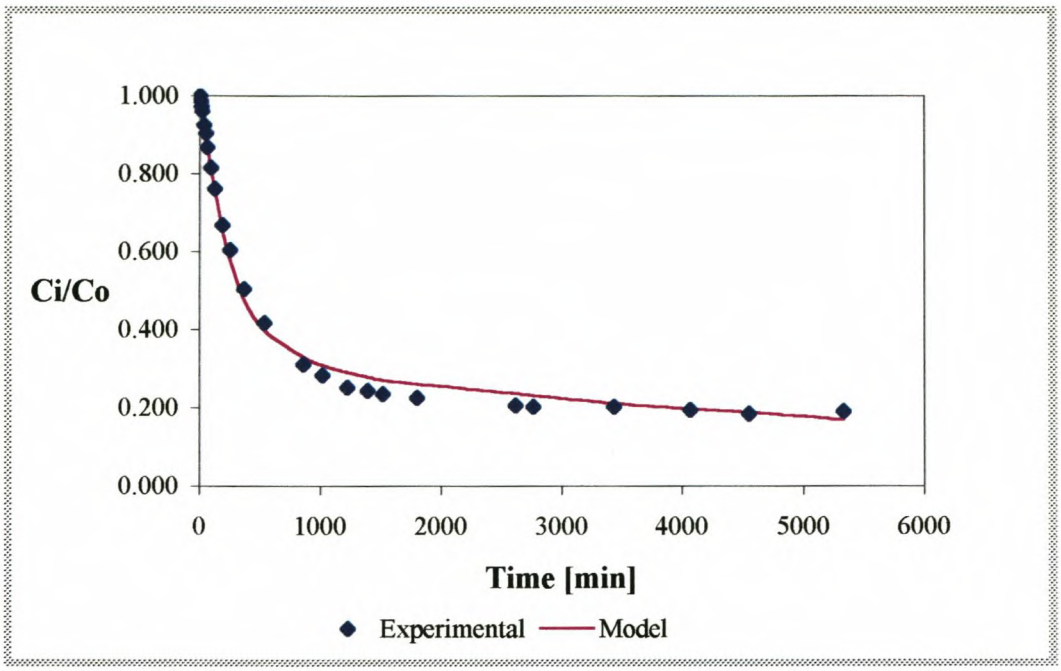

Figure 3.7 Batch kinetic gold adsorption modelling: A900_0.0425_60 (Co = 9.54 ppm, 0.25 g GAC/ℓ, 1400 < d_p < 1700 μm)

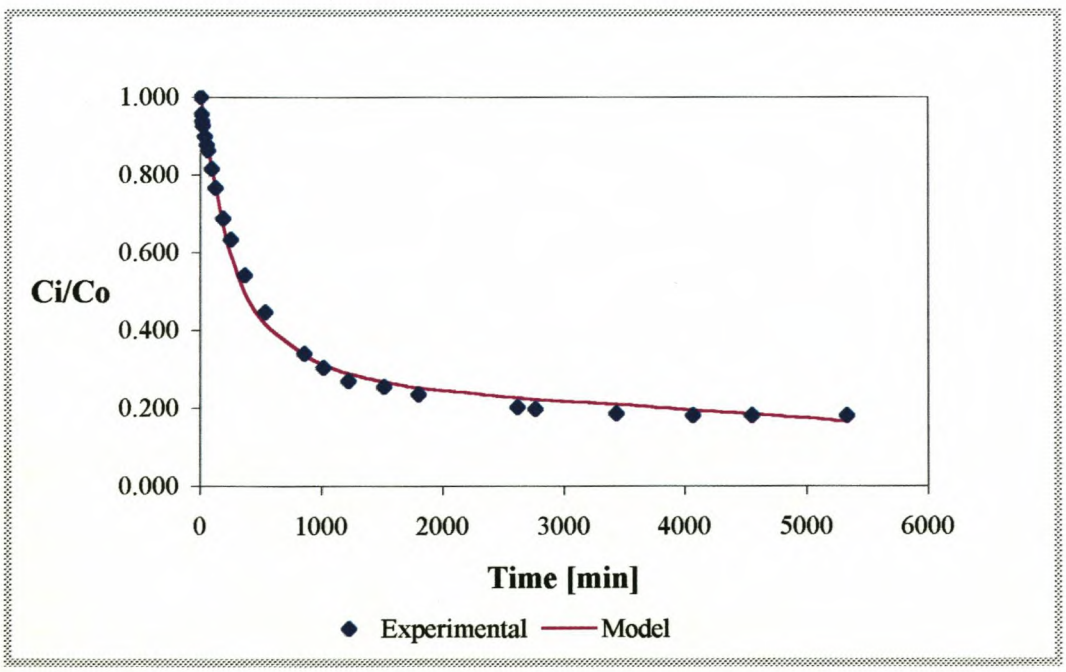

Figure 3.8 Batch kinetic gold adsorption modelling: P900_0.0425_60 (Co = 9.79 ppm, 0.25 g GAC/ℓ, 1400 < d_p < 1700 μm)

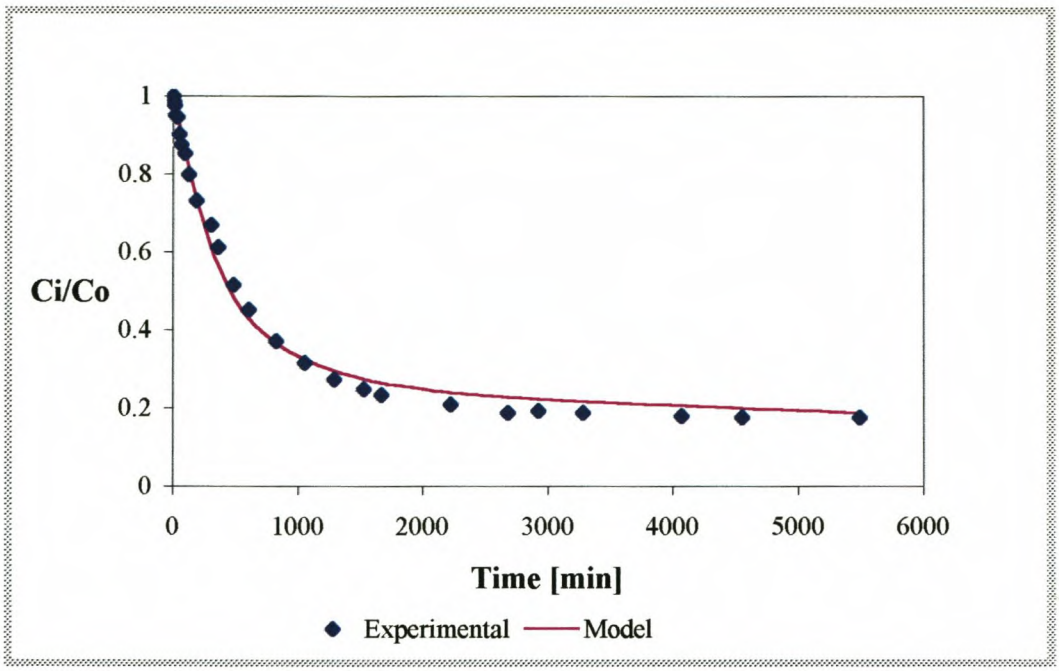

Figure 3.9 Batch kinetic gold adsorption modelling: A850_0.0533_600 (Co = 9.82 ppm, 0.25 g GAC/ℓ, 1400 < d_p < 1700 μm)

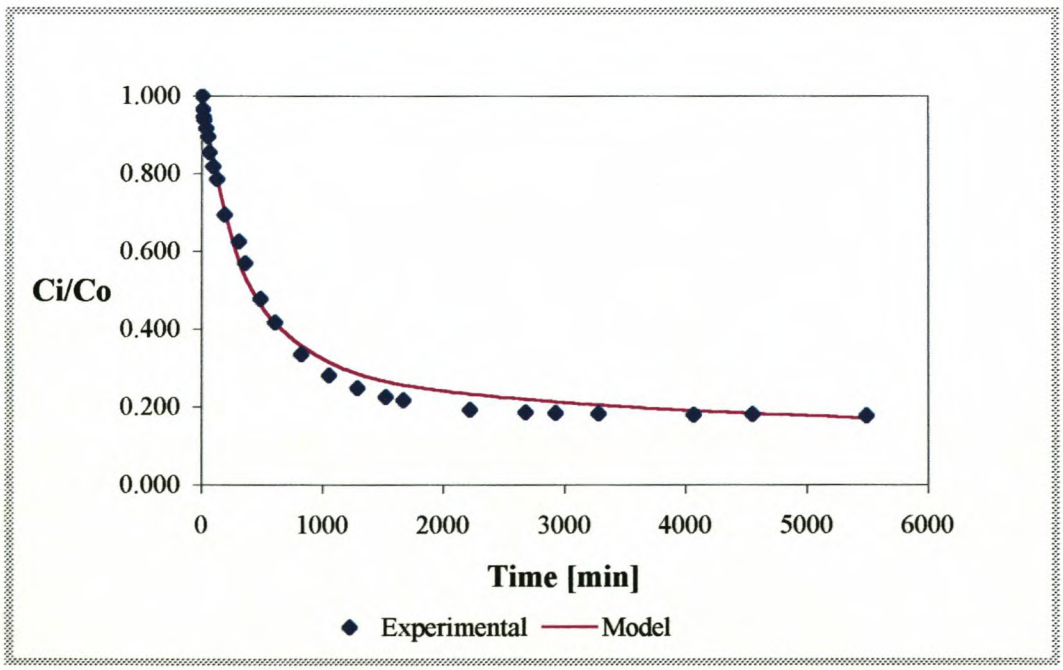

Figure 3.10 Batch kinetic gold adsorption modelling: P875_0.0533_600.25 (Co = 9.68 ppm, 0.25 g GAC/ℓ, 1400 < d_p < 1700 μm)

The following conclusions were drawn from the gold adsorption tests:

- Activated carbon produced from peach and apricot shells displays faster gold adsorption kinetics than coconut shell activated carbon.

- Activated carbons produced from peach and apricot shells display a wider pore size distribution than activated carbons produced from coconut shells.

- It is not clear from the equilibrium data which activated carbon is best suited for gold adsorption, because the equilibrium loadings of the individual activated carbon samples do not seem to vary that much.

- Apricot shell activated carbon displays more mesoporous structure than peach shell activated carbon, which leads to faster initial uptake of gold by the apricot shell activated carbon.

It is difficult to comment on the use of peach and apricot shell activated carbons for recovery of gold commercially, due to the fact that the gold adsorption properties of the activated carbon are not the only factor that determines whether a carbon is good for gold adsorption or not. An activated carbon's abrasion resistance and thermal regeneration properties are also very important.

Standard abrasion tests could not be performed on the experimentally produced activated carbons due to the small size of the samples. An attempt was made to simulate abrasion of the activated carbon in a pulp, by stirring the carbon within a pulp (silica sand) for a couple of hours and then determining the mass loss due to the reduction in size. These tests, however, failed due to the fact that fine sand particles clung to the surface of the activated carbon and could not entirely be removed by wet screening, therefore influencing the measured mass values of the activated carbon samples after each run.

Water Purification with Activated Carbon

3.1.5 Introduction

Activated carbon has been used extensively to purify, decolourize, dechlorinate and detoxicate domestic and industrial water [Bansal *et al*, 1988]. Requirements for industrial water supplies are greatly different from those of domestic water. Domestic water must be free from materials that may be harmful or poisonous to human life, occasionally free from scaling or corrosive potentials and esthetically of a nature, which will suite the standards with regard to taste, odour and colour.

Industrial wastewater is generally considered adequately neutralized if:

- Its attack on concrete, metals and other materials is minimal.
- It has little effect on fish or aquatic life in the receiving stream.
- It has little or no effect on biological matter.
- pH of the stream is in the range of 5.5 to 10.

  [Cheremisinoff and Young, 1981].

It is therefore, clear that different types of water require different treatment methods. Activated carbon is a universal adsorbed with affinity for so many organic and inorganic substances that makes it versatile for water purification.

Requirements of Activated Carbon used for Water Purification

Due to the highly developed porous structure and large specific surface area of activated carbon it exhibits a considerable adsorption capacity towards various pollutants both inorganic and organic. Activated carbons used for water purification should comply with a number of requirements, the most important of which are:

- The activated carbon should not introduce substances into the water that may be harmful to humans.
- It should not cause the formation of noxious substances when in contact with the water [Razvigorova *et al*, 1998].

Activated Carbon from Peach and Apricot Shells: Significance for South Africa

The advantages of activated carbon from peach and apricot shells for water purification in South Africa are more orientated towards domestic water than industrial waters.

In South Africa, the water infrastructure is well developed in many regions, providing treated water to a substantial portion of the population. However, large parts of the population do not have ready access to such treated water. This domestic unavailability of water supply often leads to the use of unsafe water or improper use of treated water. Even when treated pipe water is supplied it does not mean that water-related health hazards will be eliminated, because that community can be situated in a low socio-economic area. Factors such as treated piped water being contaminated due to low pipe pressure and breakdown in the system may contribute to diarrhoeal infections.

A relative cheap activated carbon made from a readily available raw material can be the answer to some of these water problems. Other applications of the activated carbons from peach and apricot shells for water purification can, however, not be excluded [Jagals *et al*, 1997].

Activated Carbon from Waste Products for Water Purification

Huge amounts of solid wastes containing relatively high amounts of organics exist. Among these solid wastes, packing papers, agricultural by-products, plastic bottles, by-products of the timber industry (e.g. sawdust), straw, rice hull, seeds or fruit stones can be mentioned. Research has been done in the past to learn more about the adsorptive behaviour/efficiencies of activated carbon produced from these waste materials for the removal of organic pollutants from water.

Activated carbon produced from grain husk, domestic waste, tyres and auto shredder light fraction by steam activation were used by László *et al* (1997) for the removal of phenol. Only the grain husk showed adsorption comparable with that of commercial activated carbons. Steam activation did, however, improve the adsorption capacities of these waste materials [László *et al*, 1997].

Trihalomethanes (THM) ($CHCl_3$, $CHBr_2Cl$, $CHBrCl_2$ and $CHBr_3$) are harmful substances formed during the disinfection step of drinking water with chlorine. They are derived from naturally occurring humic and fulvic acids combining with bromine and chlorine.

Activated carbon obtained from apricot stones by pyrolysis in a flow of water vapour was used in research by Razvigorova *et al* (1998) to see whether these activated carbons could be used for the removal of THMs. From the result obtained from equilibrium tests, the K and 1/n values (Freundlich isotherms) indicated that the magnitude of the adsorption of these chloronated organic compounds was in the following order: bromodichloromethane > dibromochloromethane > chloroform. The molecules containing bromium were adsorbed with the highest efficiency compared to the lower radius molecules (chlorine). This indicated that the adsorption was not only influenced by the size of the pores, but that the chemical character of the activated carbon also played an important role. The activated carbon from the apricot stones showed high adsorption effectiveness in relation to THMs indicating its use for water purification [Razvigorova *et al*, 1998].

In a study by Daifullah and Girgis (1998) they produced chemically activated carbon from apricot stones (H_3PO_4, 300°C-500°C) for the removal of phenols (m – cresol, 2 chlorophenol, p-cresol, 4- nitrophenol, 2,4 dichlorophenol and 2,4 dinitrophenol) from aqueous solution. It was found that carbon with surface areas of 850 – 1370 m^2/g, and pore volumes of 0.39 – 1.32 cm^3/g exhibited no corresponding change in its removal of the different phenols. Only at very high surface area or micropore volume a screening effect of the phenols could be observed. The major adsorption influencing factors were those due to the physical and chemical properties of the substances in question (solubility, molecular dimensions and acidity).

The amounts adsorbed were found to be comparable and sometimes superior to those reported for commercially available activated carbons. The adsorption of phenols seems to be determined by the distribution of pores and not merely the surface area and pore volume of the activated carbons. The feasibility of using apricot stone activated carbon for the removal of typical water pollutants was postulated, but

further work in batch and column evaluations was suggested [Daifullah and Girgis, 1998].

3.1.6 Experimental

The adsorption of phenol from aqueous solutions has frequently been used as a test for adsorbability of organic compounds by activated carbon. There are many methods for the removal of phenolic materials, e.g. steam distillation and oxidation using hydrogen peroxide. For water treatment the most frequently used method is, however, adsorption with activated carbon [Daifullah and Girgis, 1998].

Batch kinetic phenol adsorption tests were done with the A900_0.0425_60, P900_0.0425_60, P875_0.0533_60 and A850_0.0533_60 activated carbon samples. These tests were done in a 2ℓ Perspex batch reactor, equipped with four baffles and an overhead stirrer. A 10 ppm phenol solution was made up and brought into contact with 0.25g GAC/ℓ solution and stirred at a rate of 150 rpm. Samples were taken at regular time intervals and the samples analyzed at a wavelength of 269nm with a Varian, CARY UV – visible Spectrophotometer.

3.1.7 Results and Conclusions

Previous research done on the adsorption of phenol has indicated that the adsorption is a function of surface area as well as the oxygen-containing surface structures. The choice of activated carbons for the removal of phenols from aqueous solutions should therefore, favour activated carbons with high surface area and low acidic oxygen content. Activated carbon prepared at high temperatures should therefore be preferable [Bansal *et al*, 1988].

Figures 3.11 to 3.14 illustrate the concentration decline of phenol with time for the different activated carbon samples. The optimum activated carbons display better phenol adsorption than the A900_0.0425_60 and P900_0.0425_60 carbons.

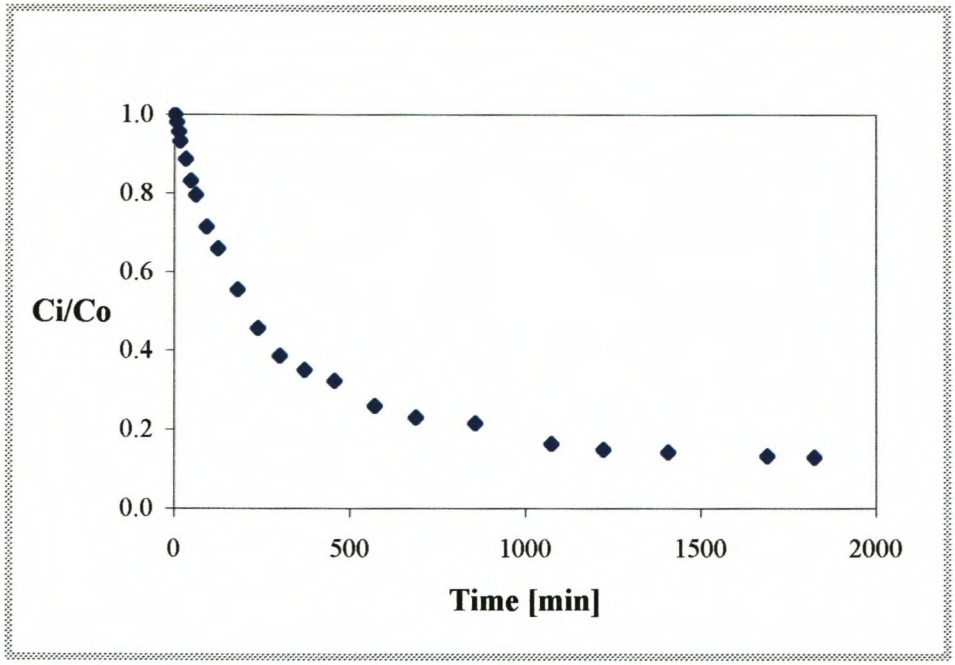

Figure 3.11 Batch kinetic phenol adsorption: A900_0.0425_60

(Co = 9.94 ppm, 0.25 g GAC/ℓ, 1400 < d_p < 1700 μm)

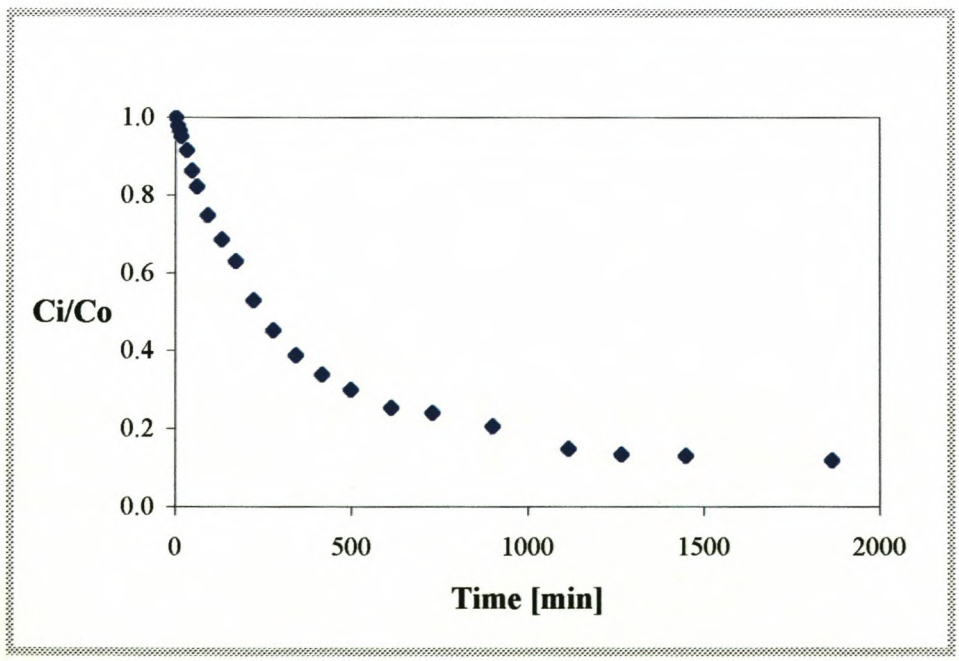

Figure 3.12 Batch kinetic phenol adsorption: P900_0.0425_60

(Co = 9.94 ppm, 0.25g GAC/ℓ, 1400 < d_p < 1700 μm)

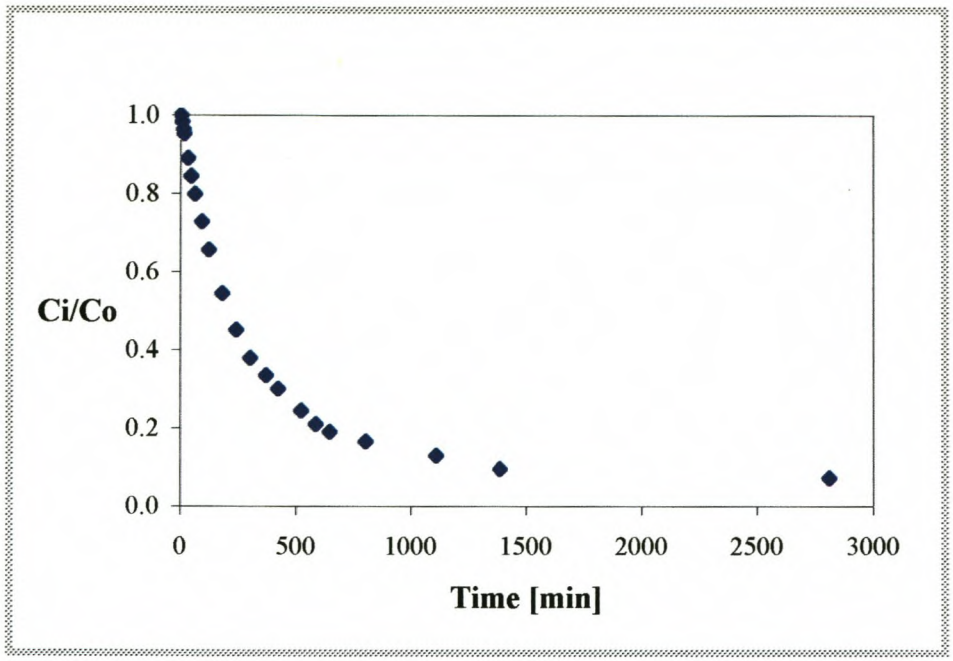

Figure 3.13 Batch kinetic phenol adsorption: A850_0.0533_60
(Co = 9.98 ppm, 0.25g GAC/ℓ, 1400 < d_p < 1700 μm)

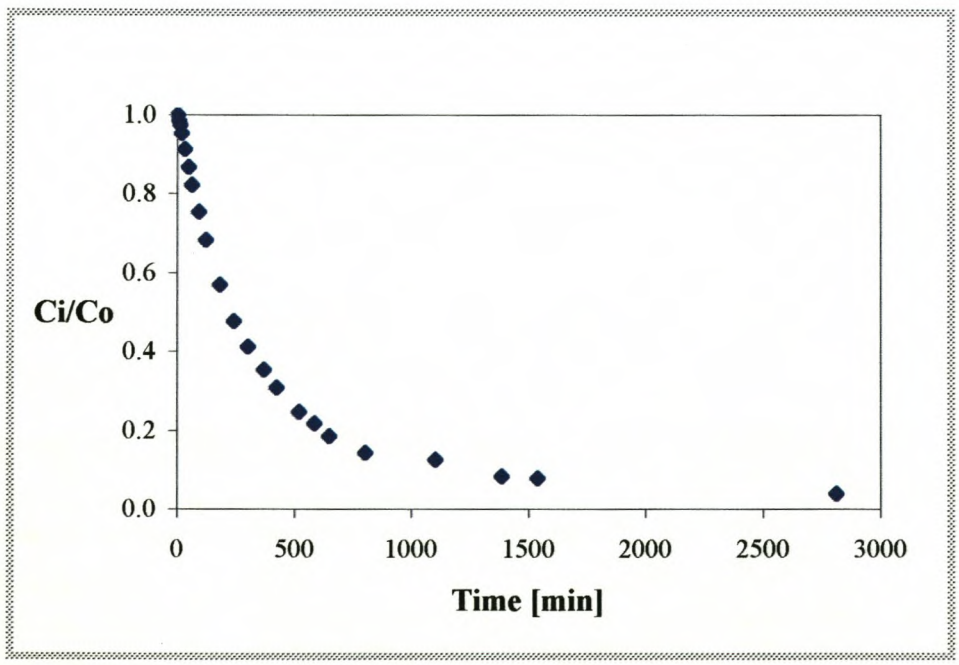

Figure 3.14 Batch kinetic phenol adsorption: P875_0.0533_60
(Co = 9.96 ppm, 0.25g GAC/ℓ, 1400 < d_p < 1700 μm)

Zhonghua Hu and Srinivasan (1999) presented a chemical activation method with KOH that yielded granular- high surface area activated carbon from coconut shells. The adsorption of these carbons for phenol was used to determine the effectiveness of these activated carbons. Phenol adsorption tests were also done with a commercial activated carbon, Filtrasorb100 (Calgon). Adsorption isotherms were determined using the batch equilibrium technique. A series of 100ml Erlenmeyer flasks containing 100ml of solution were sealed and shaken until equilibrium was reached where after the samples were filtered and the phenol concentration determined with ultraviolet adsorption.

Zhonghua Hu and Srinivasan (1999) used a Langmuir isotherm to model the phenol loading on the Filtrasorb100 and CK10 activated carbons. If the final loadings of the two optimal carbons are calculated using their Langmuir isotherms for the Filtrasorb100 and CK10 carbons, table 3.4 can be generated. The loading for the apricot and peach shell activated carbons of this study have been calculated by assuming that the values at 2808 min in figures 3.13 and 3.14 represents the equilibrium loadings.

Table 3.4 Equilibrium phenol concentrations and equilibrium loadings of optimum activated carbons and two coconut shell activated carbons

Sample	C_e Equilibrium Phenol Concentration [mg/l]	q Equilibrium Loading [mg/g]
A850_0.0533_60	0.72	37.04
Filtrasorb100	0.72	7.425
CK10	0.72	9.242
P875_0.0533_60	0.39	38.28
Filtrasorb100	0.39	4.022
CK10	0.39	5.006

From table 3.4 it can be seen that the loadings of phenol on the two optimal activated carbons are much higher than that of the one chemically activated carbon CK10 and the commercial activated carbon Filtrasorb100. If the equilibrium loadings of the two optimum activated carbons are compared then it can be seen that the peach shell activated carbon shows slightly better adsorption characteristics for phenol.

As a first indication of the possible use of the optimal activated carbons for water purification the phenol adsorption tests show very positive results, further test work would however be required.

4 Conclusions

Activated carbon was produced from peach and apricot shells at various activation conditions in order to determine the optimal activation conditions within an activation parameter range. Experiments were done to determine the suitability of peach and apricot shell activated carbon for use in the gold mining industry and for water purification. The results obtained from the experimental work led to the following conclusions:

- Activated carbons produced at low activation temperatures and long activation times shows high microporous areas. The same results can be obtained at higher temperatures, but the activation time needs to be short.

- The activation at 700°C seems to be controlled by the reaction rate, while activation at 900°C is controlled by the rate at which the reaction can be fed with steam.

- Optimal activation carbons can be produced at: 875°C, 0.0533 g steam/g char.min, 60 min for peach shells and 850°C, 0.0533 g steam/g char.min, 60 min for apricot shells.

- Apricot shell activated carbon is more mesoporous than peach shell activated carbon produced at the same activation conditions. This led to faster initial gold uptake during the batch kinetic gold adsorption tests.

- Activated carbon produced from peach and apricot shells displays faster gold adsorption kinetics than commercial coconut shell activated carbons.

- The equilibrium gold uptake of the four experimental activated carbons (A900_0.0425_60, A850_0.0533_60, P900_0.0425_60, P875_0.0533_60) and the two commercial coconut shell activated carbons (Chemquest 650, GRC 22) is for all practical purposes the same.

- Activated carbon produced from peach and apricot shells display a wider pore area distribution than coconut shell activated carbon.

- As a first indication of the use of peach and apricot shell activated carbon for phenol adsorption (relative indicator of water purification application) the results are positive.

5 Future Work

The main aim of this project was to find a "waste disposal" method for peach and apricot shells by doing product development of the products: Activated carbon from peach and apricot shells. Unknowns of the activation reaction and the adsorption properties of activated carbon from peach and apricot shells were investigated. The next step in the product development would be the large scale production, sales and delivery of the product. Unfortunately, this study only covered a small part of the initial product development. Work that still needs to be done before peach and apricot shell activated carbon can be produced commercially for gold adsorption and water purification includes the following:

- Abrasion tests on the granular activated peach and apricot shell activated carbon.
- Determination of the reactivation characteristics of peach and apricot shell activated carbon.
- Equilibrium phenol adsorption test as well as adsorption of other organic substances.
- Design and construction of a pilot plant for the production of activated carbon to determine whether data obtained from the batch production method can be scaled up.
- An economic feasibility study as well as a full market review.

6 References

1. Arriagada, R., Garcia, R., Molina-Sabio, M. and Rodriquez-Reinoso, F., Effect of steam activation on the porosity and chemical nature of activated carbons from Eucalyptus globulus and peach stones, Microporous Materials, 8, 1997, 123-130
2. ASTM Standard Test Method for Determination of Iodine Number of Activated Carbon, D4607 – 94, 1994
3. Bansal, R.C., Donnet, J.B. and Stoeckli, F., Active Carbon, Marcel Dekker, Inc., New York, 1988, 488
4. Bóta, A. and László, K. Preparation of activated carbon from apricot stones, Periodica Polytechnica Ser. Chem. Eng., 41(1), 1997, 19-24
5. Botha, K., The utilization of apricot kernels and shells, Masters Degree Thesis, University of Stellenbosch, 1998, 160
6. Chementator, Peach pits make good carbon, Chemical Engineering, February, 1998, 27
7. Cheremisinoff, P.N. and Young, R.A., Pollution Engineering Practice Handbook, Ann Arbor Science, 1981, 1073
8. Clayton, K.C. and Huie, J.M., Solid Waste Management, Ballinger Publishing Company, Cambridge, 1973
9. Daifullah, A.A.M. and Girgis, B.S., Removal of some substituted phenols by activated carbon obtained from agricultural waste, Water Research, 32(4), 1998, 1169-1177
10. Davidson, H.W., Wiggs, P.K.C., Churchouse, A.H. and Maggs, F.A.P, Manufactured Carbon, Pergamon Press LTD, Oxford, 1968, 111
11. Gergova, K. and Eser, S., Effects of activation method on the pore structure of activated carbons from apricot stones, Carbon, 34(7), 1996, 879-888
12. Hassler, J.W., Purification with activated carbon, Chemical Publishing Co., Inc., New York, 1970, 389
13. Hester, R.E. and Harrison, R.M.(ed.), Waste Treatment and Disposal, The Royal Society of Chemistry, Cambridge, 1995, 158
14. Jagals, P., Grabow, W.O.K. and Williams, E., The effects of supplied water quality on human health in an urban development with limited basic subsistence facilities., Water SA, 23(4), October 1997, 373-378

15. Jia, Y.F., Steele, C.J., Hayward, I.P. and Thomas, K.M., Mechanism of adsorption of gold and silver on activated carbons, Carbon, 36(9), 1998, 1299-1308
16. Kirubakaran, C.J., Krishnaiah. K. and Seshadri, S.K., Experimental Study of the Production of Activated Carbon in a Fluidized Bed Reactor, Ind. Eng. Chem. Res., 30(11), 1991, 2411-2416
17. László, K, Bóta, A. and Nagy, L.G., Characterization of activated carbons from waste materials by adsorption from aqueous solutions, Carbon, 35(5),1997, 593 - 598
18. Laxen, P.A., Becker, G.S.M. and Rubin, R., Developments in the application of carbon-in-pulp to the recovery of gold from South African ores, Journal of the South African Institute of Mining and Metallurgy, June, 1979, 315-326
19. MacDonald, J.A.F. and Quinn, D.F., Adsorbents for methane storage made by phosphoric acid activation of peach pips, Carbon, 34(9), 1996, 1103 – 1108
20. Mantell, C.L., Solid Wastes: origin, collection, processing and disposal, John Wiley and Sons, New York, 1975, 418.
21. McDougall, G.J., Hancock, R.D., Nicol, M.J., Wellington, O.L. and Copperthwaite, R.G., The mechanism of the adsorption of gold cyanide on activated carbon, Journal of the South African Institute of Mining and Metallurgy, September, 1980, 344-356
22. McDougall, G.L., The physical nature and manufacture of activated carbon, Journal of South African Institute of Mining and Metallurgy, 91(4), 1991, 109-120
23. McEnaney, B., Adsorption and structure in microporous carbons, Carbon, 26(3), 1988, 267-274
24. Micromeritics ASAP 2010 Operator's Manual, 1998
25. Micromeritics DFT Plus Models Library, 1997
26. Nicol, M.J., Fleming, C.A. and Cromberge, G., The adsorption of gold cyanide onto activated carbon I. The kinetics of adsorption from pulps, Journal of the South African Institute of Mining and Metallurgy, February 1984, 50-54
27. Nieuwoudt, I, Dynamic model for the competitive adsorption of metal cyanides on activated carbon in batch reactors, Masters Degree Thesis, University of Stellenbosch, 1989, 289
28. Razvigorova M., Budinova, T., Petrov, N. and Minkova, V., Purification of Water by Activated carbons from apricot stones, lignites and anthracite, Carbon, 32(7), 1988, 2135-2139

29. Sai, P.M.S, Ahmed, J., Krishnaiah, K., Production of Activated Carbon from Coconut Shell Char in a Fluidized Bed Reactor, Ind. Eng. Chem. Res., 36(9),1997, 3625-3630

30. Salunkhe, D. K. and Kadam, S.S. (ed.), Handbook of Fruit Science and Technology, Marcell Dekker, Inc., New York, 1995, 611

31. Stanley, G.G. (ed.), The Extractive Metallurgy of Gold in South Africa, Volume 1, The Chamber of Mines of South Africa, Johannesburg, 1997, 614

32. Ulrich, K.T. and Eppinger, S.D., Product Design and Development, McGraw-Hill, Inc., New York, 1995, 289

33. Van Deventer, J.S.J., Kinetic model for the adsorption of metal cyanides on activated charcoal, PhD. Thesis, University of Stellenbosch, 1984, 337

34. Van Dyk, L.D., Activated Carbon from Agricultural Waste, Final year Laboratory Project 488, University of Stellenbosch, 1998, 64

35. Webb, P.A. and Orr, C., Analytical Methods in Fine Particle Technology, Micromeritics Instrument Corporation, Norcross, USA, 1997, 301

36. Zhonghua Hu and Srinivasan, M.P., Preparation of high-surface-area activated carbons from coconut shell, Microporous and Mesoporous Materials, 27, 1999, 11-18

Appendix A: Production of Activated Carbon

A1: Carbonization Data

A1.1 Carbonization Data : Apricot Shells

Carbonization Temperature [°C]	350
Carbonization Time [min]	30
Nitrogen Flowrate [ℓ/min @ 20°C, 1 atm]	32.40-16.35
Sample Mass [g]	200

Sample Number	Mass After [g]	Mass Loss [g]	Yield %
AC 1	55.478	144.522	27.74
AC 2	53.001	146.999	26.50
AC 3	57.151	142.849	28.58
AC 4	58.987	141.013	29.49
AC 5	59.753	140.247	29.88
AC 6	58.740	141.260	29.37
AC 7	55.032	144.968	27.52
AC 8	60.650	139.350	30.33
AC 9	55.444	144.556	27.72
AC 10	60.382	139.618	30.19
AC 11	61.023	138.977	30.51
AC 12	55.655	144.345	27.83
AC 13	54.958	145.042	27.48
AC 14	57.841	142.159	28.92
AC 15	56.498	143.502	28.25
AC 16	54.845	145.155	27.42
AC 17	56.212	143.788	28.11
AC 18	53.480	146.520	26.74
AC 19	51.916	148.084	25.96
AC 20	57.982	142.018	28.99
AC 21	59.147	140.853	29.57
AC 22	55.272	144.728	27.64
AC 23	61.230	138.770	30.62
AC 24	57.923	142.077	28.96
AC 25	54.160	145.840	27.08
AC 26	60.575	139.425	30.29
AC 27	57.877	142.123	28.94

A1.1 Carbonization Data: Apricot Shells

Sample Number	Mass After [g]	Mass Loss [g]	Yield %
AC 28	58.056	141.944	29.03
AC 29	56.432	143.568	28.22
AC 30	59.010	140.990	29.51
AC 31	57.339	142.661	28.67
AC 32	57.860	142.140	28.93
AC 33	60.584	139.416	30.29
AC 34	60.123	139.877	30.06
AC 35	57.794	142.206	28.90
AC 36	57.221	142.779	28.61
AC 37	59.158	140.842	29.58
AC 38	63.393	136.607	31.70
AC 39	56.681	143.319	28.34
AC 40	57.789	142.211	28.89
AC 41	57.775	142.225	28.89
AC 42	60.929	139.071	30.46
AC 43	56.938	143.062	28.47
AC 44	57.940	142.060	28.97
AC 45	58.542	141.458	29.27
AC 46	62.184	137.816	31.09
AC 47	57.283	142.717	28.64
AC 48	57.349	142.651	28.67
AC 49	60.478	139.522	30.24

Yield % After Carbonization: 28.90

A1.2 Carbonization Data : Peach Shells

Carbonization Temperature [°C] 345

Carbonization Time [min] 30

Nitrogen Flowrate [ℓ/min @ 20°C, 1 atm] 32.40-16.35

Sample Mass [g] 200

Sample Number	Mass After [g]	Mass Loss [g]	Yield %
PC 1	69.683	130.317	34.84
PC 2	62.342	137.658	31.17
PC 3	63.261	136.739	31.63
PC 4	62.765	137.235	31.38
PC 5	67.968	132.032	33.98
PC 6	63.205	136.795	31.60
PC 7	63.210	136.790	31.61
PC 8	61.966	138.034	30.98
PC 9	67.087	132.913	33.54
PC 10	61.973	138.027	30.99
PC 11	57.679	142.321	28.84
PC 12	62.114	137.886	31.06
PC 13	66.036	133.964	33.02
PC 14	63.313	136.687	31.66
PC 15	63.243	136.757	31.62
PC 16	61.696	138.304	30.85
PC 17	67.424	132.576	33.71
PC 18	62.427	137.573	31.21
PC 19	63.169	136.831	31.58
PC 20	63.653	136.347	31.83
PC 21	67.846	132.154	33.92
PC 22	63.078	136.922	31.54
PC 23	61.949	138.051	30.97
PC 24	65.342	134.658	32.67
PC 25	65.122	134.878	32.56
PC 26	63.132	136.868	31.57
PC 27	64.762	135.238	32.38
PC 28	61.662	138.338	30.83
PC 29	64.377	135.623	32.19
PC 30	66.017	133.983	33.01
PC 31	62.667	137.333	31.33
PC 32	62.358	137.642	31.18

A1.2 Carbonization Data: Peach Shells

Sample Number	Mass After [g]	Mass Loss [g]	Yield %
PC 33	68.431	131.569	34.22
PC 34	61.717	138.283	30.86
PC 35	61.130	138.870	30.57
PC 36	62.438	137.562	31.22
PC 37	66.668	133.332	33.33
PC 38	61.770	138.230	30.89
PC 39	62.073	137.927	31.04
PC 40	61.183	138.817	30.59
PC 41	66.363	133.637	33.18
PC 42	61.036	138.964	30.52
PC 43	64.450	135.550	32.23
PC 44	62.244	137.756	31.12
PC 45	61.226	138.774	30.61
PC 46	60.932	139.068	30.47
PC 47	64.885	135.115	32.44
PC 48	61.165	138.835	30.58
PC 49	66.121	133.879	33.06
PC 50	61.801	138.199	30.90
PC 51	62.166	137.834	31.08
PC 52	62.593	137.407	31.30

Yield % After Carbonization: 31.76

A2 : Activated Carbon Fact Sheets

A2.1 Activated Carbon Fact Sheet: A700_0.0425_30

Raw Material

Apricot Shell

Activation Conditions

Activation Time [min]	30
Activation Temperature [°C]	700
Steam Flowrate [g/g.min]	0.0425
Nitrogen Flowrate [ℓ/min @ 20°C, 1 atm]	14

Total Yield (Raw Material to GAC)

Mass of Char before Activation [g]	100.00
Mass of Activated Carbon Produced [g]	66.389
Mass Loss [g]	33.61
Yield %	19.19

BET Surface Area

Micropore Surface Area [m^2/g]	412.3
External/ Mesoporous Surface Area [m^2/g]	58.8
Micropore Volume [cm^3/g]	0.191788

Iodine Number [mg/g]

492.1

A2.2 Activated Carbon Fact Sheet: A700_0.0425_60

Raw Material Apricot Shell

Activation Conditions

Activation Time [min]	60
Activation Temperature [°C]	700
Steam Flowrate [g/g.min]	0.0425
Nitrogen Flowrate [ℓ/min @ 20°C, 1 atm]	14

Total Yield (Raw Material to GAC)

Mass of Char before Activation [g]	100.00
Mass of Activated Carbon Produced [g]	61.718
Mass Loss [g]	38.28
Yield %	17.84

BET Surface Area

Micropore Surface Area [m^2/g]	463.5
External/ Mesoporous Surface Area [m^2/g]	79.3
Micropore Volume [cm^3/g]	0.215379

Iodine Number [mg/g] 662.3

A2.3 Activated Carbon Fact Sheet: A700_0.0629_30

Raw Material	Apricot Shell

Activation Conditions

Activation Time [min]	30
Activation Temperature [°C]	700
Steam Flowrate [g/g.min]	0.0629
Nitrogen Flowrate [ℓ/min @ 20°C, 1 atm]	14

Total Yield (Raw Material to GAC)

Mass of Char before Activation [g]	100.00
Mass of Activated Carbon Produced [g]	65.922
Mass Loss [g]	34.08
Yield %	19.05

BET Surface Area

Micropore Surface Area [m^2/g]	426.1
External/Mesoporous Surface Area [m^2/g]	66.0
Micropore Volume [cm^3/g]	0.198115

Iodine Number [mg/g]	561.9

A2.4 Activated Carbon Fact Sheet: A700_0.0629_60

Raw Material

Apricot Shell

Activation Conditions

Activation Time [min]	60
Activation Temperature [°C]	700
Steam Flowrate [g/g.min]	0.0629
Nitrogen Flowrate [ℓ/min @ 20°C, 1 atm]	14

Total Yield (Raw Material to GAC)

Mass of Char before Activation [g]	100.00
Mass of Activated Carbon Produced [g]	58.962
Mass Loss [g]	41.04
Yield %	17.04

BET Surface Area

Micropore Surface Area [m^2/g]	491.8
External/ Mesoporous Surface Area [m^2/g]	116.6
Micropore Volume [cm^3/g]	0.228467

Iodine Number [mg/g]

746.2

A2.5 Activated Carbon Fact Sheet: A700_0.10_60

Raw Material	Apricot Shell

Activation Conditions

Activation Time [min]	60
Activation Temperature [°C]	700
Steam Flowrate [g/g.min]	0.1
Nitrogen Flowrate [ℓ/min @ 20°C, 1 atm]	14

Total Yield (Raw Material to GAC)

Mass of Char before Activation [g]	100.00
Mass of Activated Carbon Produced [g]	53.299
Mass Loss [g]	46.70
Yield %	15.40

Iodine Number [mg/g]	879.6

A2.6 Activated Carbon Fact Sheet: A800_0.0425_30

Raw Material	Apricot Shell

Activation Conditions

Activation Time [min]	30
Activation Temperature [°C]	800
Steam Flowrate [g/g.min]	0.0425
Nitrogen Flowrate [ℓ/min @ 20°C, 1 atm]	14

Total Yield (Raw Material to GAC)

Mass of Char before Activation [g]	100.00
Mass of Activated Carbon Produced [g]	60.183
Mass Loss [g]	39.82
Yield %	17.39

Iodine Number [mg/g]	690.0

A2.7 Activated Carbon Fact Sheet: A800_0.0425_60

Raw Material	Apricot Shell

Activation Conditions

Activation Time [min]	60
Activation Temperature [°C]	800
Steam Flowrate [g/g.min]	0.0425
Nitrogen Flowrate [ℓ/min @ 20°C, 1 atm]	14

Total Yield (Raw Material to GAC)

Mass of Char before Activation [g]	100.00
Mass of Activated Carbon Produced [g]	52.149
Mass Loss [g]	47.85
Yield %	15.07

BET Surface Area

Micropore Surface Area [m^2/g]	535.2
External Surface Area [m^2/g]	195.7
Micropore Volume [cm^3/g]	0.249491

Iodine Number [mg/g]	894.3

A2.8 Activated Carbon Fact Sheet: A800_0.0425_90

Raw Material	Apricot Shell

Activation Conditions

Activation Time [min]	90
Activation Temperature [°C]	800
Steam Flowrate [g/g.min]	0.0425
Nitrogen Flowrate [ℓ/min @ 20°C, 1 atm]	14

Total Yield (Raw Material to GAC)

Mass of Char before Activation [g]	100.00
Mass of Activated Carbon Produced [g]	34.544
Mass Loss [g]	65.46
Yield %	9.98

Iodine Number [mg/g]	1267.9

A2.9 Activated Carbon Fact Sheet: A900_0.0425_30

Raw Material	Apricot Shell

Activation Conditions

Activation Time [min]	30
Activation Temperature [°C]	900
Steam Flowrate [g/g.min]	0.0425
Nitrogen Flowrate [ℓ/min @ 20°C, 1 atm]	14

Total Yield (Raw Material to GAC)

Mass of Char before Activation [g]	100.00
Mass of Activated Carbon Produced [g]	50.523
Mass Loss [g]	49.48
Yield %	14.60

BET Surface Area

Micropore Surface Area [m^2/g]	533.9
External/ Mesoporous Surface Area [m^2/g]	208.0
Micropore Volume [cm^3/g]	0.249916

Iodine Number [mg/g]	904.3

A2.10 Activated Carbon Fact Sheet: A900_0.0425_60

Raw Material

Apricot Shell

Activation Conditions

Activation Time [min]	60
Activation Temperature [°C]	900
Steam Flowrate [g/g.min]	0.0425
Nitrogen Flowrate [ℓ/min @ 20°C, 1 atm]	14

Total Yield (Raw Material to GAC)

Mass of Char before Activation [g]	100.00
Mass of Activated Carbon Produced [g]	31.84
Mass Loss [g]	68.16
Yield %	9.20

BET Surface Area

Micropore Surface Area [m^2/g]	645.3
External/ Mesoporous Surface Area [m^2/g]	458.0
Micropore Volume [cm^3/g]	0.299496

Iodine Number [mg/g]

1300.9

A2.11 Activated Carbon Fact Sheet: A900_0.0629_30

Raw Material	Apricot Shell

Activation Conditions

Activation Time [min]	30
Activation Temperature [°C]	900
Steam Flowrate [g/g.min]	0.0629
Nitrogen Flowrate [ℓ/min @ 20°C, 1 atm]	14

Total Yield (Raw Material to GAC)

Mass of Char before Activation [g]	100.00
Mass of Activated Carbon Produced [g]	45.544
Mass Loss [g]	54.46
Yield %	13.16

BET Surface Area

Micropore Surface Area [m^2/g]	559.1
External/ Mesoporous Surface Area [m^2/g]	305.4
Micropore Volume [cm^3/g]	0.260029

Iodine Number [mg/g]	1003.7

A2.12 Activated Carbon Fact Sheet: A900_0.0629_60

Raw Material	Apricot Shell

Activation Conditions

Activation Time [min]	60
Activation Temperature [°C]	900
Steam Flowrate [g/g.min]	0.0629
Nitrogen Flowrate [ℓ/min @ 20°C, 1 atm]	14

Total Yield (Raw Material to GAC)

Mass of Char before Activation [g]	100.00
Mass of Activated Carbon Produced [g]	16.848
Mass Loss [g]	83.15
Yield %	4.87

BET Surface Area

Micropore Surface Area [m^2/g]	687.4
External/ Mesoporous Surface Area [m^2/g]	821.1
Micropore Volume [cm^3/g]	0.314559

Iodine Number [mg/g]	1569.3

A2.13 Activated Carbon Fact Sheet: A850_0.0533_60

Raw Material	Apricot Shell

Activation Conditions

Activation Time [min]	60
Activation Temperature [°C]	850
Steam Flowrate [g/g.min]	0.0533
Nitrogen Flowrate [ℓ/min @ 20°C, 1 atm]	14

Total Yield (Raw Material to GAC)

Mass of Char before Activation [g]	100.00
Mass of Activated Carbon Produced [g]	37.369
Mass Loss [g]	62.63
Yield %	10.80

BET Surface Area

Micropore Surface Area [m^2/g]	610.8
External/ Mesoporous Surface Area [m^2/g]	391.9
Micropore Volume [cm^3/g]	0.283657

Iodine Number [mg/g]	1194.2

A2.14 Activated Carbon Fact Sheet: P700_0.0425_30

Raw Material	Peach Shell

Activation Conditions

Activation Time [min]	30
Activation Temperature [°C]	700
Steam Flowrate [g/g.min]	0.0425
Nitrogen Flowrate [ℓ/min @ 20°C, 1 atm]	14

Total Yield (Raw Material to GAC)

Mass of Char before Activation [g]	100.00
Mass of Activated Carbon Produced [g]	64.216
Mass Loss [g]	35.78
Yield %	20.39

BET Surface Area

Micropore Surface Area [m^2/g]	404.0
External/ Mesoporous Surface Area [m^2/g]	53.1
Micropore Volume [cm^3/g]	0.187974

Iodine Number [mg/g]	489.7

A2.15 Activated Carbon Fact Sheet: P700_0.0425_60

Raw Material

Peach Shell

Activation Conditions

Activation Time [min]	60
Activation Temperature [°C]	700
Steam Flowrate [g/g.min]	0.0425
Nitrogen Flowrate [ℓ/min @ 20°C, 1 atm]	14

Total Yield (Raw Material to GAC)

Mass of Char before Activation [g]	100.00
Mass of Activated Carbon Produced [g]	61.579
Mass Loss [g]	38.42
Yield %	19.62

BET Surface Area

Micropore Surface Area [m^2/g]	459.7
External/ Mesoporous Surface Area [m^2/g]	67.7
Micropore Volume [cm^3/g]	0.187974

Iodine Number [mg/g]

625.2

A2.16 Activated Carbon Fact Sheet: P700_0.0629_30

Raw Material	Peach Shell

Activation Conditions

Activation Time [min]	30
Activation Temperature [°C]	700
Steam Flowrate [g/g.min]	0.0629
Nitrogen Flowrate [ℓ/min @ 20°C, 1 atm]	14

Total Yield (Raw Material to GAC)

Mass of Char before Activation [g]	100.00
Mass of Activated Carbon Produced [g]	63.668
Mass Loss [g]	36.33
Yield %	20.22

BET Surface Area

Micropore Surface Area [m^2/g]	421.1
External/ Mesoporous Surface Area [m^2/g]	55.6
Micropore Volume [cm^3/g]	0.195903

Iodine Number [mg/g]	551.0

A2.17 Activated Carbon Fact Sheet: P700_0.0629_60

Raw Material	Peach Shell

Activation Conditions

Activation Time [min]	60
Activation Temperature [°C]	700
Steam Flowrate [g/g.min]	0.0629
Nitrogen Flowrate [ℓ/min @ 20°C, 1 atm]	14

Total Yield (Raw Material to GAC)

Mass of Char before Activation [g]	100.00
Mass of Activated Carbon Produced [g]	58.962
Mass Loss [g]	41.04
Yield %	18.73

BET Surface Area

Micropore Surface Area [m^2/g]	498.2
External/ Mesoporous Surface Area [m^2/g]	87.5
Micropore Volume [cm^3/g]	0.231571

Iodine Number [mg/g]	726.5

A2.18 Activated Carbon Fact Sheet: P800_0.0425_60

Raw Material Peach Shell

Activation Conditions

Activation Time [min]	60
Activation Temperature [°C]	800
Steam Flowrate [g/g.min]	0.0425
Nitrogen Flowrate [ℓ/min @ 20°C, 1 atm]	14

Total Yield (Raw Material to GAC)

Mass of Char before Activation [g]	100.00
Mass of Activated Carbon Produced [g]	51.837
Mass Loss [g]	48.16
Yield %	16.46

BET Surface Area

Micropore Surface Area [m^2/g]	567.3
External/ Mesoporous Surface Area [m^2/g]	165.0
Micropore Volume [cm^3/g]	0.264271

Iodine Number [mg/g] 858.9

A2.19 Activated Carbon Fact Sheet: P900_0.0425_30

Raw Material	Peach Shell

Activation Conditions

Activation Time [min]	30
Activation Temperature [°C]	900
Steam Flowrate [g/g.min]	0.0425
Nitrogen Flowrate [ℓ/min @ 20°C, 1 atm]	14

Total Yield (Raw Material to GAC)

Mass of Char before Activation [g]	100.00
Mass of Activated Carbon Produced [g]	51.104
Mass Loss [g]	48.90
Yield %	16.23

BET Surface Area

Micropore Surface Area [m^2/g]	550.6
External/ Mesoporous Surface Area [m^2/g]	165.3
Micropore Volume [cm^3/g]	0.256472

Iodine Number [mg/g]	882.7

A2.20 Activated Carbon Fact Sheet: P900_0.0425_60

Raw Material	Peach Shell

Activation Conditions

Activation Time [min]	60
Activation Temperature [°C]	900
Steam Flowrate [g/g.min]	0.0425
Nitrogen Flowrate [ℓ/min @ 20°C, 1 atm]	14

Total Yield (Raw Material to GAC)

Mass of Char before Activation [g]	100.00
Mass of Activated Carbon Produced [g]	40.298
Mass Loss [g]	59.70
Yield %	12.80

BET Surface Area

Micropore Surface Area [m^2/g]	641.4
External/ Mesoporous Surface Area [m^2/g]	294.0
Micropore Volume [cm^3/g]	0.29803

Iodine Number [mg/g]	1127.0

A2.21 Activated Carbon Fact Sheet: P900_0.0629_30

Raw Material

Peach Shell

Activation Conditions

Activation Time [min]	30
Activation Temperature [°C]	900
Steam Flowrate [g/g.min]	0.0629
Nitrogen Flowrate [ℓ/min @ 20°C, 1 atm]	14

Total Yield (Raw Material to GAC)

Mass of Char before Activation [g]	100.00
Mass of Activated Carbon Produced [g]	50.083
Mass Loss [g]	49.92
Yield %	15.91

BET Surface Area

Micropore Surface Area [m^2/g]	567.9
External/ Mesoporous Surface Area [m^2/g]	182.2
Micropore Volume [cm^3/g]	0.264339

Iodine Number [mg/g]

929.6

A2.22 Activated Carbon Fact Sheet: P900_0.0629_60

Raw Material	Peach Shell

Activation Conditions

Activation Time [min]	60
Activation Temperature [°C]	900
Steam Flowrate [g/g.min]	0.0629
Nitrogen Flowrate [ℓ/min @ 20°C, 1 atm]	14

Total Yield (Raw Material to GAC)

Mass of Char before Activation [g]	100.00
Mass of Activated Carbon Produced [g]	19.415
Mass Loss [g]	80.59
Yield %	6.17

BET Surface Area

Micropore Surface Area [m^2/g]	788.6
External/ Mesoporous Surface Area [m^2/g]	653.4
Micropore Volume [cm^3/g]	0.362756

Iodine Number [mg/g]	1556.6

A2.23 Activated Carbon Fact Sheet: P875_0.0533_60

Raw Material

Peach Shell

Activation Conditions

Activation Time [min]	60
Activation Temperature [°C]	875
Steam Flowrate [g/g.min]	0.0533
Nitrogen Flowrate [ℓ/min @ 20°C, 1 atm]	14

Total Yield (Raw Material to GAC)

Mass of Char before Activation [g]	100.00
Mass of Activated Carbon Produced [g]	40.662
Mass Loss [g]	59.34
Yield %	12.91

BET Surface Area

Micropore Surface Area [m^2/g]	649.9
External/ Mesoporous Surface Area [m^2/g]	354.7
Micropore Volume [cm^3/g]	0.301448

Iodine Number [mg/g]

1152.3

A2.24 Activated Carbon Fact Sheet: GRC 22

Raw Material Coconut Shell

BET Surface Area

Micropore Surface Area [m^2/g]	763.8
External/ Mesoporous Surface Area [m^2/g]	126.0
Micropore Volume [cm^3/g]	0.355245

Iodine Number [mg/g] 1085.9

A2.25 Activated Carbon Fact Sheet: Chemquest 650 (CQ650)

Raw Material Coconut Shell

BET Surface Area

Micropore Surface Area [m^2/g]	916.9
External/ Mesoporous Surface Area [m^2/g]	283.6
Micropore Volume [cm^3/g]	0.423285

Iodine Number [mg/g] 1262.1

Appendix A3: Iodine Adsorption Isotherms

A3.1 Iodine Adsorption Isotherm: A700_0.0425_30

Mass GAC [mg]	Residual Iodine Concentration [N]	Iodine Adsorbed/g GAC [mg/g]
2.713	0.0072	425.3
2.130	0.0168	478.9
1.734	0.0262	512.2

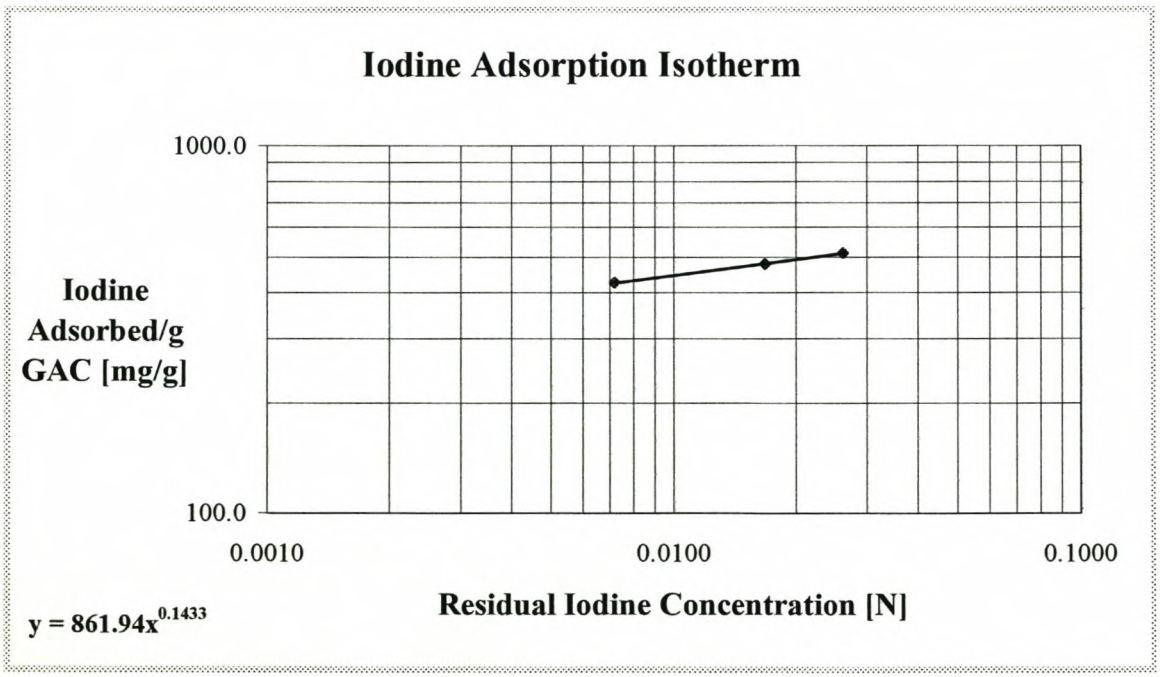

Iodine Number [mg/g] : 492.1

A3.2 Iodine Adsorption Isotherm: A700_0.0425_60

Mass GAC [mg]	Residual Iodine Concentration [N]	Iodine Adsorbed/g GAC [mg/g]
2.699	0.0007	457.3
1.865	0.0077	609.8
1.318	0.0257	671.2

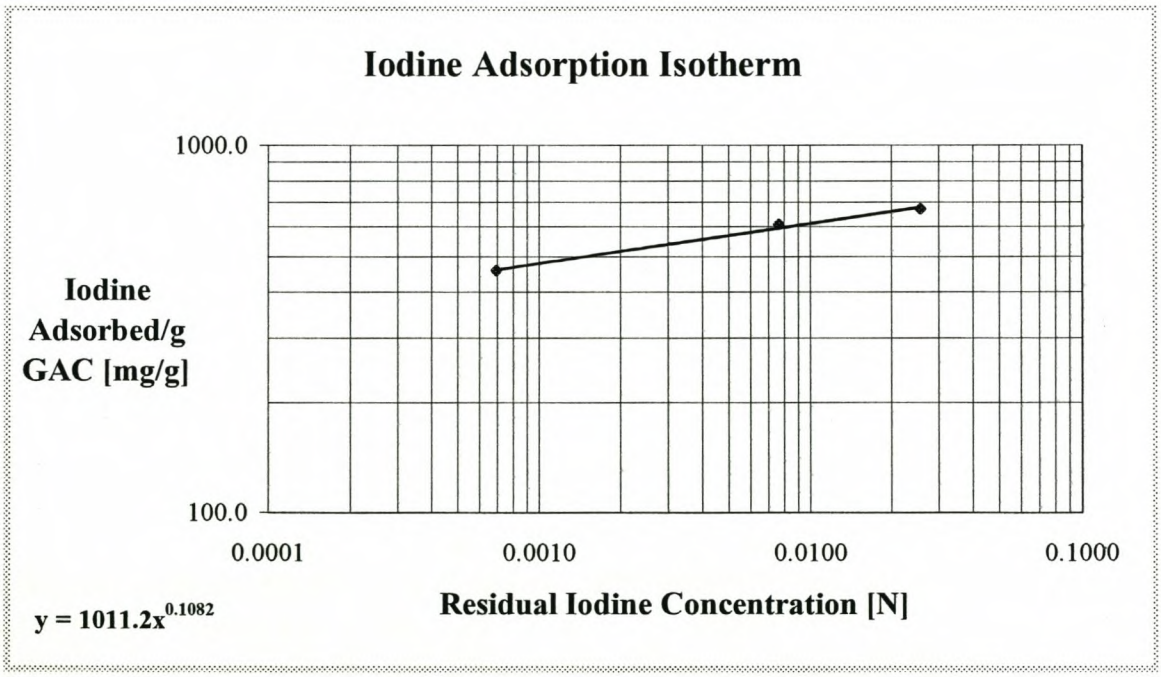

Iodine Number [mg/g] : 662.3

A3.3 Iodine Adsorption Isotherm: A700_0.0629_30

Mass GAC [mg]	Residual Iodine Concentration [N]	Iodine Adsorbed/g GAC [mg/g]
2.025	0.0124	532.7
1.669	0.0216	569.6
1.374	0.0317	588.4

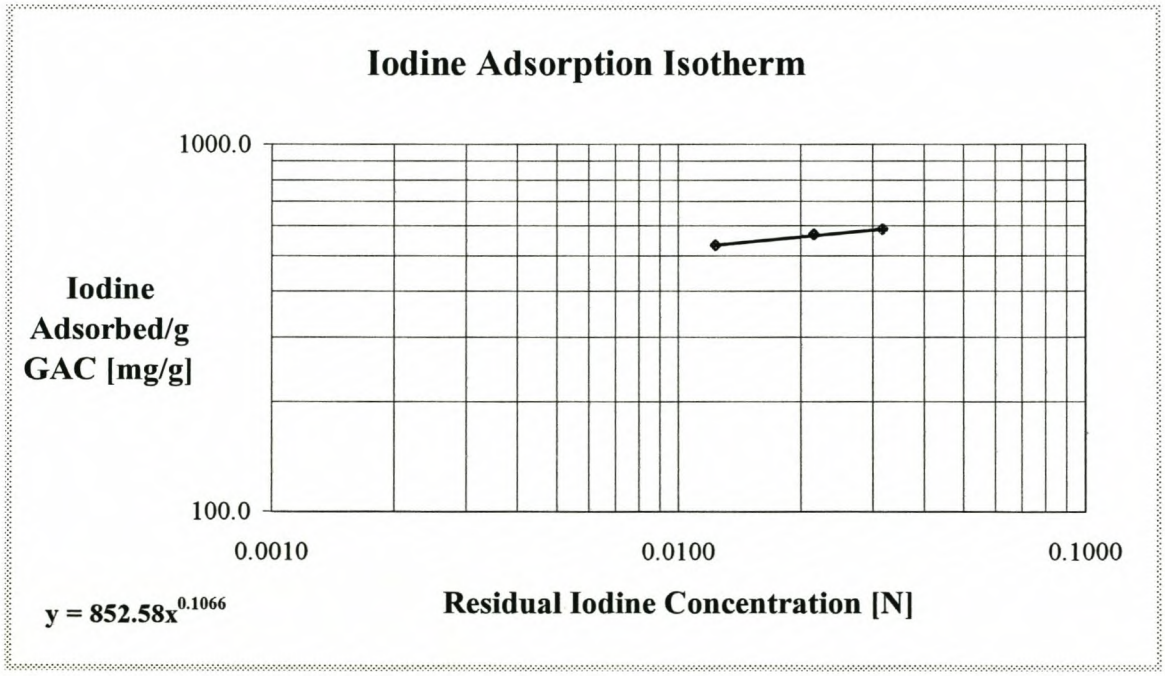

Iodine Number [mg/g] : 561.9

A3.4 Iodine Adsorption Isotherm: A700_0.0629_60

Mass GAC [mg]	Residual Iodine Concentration [N]	Iodine Adsorbed/g GAC [mg/g]
1.546	0.0108	713.6
1.272	0.0214	751.0
1.049	0.0319	770.9

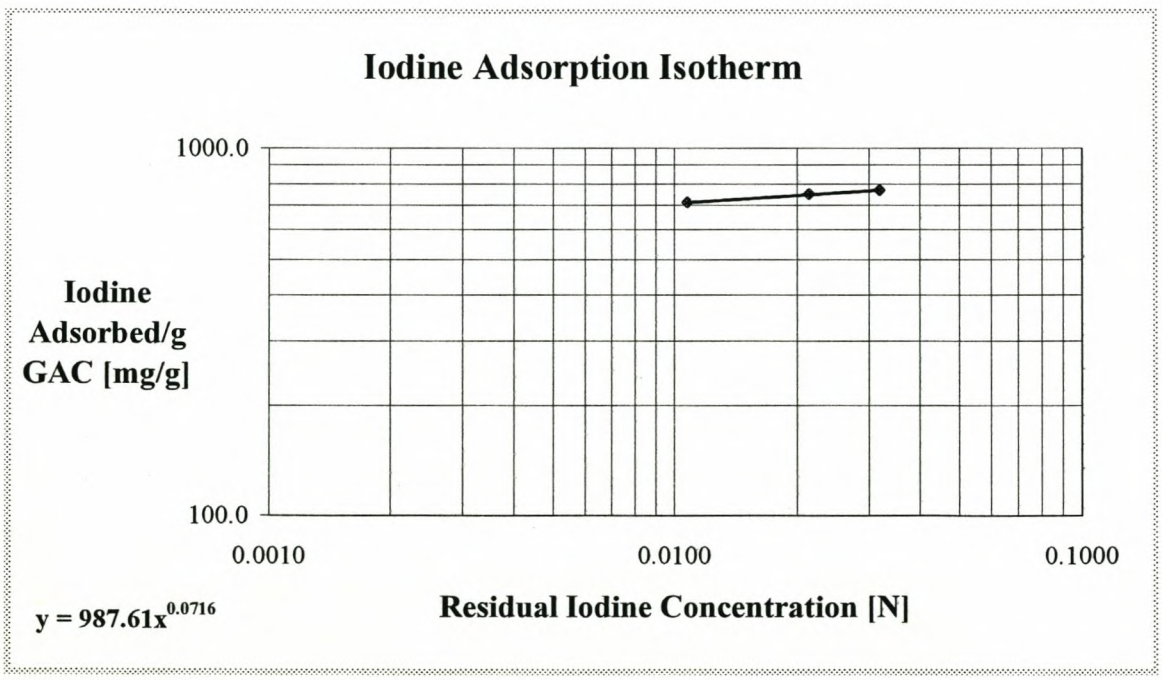

Iodine Number [mg/g] : 746.2

A3.5 Iodine Adsorption Isotherm: A700_0.10_60

Mass GAC [mg]	Residual Iodine Concentration [N]	Iodine Adsorbed/g GAC [mg/g]
1.891	0.0011	649.8
1.332	0.0099	829.8
1.080	0.0213	876.4

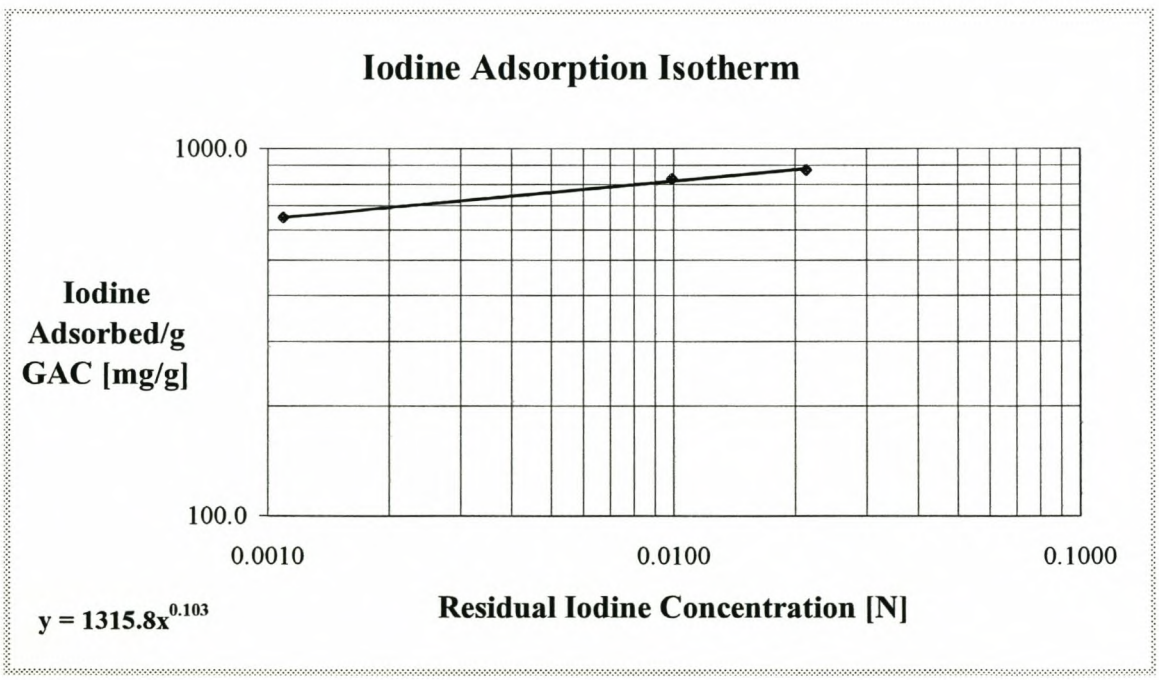

Iodine Number [mg/g] : 879.6

A3.6 Iodine Adsorption Isotherm: A800_0.0425_30

Mass GAC [mg]	Residual Iodine Concentration [N]	Iodine Adsorbed/g GAC [mg/g]
1.656	0.0112	661.5
1.364	0.0259	701.2
1.132	0.0316	715.4

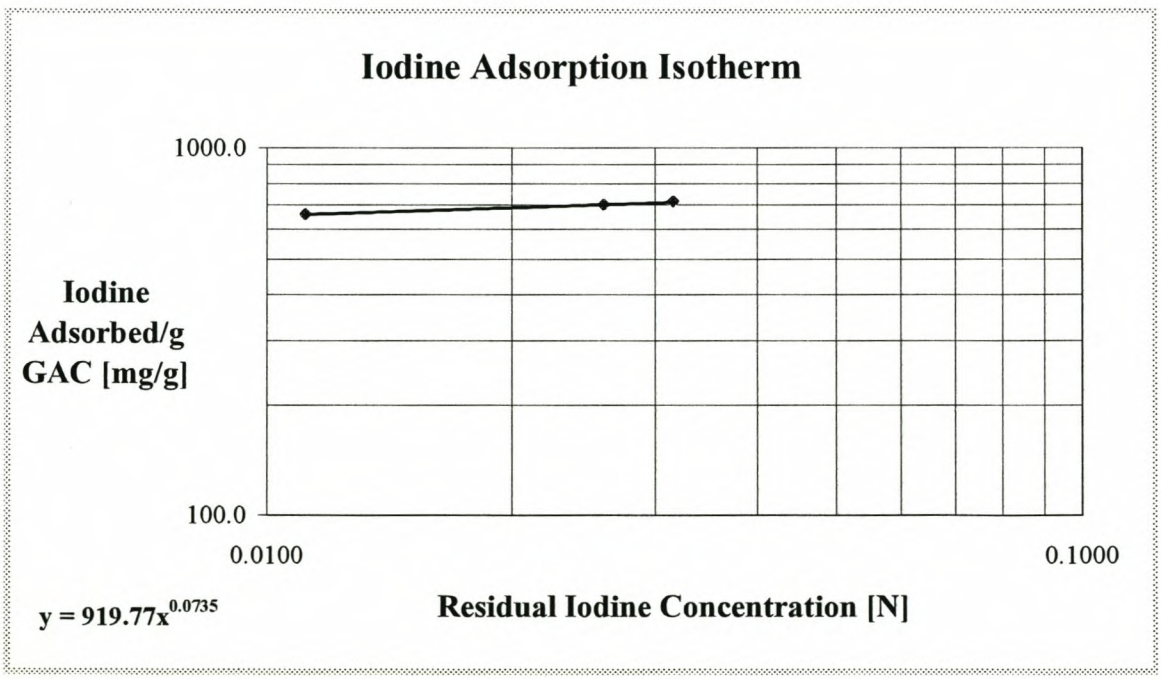

Iodine Number [mg/g] : 690.0

A3.7 Iodine Adsorption Isotherm: A800_0.0425_60

Mass GAC [mg]	Residual Iodine Concentration [N]	Iodine Adsorbed/g GAC [mg/g]
1.215	0.0144	870.9
0.993	0.0255	910.0
0.824	0.0348	938.4

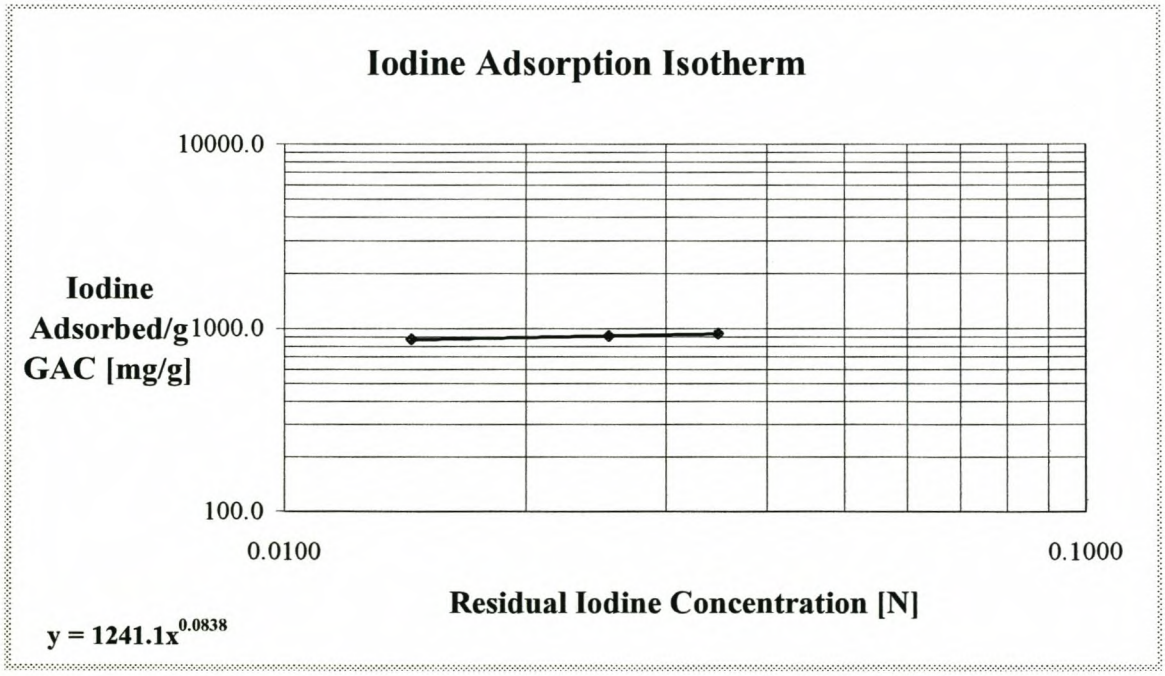

Iodine Number [mg/g] : 894.3

A3.8 Iodine Adsorption Isotherm: A800_0.0425_90

Mass GAC [mg]	Residual Iodine Concentration [N]	Iodine Adsorbed/g GAC [mg/g]
0.924	0.0108	1185.6
0.712	0.0235	1290.8
0.594	0.0324	1336.1

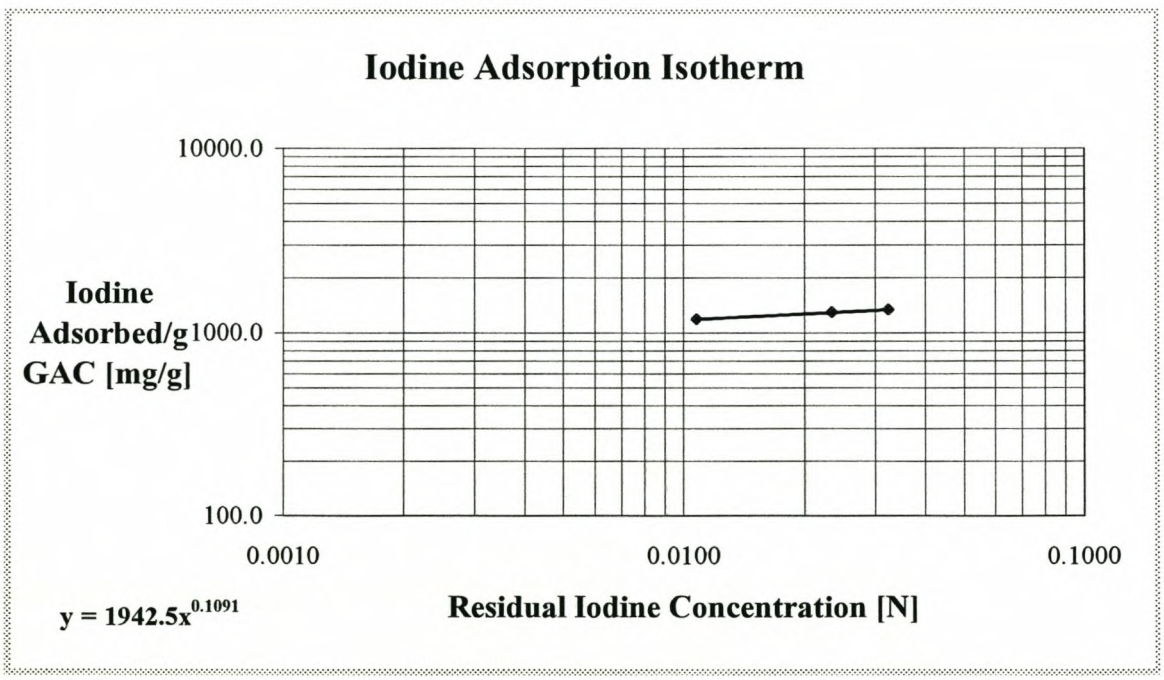

Iodine Number [mg/g] : 1267.9

A3.9 Iodine Adsorption Isotherm: A900_0.0425_30

Mass GAC [mg]	Residual Iodine Concentration [N]	Iodine Adsorbed/g GAC [mg/g]
1.254	0.0122	865.7
1.037	0.0221	914.3
0.850	0.0326	942.3

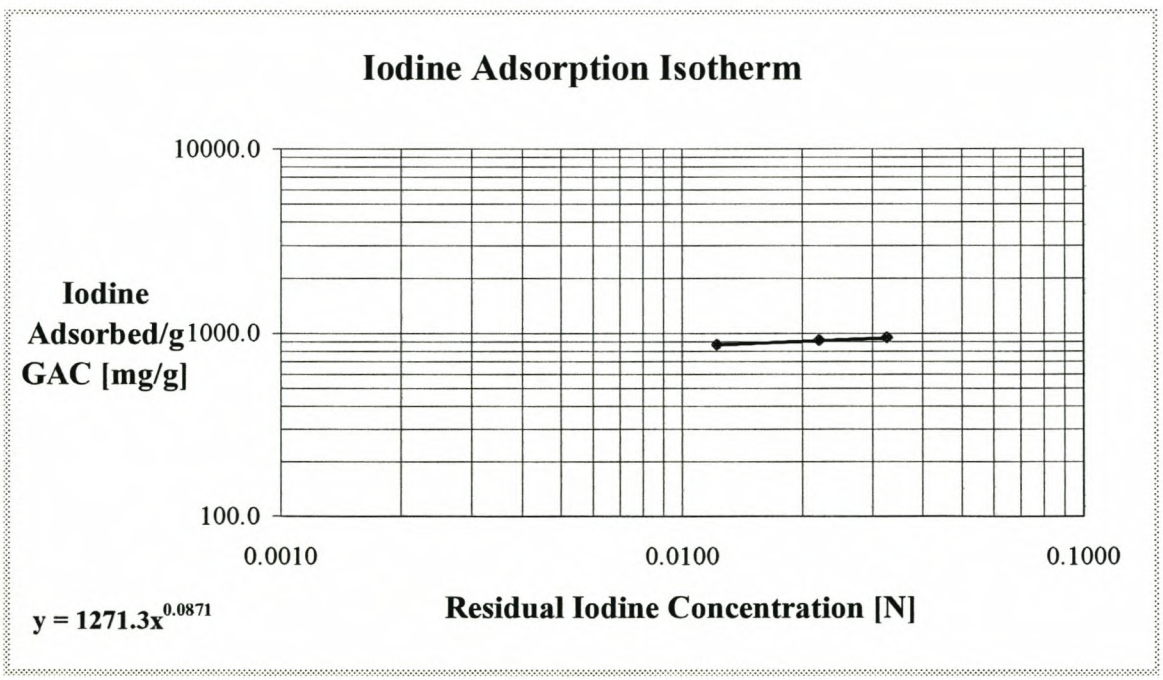

Iodine Number [mg/g] : 904.3

A3.10 Iodine Adsorption Isotherm: A900_0.0425_60

Mass GAC [mg]	Residual Iodine Concentration [N]	Iodine Adsorbed/g GAC [mg/g]
0.863	0.0126	1240.5
0.684	0.0243	1326.3
0.560	0.0341	1375.6

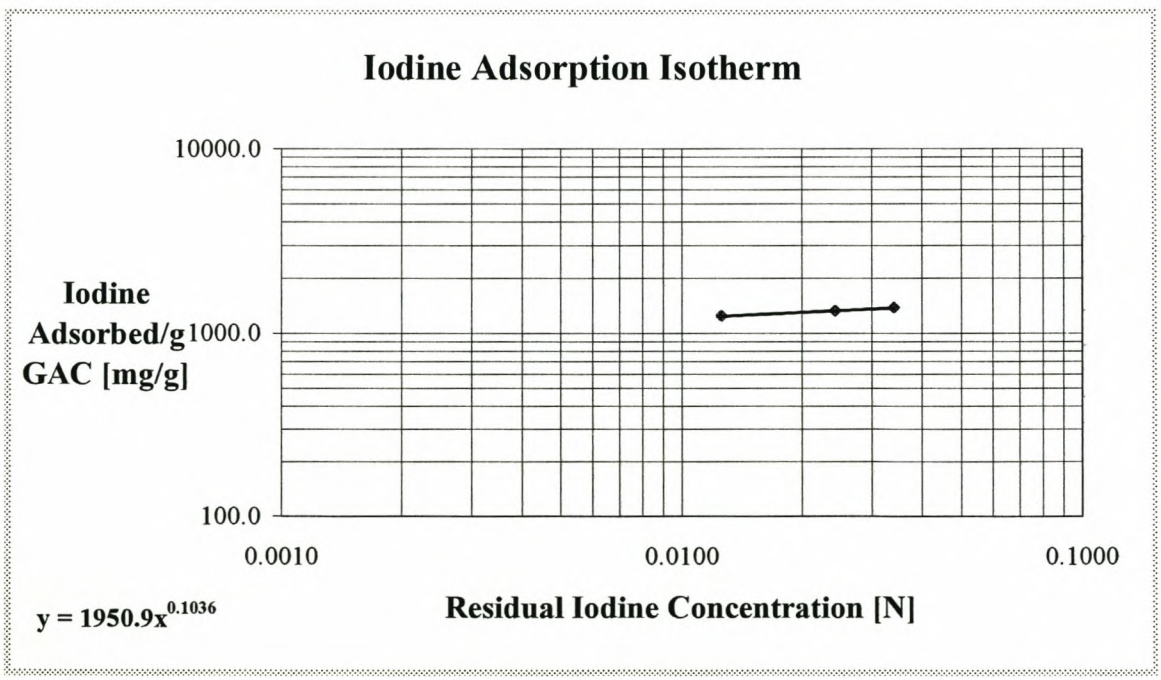

Iodine Number [mg/g] : 1300.9

A3.11 Iodine Adsorption Isotherm: A900_0.0629_30

Mass GAC [mg]	Residual Iodine Concentration [N]	Iodine Adsorbed/g GAC [mg/g]
1.257	0.0072	913.7
1.056	0.0151	983.1
0.871	0.0256	1023.6

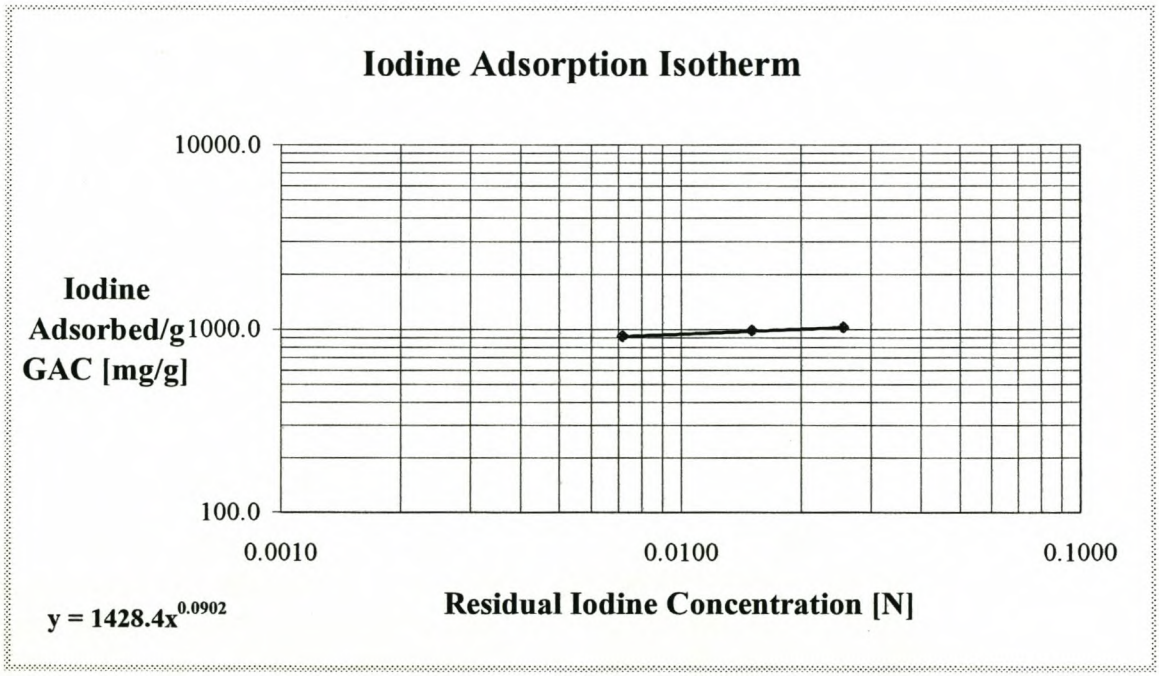

Iodine Number [mg/g] : 1003.7

A3.12 Iodine Adsorption Isotherm: A900_0.0629_60

Mass GAC [mg]	Residual Iodine Concentration [N]	Iodine Adsorbed/g GAC [mg/g]
0.763	0.0102	1440.8
0.602	0.0209	1578.4
0.478	0.0319	1664.3

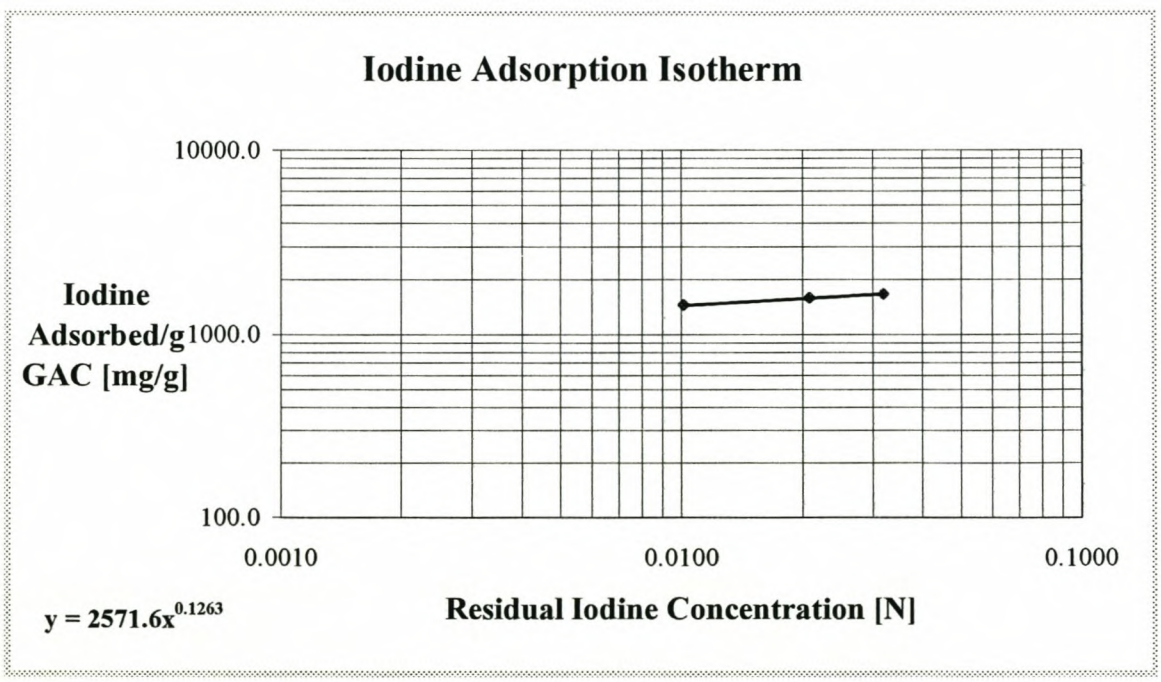

Iodine Number [mg/g] : 1569.3

A3.13 Iodine Adsorption Isotherm: A850_0.0533_60

Mass GAC [mg]	Residual Iodine Concentration [N]	Iodine Adsorbed/g GAC [mg/g]
1.065	0.0078	1077.7
0.889	0.0158	1165.4
0.712	0.0271	1233.5

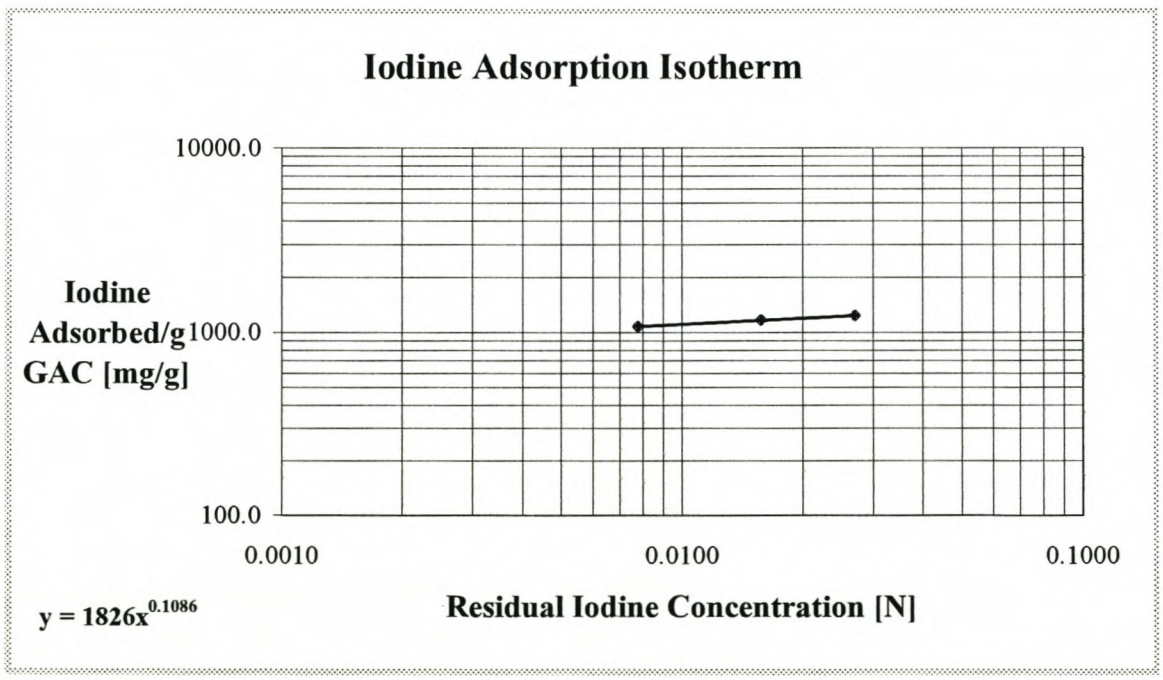

Iodine Number [mg/g] : 1194.2

A3.14 Iodine Adsorption Isotherm: P700_0.0425_30

Mass GAC [mg]	Residual Iodine Concentration [N]	Iodine Adsorbed/g GAC [mg/g]
2.706	0.0076	422.3
2.124	0.0172	475.0
1.720	0.0262	513.2

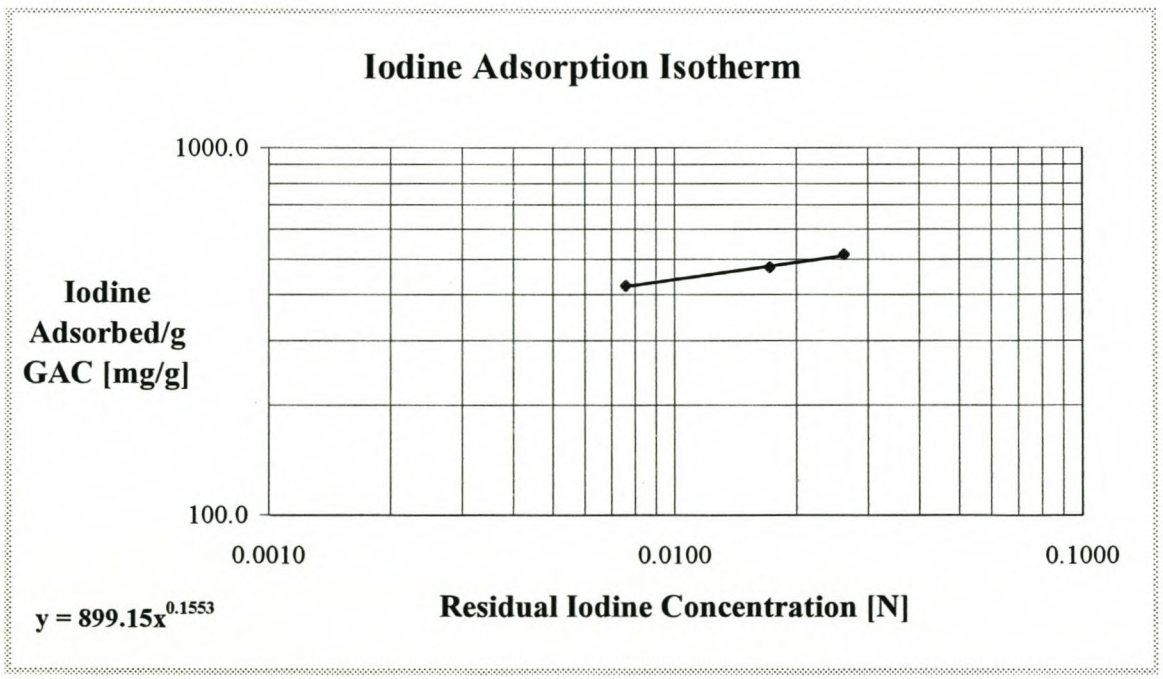

Iodine Number [mg/g] : 489.7

A3.15 Iodine Adsorption Isotherm: P700_0.0425_60

Mass GAC [mg]	Residual Iodine Concentration [N]	Iodine Adsorbed/g GAC [mg/g]
1.752	0.0132	603.6
1.410	0.0247	636.3
1.143	0.0352	655.8

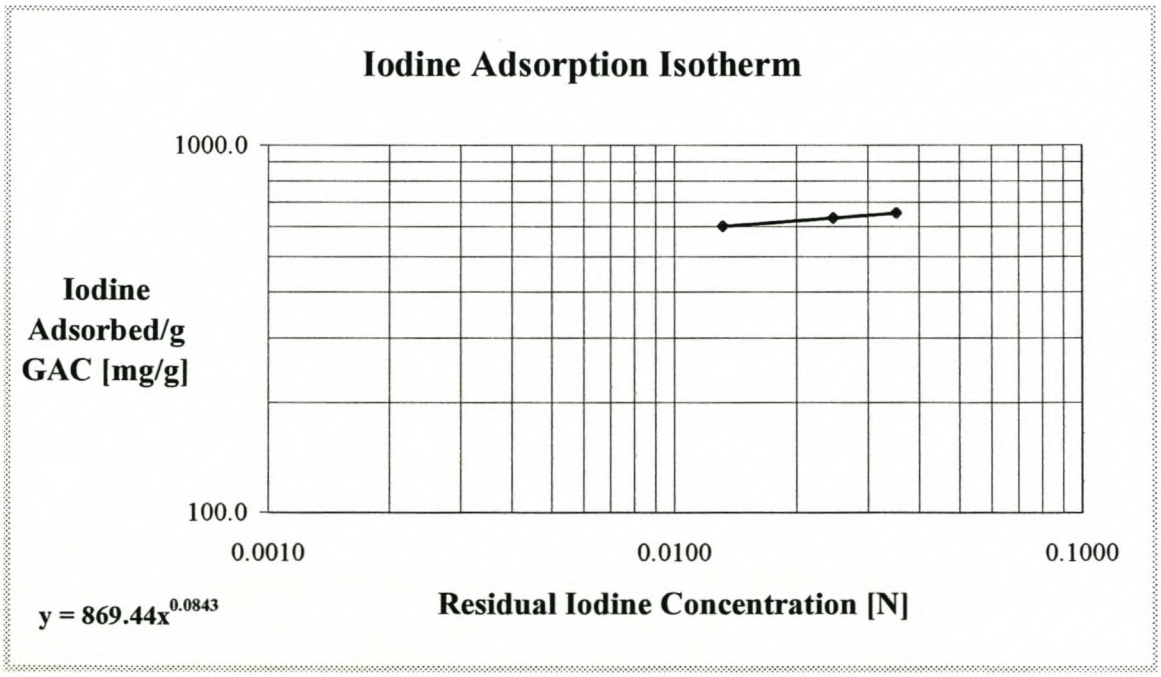

Iodine Number [mg/g] : 625.2

A3.16 Iodine Adsorption Isotherm: P700_0.0629_30

Mass GAC [mg]	Residual Iodine Concentration [N]	Iodine Adsorbed/g GAC [mg/g]
2.239	0.0080	504.7
1.771	0.0188	550.0
1.414	0.0309	572.5

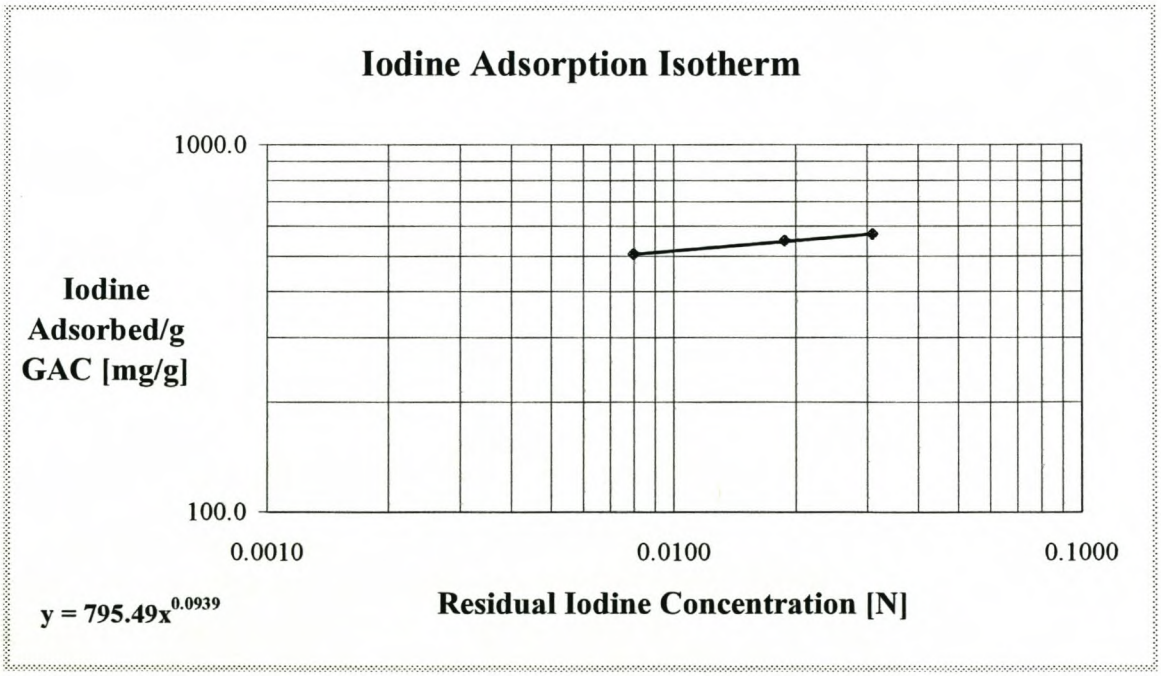

Iodine Number [mg/g] : 551.0

A3.17 Iodine Adsorption Isotherm: P700_0.0629_60

Mass GAC [mg]	Residual Iodine Concentration [N]	Iodine Adsorbed/g GAC [mg/g]
1.851	0.0045	643.6
1.517	0.0131	706.1
1.251	0.0240	734.6

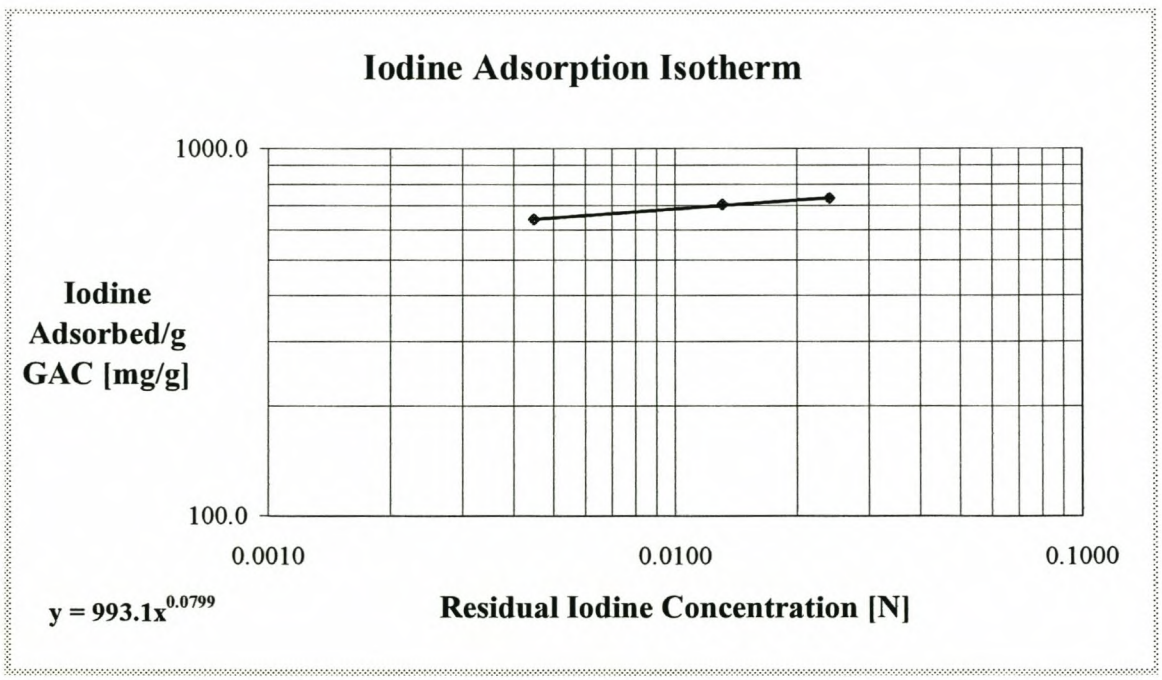

Iodine Number [mg/g] : 726.5

A3.18 Iodine Adsorption Isotherm: P800_0.0425_60

Mass GAC [mg]	Residual Iodine Concentration [N]	Iodine Adsorbed/g GAC [mg/g]
1.314	0.0116	827.3
1.093	0.0217	865.5
0.906	0.0320	885.4

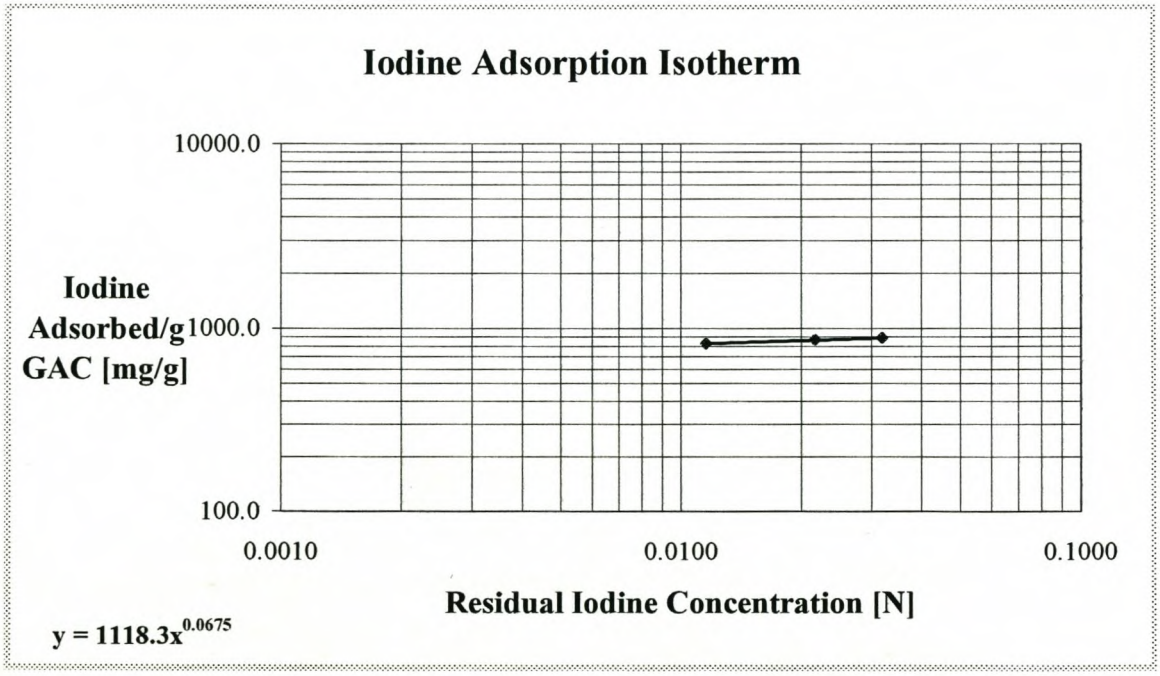

Iodine Number [mg/g] : 858.9

A3.19 Iodine Adsorption Isotherm: P900_0.0425_30

Mass GAC [mg]	Residual Iodine Concentration [N]	Iodine Adsorbed/g GAC [mg/g]
1.233	0.0142	856.7
1.022	0.0242	896.4
0.836	0.0343	926.5

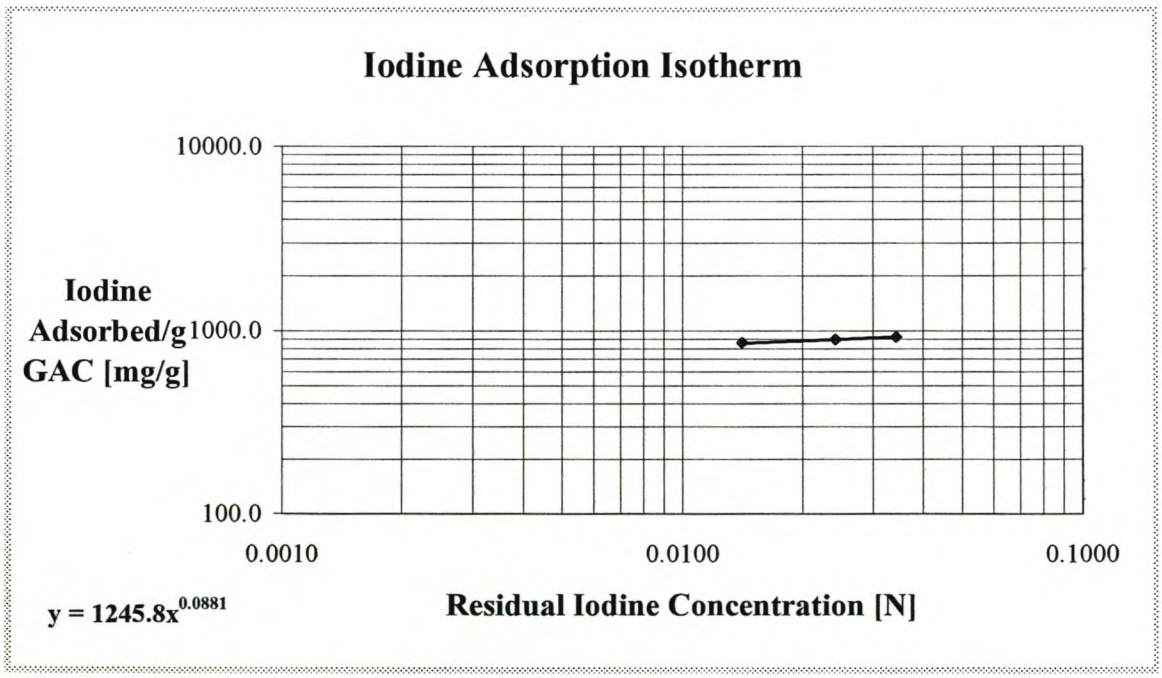

Iodine Number [mg/g] : 882.7

A3.20 Iodine Adsorption Isotherm: P900_0.0425_60

Mass GAC [mg]	Residual Iodine Concentration [N]	Iodine Adsorbed/g GAC [mg/g]
0.928	0.0163	1106.1
0.754	0.0326	1176.4
0.619	0.0368	1195.9

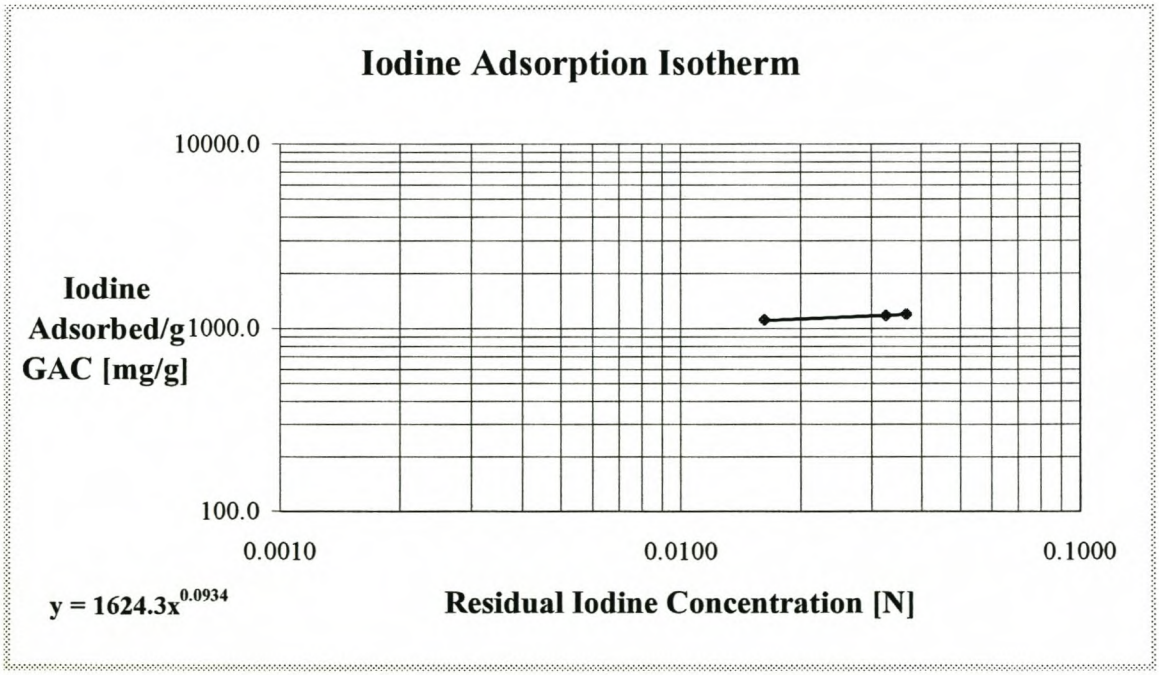

Iodine Number [mg/g] : 1127.0

A3.21 Iodine Adsorption Isotherm: P900_0.0629_30

Mass GAC [mg]	Residual Iodine Concentration [N]	Iodine Adsorbed/g GAC [mg/g]
1.251	0.0106	880.1
1.054	0.0193	929.3
0.868	0.0323	966.6

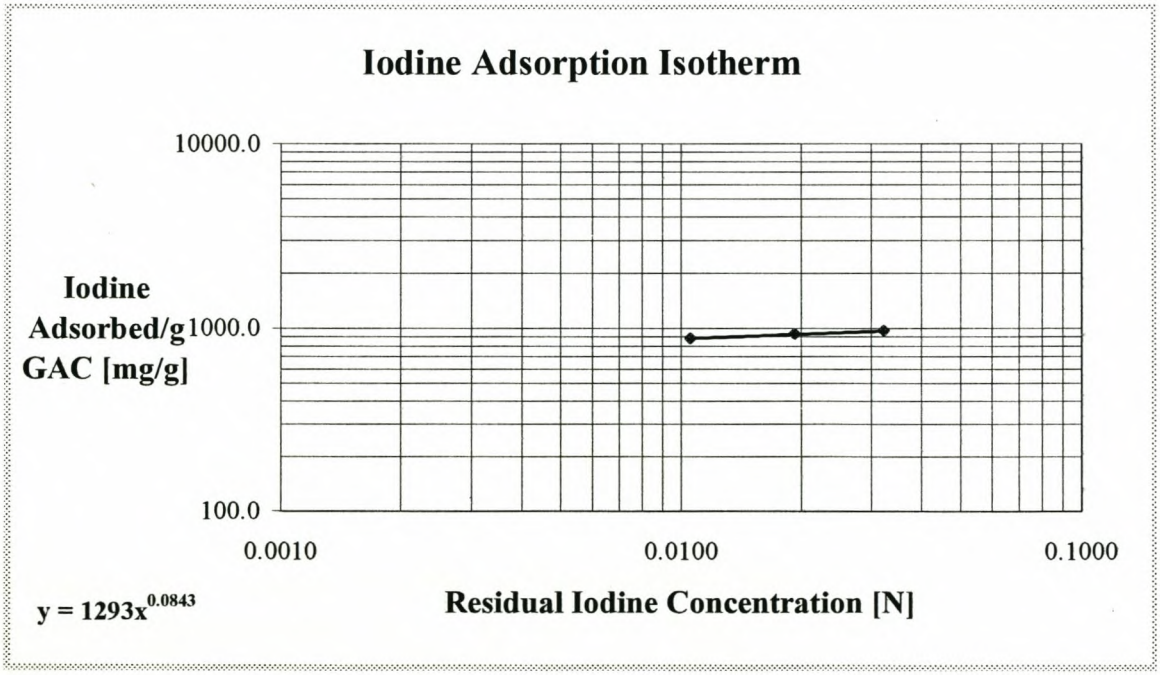

Iodine Number [mg/g] : 929.6

A3.22 Iodine Adsorption Isotherm: P900_0.0629_60

Mass GAC [mg]	Residual Iodine Concentration [N]	Iodine Adsorbed/g GAC [mg/g]
0.929	0.0050	1271.7
0.735	0.0126	1464.3
0.588	0.0230	1582.4

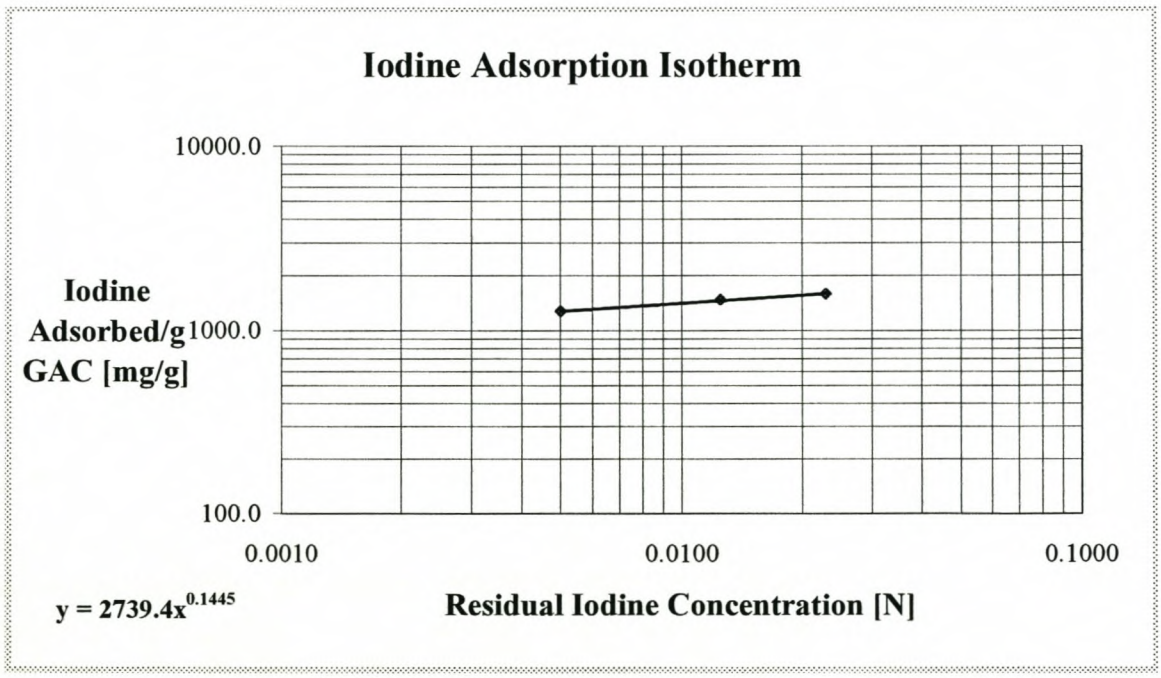

Iodine Number [mg/g] : 1556.6

A3.23 Iodine Adsorption Isotherm: P875_0.0533_60

Mass GAC [mg]	Residual Iodine Concentration [N]	Iodine Adsorbed/g GAC [mg/g]
1.018	0.0105	1087.9
0.824	0.0212	1162.7
0.685	0.0312	1194.8

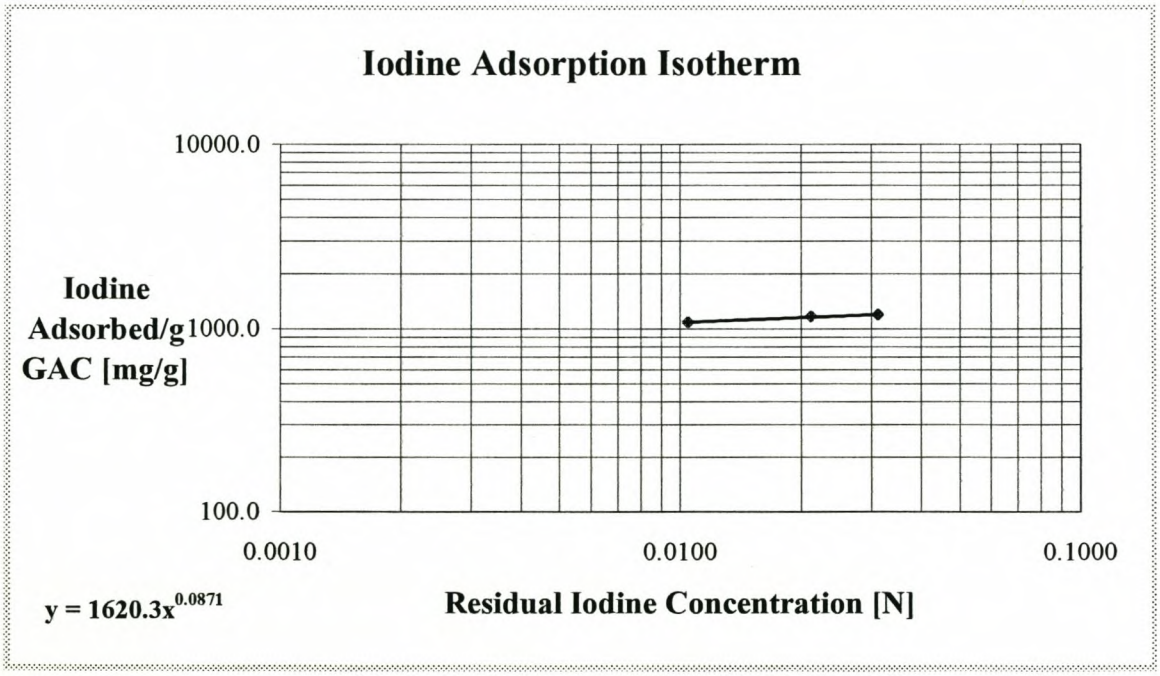

Iodine Number [mg/g] : 1152.3

A3.24 Iodine Adsorption Isotherm: GRC 22

Mass GAC [mg]	Residual Iodine Concentration [N]	Iodine Adsorbed/g GAC [mg/g]
1.128	0.0084	1002.8
0.871	0.0211	1096.3
0.643	0.0368	1144.0

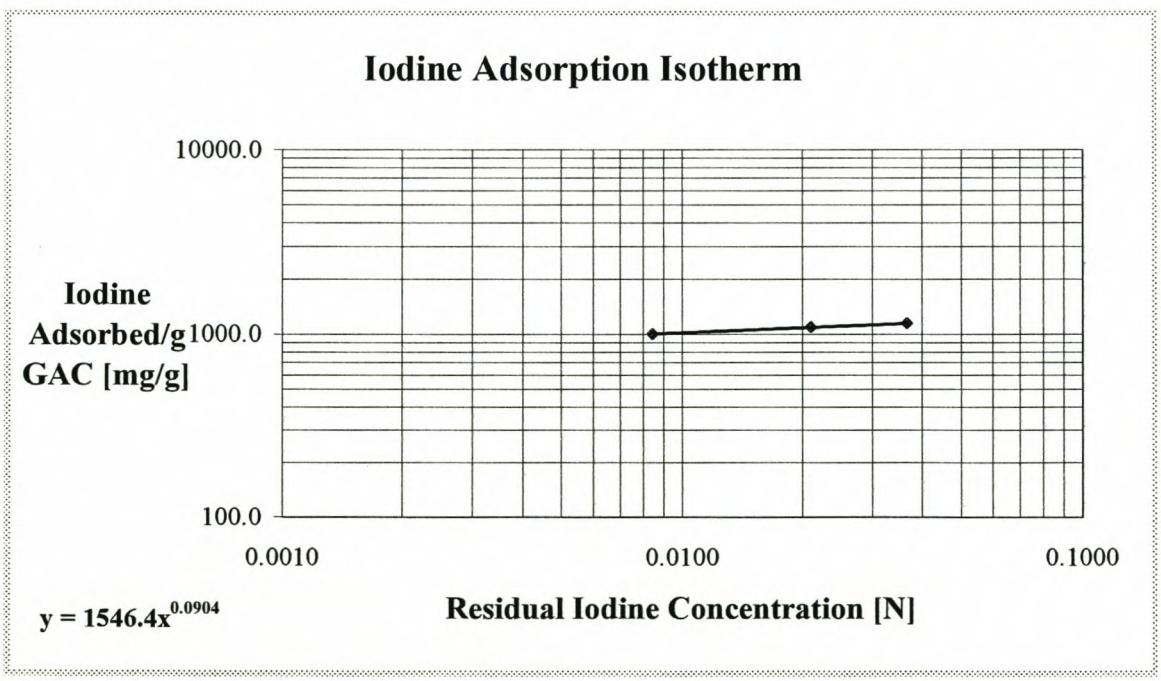

Iodine Number [mg/g] : 1085.9

A3.25 Iodine Adsorption Isotherm: Chemquest 650

Mass GAC [mg]	Residual Iodine Concentration [N]	Iodine Adsorbed/g GAC [mg/g]
1.139	0.0043	1044.3
0.885	0.0128	1209.1
0.673	0.0268	1299.2

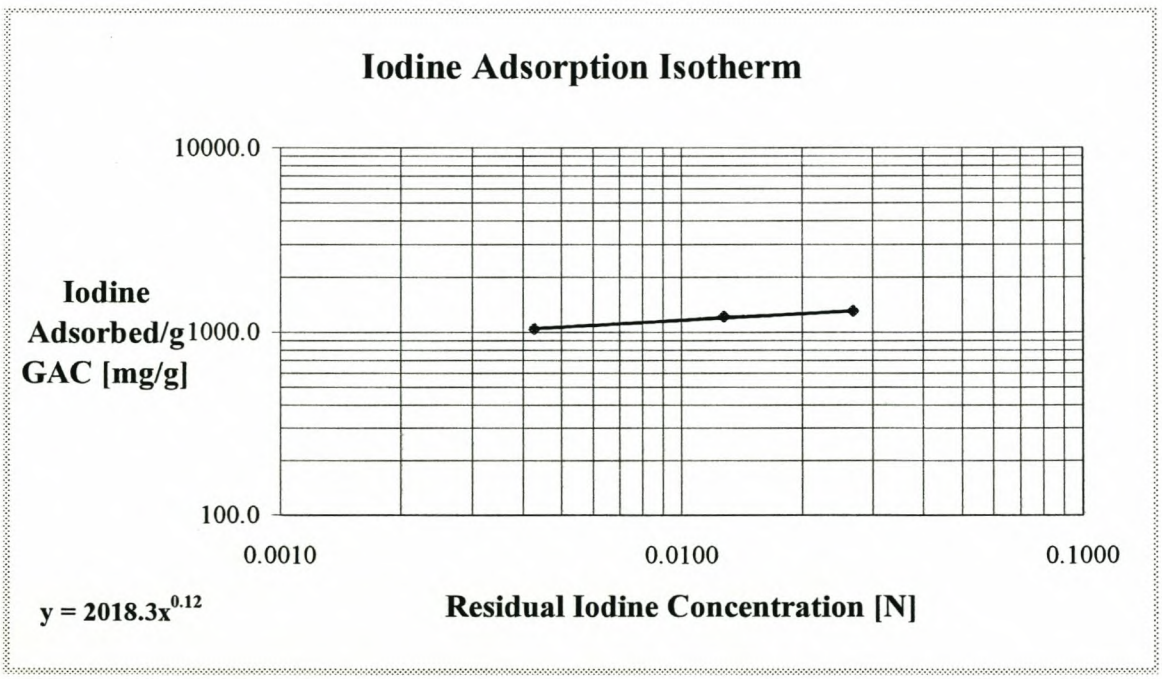

Iodine Number [mg/g] : 1262.1

A4: Standard Test Method for Determination of Iodine Number of Activated Carbon

The iodine numbers of the activated carbon samples were determined with the ASTM Standard Test Method D4607 – 94 (1994). A summary of the test method will follow:

Procedure for the determination of the iodine number:

1. Grind/ Pulverize activated carbon sample in a concentric circle crusher until 60 wt % or more will pass through a 44 μm sieve and 95wt % or more will pass through a 150 μm sieve.
2. Dry sample at 140°C for two hours and allow sample to cool in a dessicator to prevent any uptake of water from the atmosfere.
3. Estimate activated carbon dosages
4. Weigh appropriate amount of dry carbon and record weight
5. Transfer weight of carbon sample to a clean, dry 250mℓ- Erlenmeyer flask equipped with glass stopper.
6. Pipet 10.0 mℓ of 5 wt% hydrochloric acid solution into flask containing carbon.
7. Stopper flask and swirl gently until the carbon is completely wetted.
8. Boil for 30 ± 2 s to remove any sulfur which may interfere with test results.
9. Remove from hot plate and cool to room temperature.
10. Pipet 100.0 mℓ of 0.100 N iodine solution into flask. (standardize the iodine solution prior to use)
11. Immediately stopper solution and shake vigorously for 30 ± 1s.
12. Quickly filter mixture (Filter paper: Whatman 2V or equivalent)
13. Mix filtrate and pipet 50.0 mℓ into a clean 250- mℓ Erlenmeyer flask.
14. Titrate with standarized 0.1 N sodium thiosulfate solution until solution is pale yellow. Add 2 mℓ of starch indicator solution and continue titration until a colourless solution is reached.
15. Record the volume of the sodium thiosulfate used.

Steps 5-16 have to be repeated for three different weights of the pulverized activated carbon sample.

Calculations

Estimation of activated carbon dosage

The capacity of activated carbon for iodine is dependent on the concentration of the iodine solution. In order to estimate appropriate carbon weights to produce final iodine concentrations agreeing with the iodine number the concentration of the standard iodine solution and filtrates must be specified or be known.

To estimate the carbon dosages the following constants need to be derived first:

$$A = (N_2)(12693.0) \qquad \text{(A4.1)}$$

N_2 = iodine concentration, (N)

$$B = (N_1)(126.93) \qquad \text{(A4.2)}$$

N_1 = sodium thiosulfate concentration, (N)

$$DF = (I + H)/F \qquad \text{(A4.3)}$$

DF = dilution factor

I = iodine (mℓ)

H = 5 % hydrochloric acid used, (mℓ), and

F = filtrate, (mℓ)

For example:

If 10 mℓ of HCl and 50 mℓ of filtrate are used: DF = (100 + 10)/50 = 2.2

The carbon dosage can be estimated as follows:

$$M = [A - (DF)(C)(126.93)(50)]/E \qquad \text{(A4.4)}$$

E = Estimated iodine number of the carbon

C = 0.01, 0.02 or 0.03

Determination of the Iodine Number

Iodine Adsorbed per Gram of Carbon:

$$X/M = [\ A - (DF)(B)(S)]/M \qquad (A4.5)$$

S = sodium tiosulfate (mℓ) and

M = carbon used (g)

Residual Iodine Concentration:

$$C = (N_1.S)/F \qquad (A4.6)$$

F = filtrate, (mℓ)(50.0)

Plot X/M (as the ordinate) versus C (as the abscissa) for each of the three carbon dosages. Calculate least square fit for the three points and plot. The iodine number is the X/M value at a residual concentration (C) of 0.02N.

This was done on Microsoft Excel by plotting X/M vs. C with a logarithmic scale and adding a power trend line. The equation of the trend line was used to determine the iodine number. The regression coefficient for the least square fit (trend line) was also displayed.

A5: Model for Optimum Activation Conditions

The equations for the determination of the optimal activation conditions are summarized in tables A5.1 to A5.6. Because the peristaltic pump could only deliver water at certain constant flowrates, the equations were determined at flow rates of 0.0425, 0.0533 and 0.0629 [g/g.min].

General Equation

$$X = a + bT + cT_i + d \cdot S \cdot T + e \cdot T \cdot T_i + f \cdot S \cdot T_i + g \cdot S \cdot T \cdot T_i + h \qquad \text{(A5.1)}$$

X : Iodine Number [mg/g] or Yield [%] or Mesoporous Area [m^2/g]

T : Temperature [°C]

T_i : Time [min]

S : Steam Flowrate [g/g.min]

a, b, c, d, e, f, g, h : Coefficients

Apricot Shell GAC

Table A5.1 Model coefficients for apricot shell activated carbon produced at a steam flowrate of 0.0425 [g/g.min]

Coefficient	X		
	Iodine Number [mg/g]	**Mesoporous Area [m^2/g]**	**Yield [%]**
a	-1358.0875	-692.0468917	28.12791667
b	2.234208333	1.111738083	-0.0123875
c	15.93013889	29.05624347	-0.068680556
d	-30.71078431	-35.6129902	0.227941176
e	-0.016051389	-0.043526335	9.93056E-05
f	-862.8267974	-1297.704984	11.6748366
g	1.265522876	1.924265523	-0.018218954
h	1029.6875	1011.65229	-5.6979167

Table A5.2 Model coefficients for apricot shell activated carbon produced at a steam flowrate of 0.0533 [g/g.min]

Coefficient	*X*		
	Iodine Number [mg/g]	**Mesoporous Area [m^2/g]**	**Yield [%]**
a	-1358.0875	-692.0468917	28.12791667
b	2.234208333	1.111738083	-0.0123875
c	15.93013889	29.05624347	-0.068680556
d	-30.71078431	-35.6129902	0.227941176
e	-0.016051389	-0.043526335	9.93056E-05
f	-862.8267974	-1297.704984	11.6748366
g	1.265522876	1.924265523	-0.018218954
h	1291.34926	1268.73099	-7.1458578

Table A5.3 Model coefficients for apricot shell activated carbon produced at a steam flowrate of 0.0629 [g/g.min]

Coefficient	*X*		
	Iodine Number [mg/g]	**Mesoporous Area [m^2/g]**	**Yield [%]**
a	-1358.0875	-692.0468917	28.12791667
b	2.234208333	1.111738083	-0.0123875
c	15.93013889	29.05624347	-0.068680556
d	-30.71078431	-35.6129902	0.227941176
e	-0.016051389	-0.043526335	9.93056E-05
f	-862.8267974	-1297.704984	11.6748366
g	1.265522876	1.924265523	-0.018218954
h	1523.9375	1497.24539	-8.4329167

Table A5.4 Model coefficients for peach shell activated carbon produced at a steam flowrate of 0.0425 [g/g.min]

Coefficient	*X*		
	Iodine Number [mg/g]	**Mesoporous Area [m^2/g]**	**Yield [%]**
a	-3288.729167	-2189.1824	64.93083333
b	5.140791667	3.226508667	-0.064166667
c	72.34069444	64.99200111	-1.024013889
d	-87.5245098	-76.1477451	1.333333333
e	-0.100859722	-0.093867194	0.001497639
f	-1894.526144	-1831.104575	30.79248366
g	2.799836601	2.656251634	-0.045669935
h	2648.22917	2234.54375	-38.520833

Table A5.5 Model coefficients for peach shell activated carbon produced at a steam flowrate of 0.0533 [g/g.min]

Coefficient	*X*		
	Iodine Number [mg/g]	**Mesoporous Area [m^2/g]**	**Yield [%]**
a	-3288.729167	-2189.1824	64.93083333
b	5.140791667	3.226508667	-0.064166667
c	72.34069444	64.99200111	-1.024013889
d	-87.5245098	-76.1477451	1.333333333
e	-0.100859722	-0.093867194	0.001497639
f	-1894.526144	-1831.104575	30.79248366
g	2.799836601	2.656251634	-0.045669935
h	3321.19093	2802.38075	-48.309657

Table A5.6 Model coefficients for peach shell activated carbon produced at a steam flowrate of 0.0629 [g/g.min]

Coefficient	*X*		
	Iodine Number [mg/g]	**Mesoporous Area [m^2/g]**	**Yield [%]**
a	-3288.729167	-2189.1824	64.93083333
b	5.140791667	3.226508667	-0.064166667
c	72.34069444	64.99200111	-1.024013889
d	-87.5245098	-76.1477451	1.333333333
e	-0.100859722	-0.093867194	0.001497639
f	-1894.526144	-1831.104575	30.79248366
g	2.799836601	2.656251634	-0.045669935
h	3919.37917	3307.12475	-57.010833

Appendix B: Gold Adsorption

B1: Preparation of Gold Solutions

10 ppm Gold (Au^+) and 100 ppm Cyanide (CN^-) Solution

Transfer 0.01470g of $KAu(CN)_2$ (68% Au^+) and 0.18104g of NaCN (95%) into a 1ℓ volumetric flask. Fill with distilled water and adjust pH with 0.1 KOH solution. For the gold adsorption tests the pH was adjusted to 10.5 – 11.

10 ppm Gold (Au^+) and 100 ppm Cyanide (CN^-) Solution

Transfer 0.1470g of $KAu(CN)_2$ (68% Au^+) and 0.12124g of NaCN (95%) into a 1ℓ volumetric flask. Fill with distilled water and adjust pPH with 0.1 KOH solution. For the gold adsorption tests the pH was adjusted to 10.5 – 11.

B2: Batch Kinetic Gold Adsorption

B2.1 Batch Kinetic Gold Adsorption P900_0.0425_60

0.25g Activated Carbon per 1000mℓ GoldCyanide Solution

Particle Size 1400-1700 micrometer

pH 10.5 - 11

Time [min]	Ci [ppm]	Ci/Co
0	9.79	1.000
5	9.35	0.955
10	9.18	0.938
15	9.06	0.925
30	8.80	0.899
45	8.58	0.876
60	8.44	0.862
90	7.97	0.814
120	7.49	0.765
186	6.72	0.686
246	6.19	0.632
366	5.29	0.540
532	4.36	0.445
853	3.32	0.339
1014	2.97	0.303
1219	2.63	0.269
1514	2.49	0.254
1797	2.30	0.235
2611	1.98	0.202
2760	1.92	0.196
3430	1.81	0.185
4063	1.76	0.180
4546	1.77	0.181
5324	1.76	0.180

B2.2 Batch Kinetic Gold Adsorption A900_0.0425_60

0.25g Activated Carbon per 1000mℓ GoldCyanide Solution

Particle Size 1400-1700 micrometer

pH 10.5 - 11

Time [min]	Ci [ppm]	Ci/Co
0	9.54	1.000
5	9.41	0.986
10	9.28	0.973
15	9.17	0.961
30	8.82	0.925
45	8.61	0.903
60	8.27	0.867
90	7.77	0.814
120	7.26	0.761
186	6.36	0.667
246	5.76	0.604
366	4.80	0.503
532	3.97	0.416
853	2.96	0.310
1014	2.69	0.282
1219	2.40	0.252
1386	2.32	0.243
1514	2.23	0.234
1797	2.14	0.224
2611	1.96	0.205
2760	1.93	0.202
3430	1.92	0.201
4063	1.85	0.194
4546	1.75	0.183
5324	1.81	0.190

B2.3 Batch Kinetic Gold Adsorption A850_0.0533_60

0.25g Activated Carbon per 1000mℓ GoldCyanide Solution

Particle Size 1400-1700 micrometer

pH 10.5 - 11

Time [min]	Ci [ppm]	Ci/Co
0	9.82	1.000
5	9.68	0.986
10	9.58	0.976
15	9.33	0.950
30	9.29	0.946
45	8.86	0.902
60	8.59	0.875
90	8.37	0.852
120	7.84	0.798
182	7.18	0.731
302	6.57	0.669
355	6.01	0.612
480	5.06	0.515
600	4.43	0.451
818	3.64	0.371
1047	3.09	0.315
1285	2.67	0.272
1523	2.43	0.247
1668	2.28	0.232
2220	2.04	0.208
2677	1.83	0.186
2921	1.88	0.191
3279	1.83	0.186
4062	1.75	0.178
4548	1.72	0.175
5489	1.72	0.175

B2.4 Batch Kinetic Gold Adsorption P875_0.0533_60

0.25g Activated Carbon per 1000mℓ GoldCyanide Solution

Particle Size 1400-1700 micrometer

pH 10.5 - 11

Time [min]	Ci [ppm]	Ci/Co
0	9.68	1.000
5	9.34	0.965
10	9.16	0.946
15	9.07	0.937
30	8.87	0.916
45	8.67	0.896
60	8.26	0.853
90	7.92	0.818
120	7.60	0.785
182	6.71	0.693
302	6.05	0.625
355	5.51	0.569
480	4.61	0.476
600	4.03	0.416
818	3.24	0.335
1047	2.71	0.280
1285	2.39	0.247
1523	2.17	0.224
1668	2.1	0.217
2220	1.85	0.191
2677	1.79	0.185
2921	1.78	0.184
3279	1.76	0.182
4062	1.73	0.179
4548	1.74	0.180
5489	1.72	0.178

B2.5 Batch Kinetic Gold Adsorption GRC 22

0.25g Activated Carbon per 1000mℓ GoldCyanide Solution

Particle Size 1400-1700 micrometer

pH 10.5 - 11

Time [min]	Ci [ppm]	Ci/Co
0	10.03	1.000
5	9.72	0.969
10	9.62	0.959
15	9.53	0.950
30	9.36	0.933
45	9.01	0.898
60	8.98	0.895
90	8.45	0.842
120	8.22	0.820
180	7.66	0.764
242	7.15	0.713
300	6.61	0.659
382	6.21	0.619
540	5.35	0.533
719	4.81	0.480
945	4.26	0.425
1125	3.92	0.391
1507	3.35	0.334
1895	2.98	0.297
2384	2.81	0.280
3104	2.52	0.251
4119	2.31	0.230

B2.6 Batch Kinetic Gold Adsorption Chemquest 650

0.25g Activated Carbon per 1000mℓ GoldCyanide Solution

Particle Size 1400-1700 micrometer

pH 10.5 - 11

Time [min]	Ci [ppm]	Ci/Co
0	9.76	1.000
5	9.62	0.986
10	9.43	0.966
15	9.21	0.944
30	9.14	0.936
45	8.93	0.915
60	8.89	0.911
90	8.42	0.863
120	8.09	0.829
180	7.51	0.769
242	6.87	0.704
300	6.45	0.661
382	6.10	0.625
540	5.36	0.549
719	4.86	0.498
945	4.31	0.442
1125	4.14	0.424
1507	3.85	0.394
1895	3.70	0.379
2384	3.45	0.353
3104	3.27	0.335
4119	3.18	0.326

B3: Equilibrium Gold Adsorption

B3.1 Equilibrium Gold Adsorption P900_0.0425_60

Particle Size 1400-1700 micrometer

pH 10.5 - 11

Mass of Carbon [g]	Residual Au Conc. [mg/ℓ]	Residual Gold [mg]	Gold Adsorbed /g GAC
0.0000	97.9	48.95	
0.2596	68.1	34.05	57.4
0.5679	36.7	18.35	53.9
1.0030	13.5	6.75	42.1
1.4779	4.1	2.05	31.7

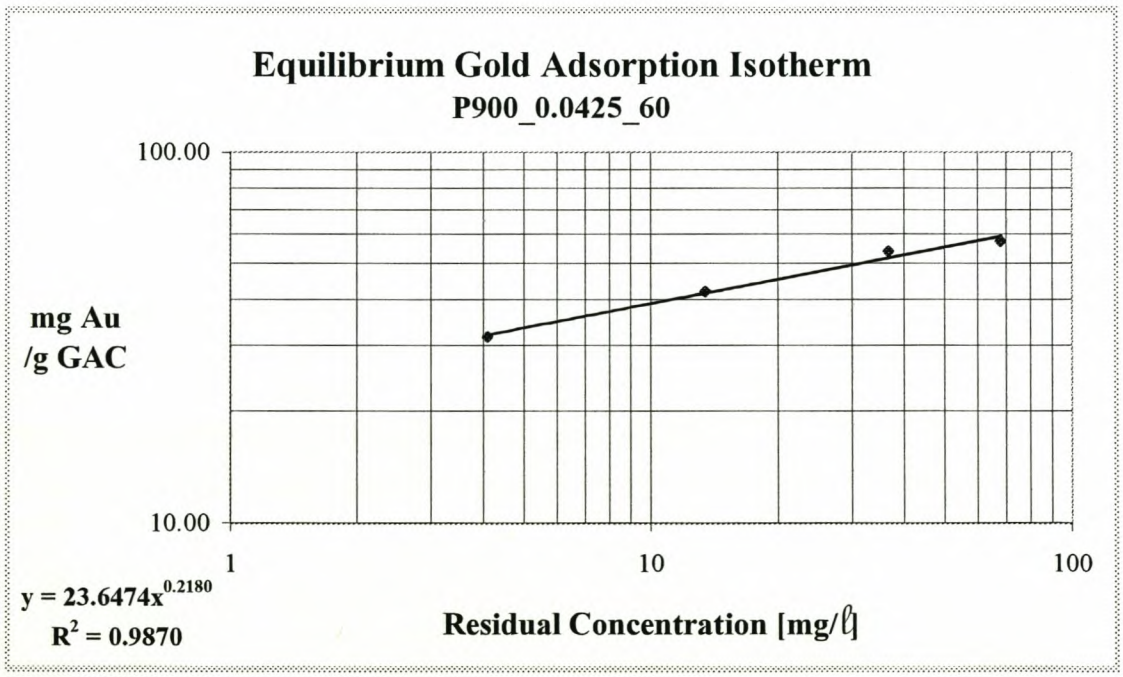

B3.2 Equilibrium Gold Adsorption A900_0.0425_60

Particle Size 1400-1700 micrometer

pH 10.5 - 11

Mass of Carbon [g]	Residual Au Conc. [mg/ℓ]	Residual Gold [mg]	Gold Adsorbed /g GAC
0.0000	98.2	49.1	
0.2599	69.5	34.75	55.2
0.5714	39.1	19.55	51.7
1.0008	14.6	7.3	41.8
1.4767	5.3	2.65	31.5

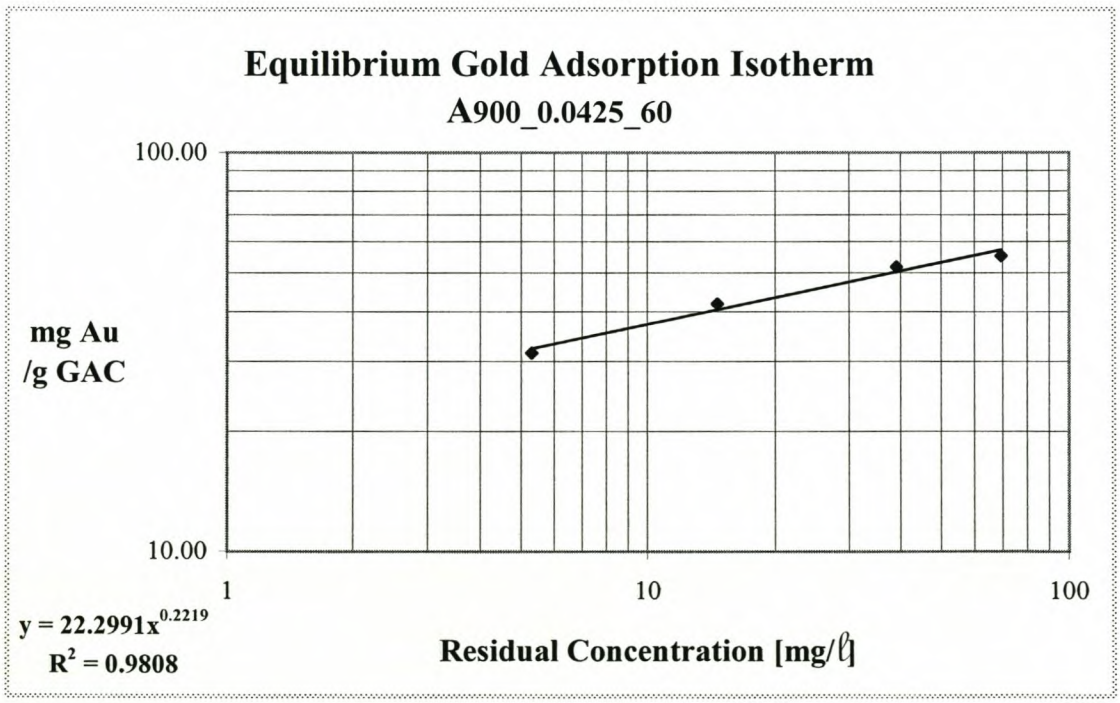

B3.3 Equilibrium Gold Adsorption A850_0.0533_60

Particle Size 1400-1700 micrometer

pH 10.5 - 11

Mass of Carbon [g]	Residual Au Conc. [mg/ℓ]	Residual Gold [mg]	Gold Adsorbed /g GAC
0.0000	98.6	49.3	
0.2593	68.2	34.1	58.6
0.5668	36.2	18.1	55.0
1.0028	13.6	6.8	42.4
1.4733	4.1	2.05	32.1

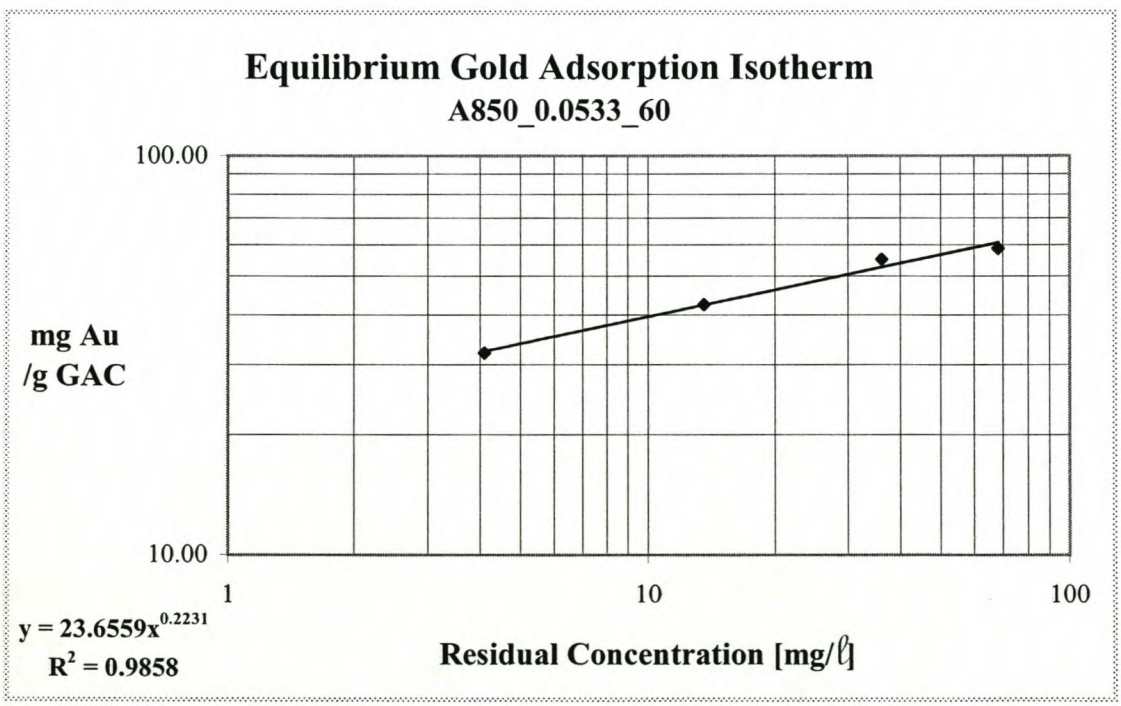

B3.4 Equilibrium Gold Adsorption P875_0.0533_60

Particle Size 1400-1700 micrometer

pH 10.5 - 11

Mass of Carbon [g]	Residual Au Conc. [mg/ℓ]	Residual Gold [mg]	Gold Adsorbed /g GAC
0.0000	98.5	49.25	
0.2593	68.1	34.05	58.6
0.5683	36.8	18.4	54.3
1.0010	14.1	7.05	42.2
1.4751	4.1	2.05	32.0

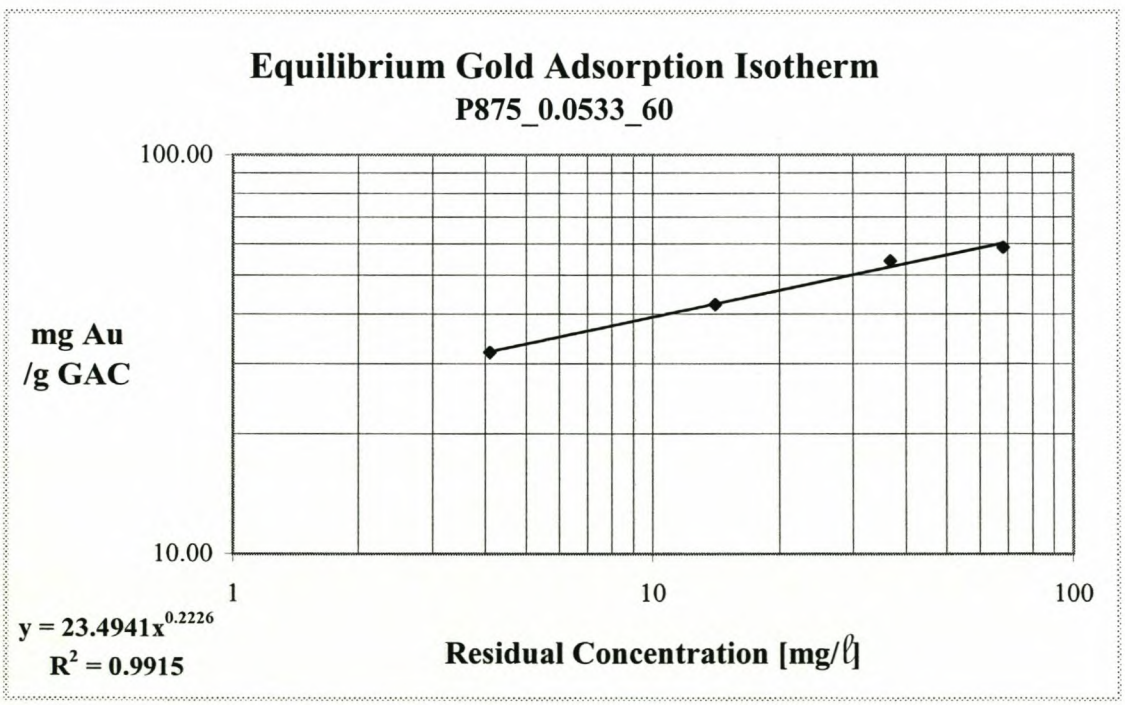

B3.5 Equilibrium Gold Adsorption GRC22

Particle Size 1400-1700 micrometer

pH 10.5 - 11

Mass of Carbon [g]	Residual Au Conc. [mg/ℓ]	Residual Gold [mg]	Gold Adsorbed /g GAC
0.0000	97.3	48.65	
0.2606	67.3	33.65	57.5
0.5662	39.3	19.65	51.2
1.0015	14.2	7.1	41.5
1.4798	4	2	31.5

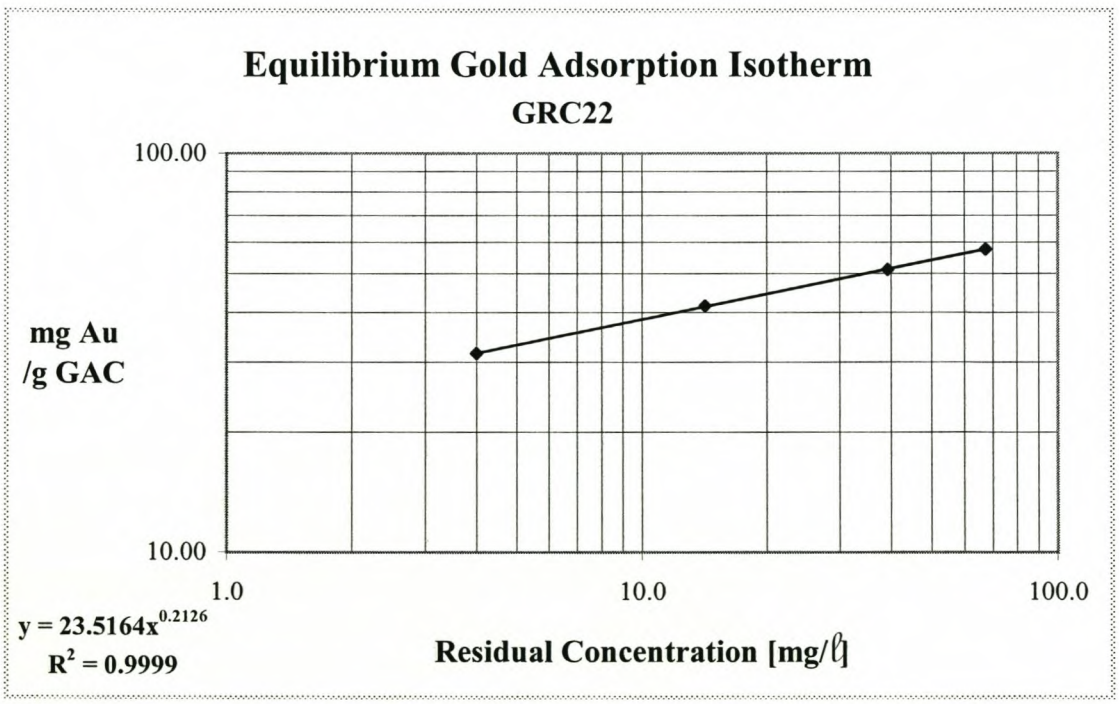

B3.6 Equilibrium Gold Adsorption Chemquest 650

Particle Size 1400-1700 micrometer

pH 10.5 - 11

Mass of Carbon [g]	Residual Au Conc. [mg/ℓ]	Residual Gold [mg]	Gold Adsorbed /g GAC
0.0000	100.8	50.4	
0.2583	71.6	35.8	56.5
0.5698	42.7	21.35	51.0
1.0026	18.6	9.3	41.0
1.4805	6	3	32.0

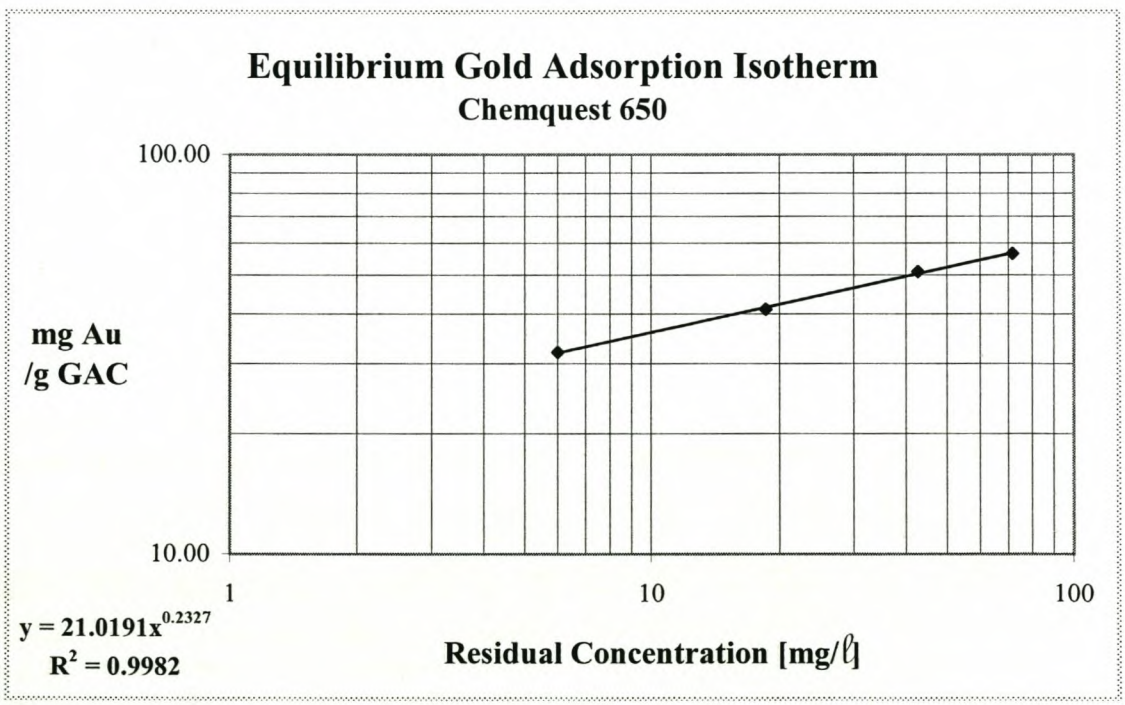

B4: Activated Carbon Pore Area Distributions

B4.1 Pore Area Distribution (6 – 150 Å): P900_0.0425_60

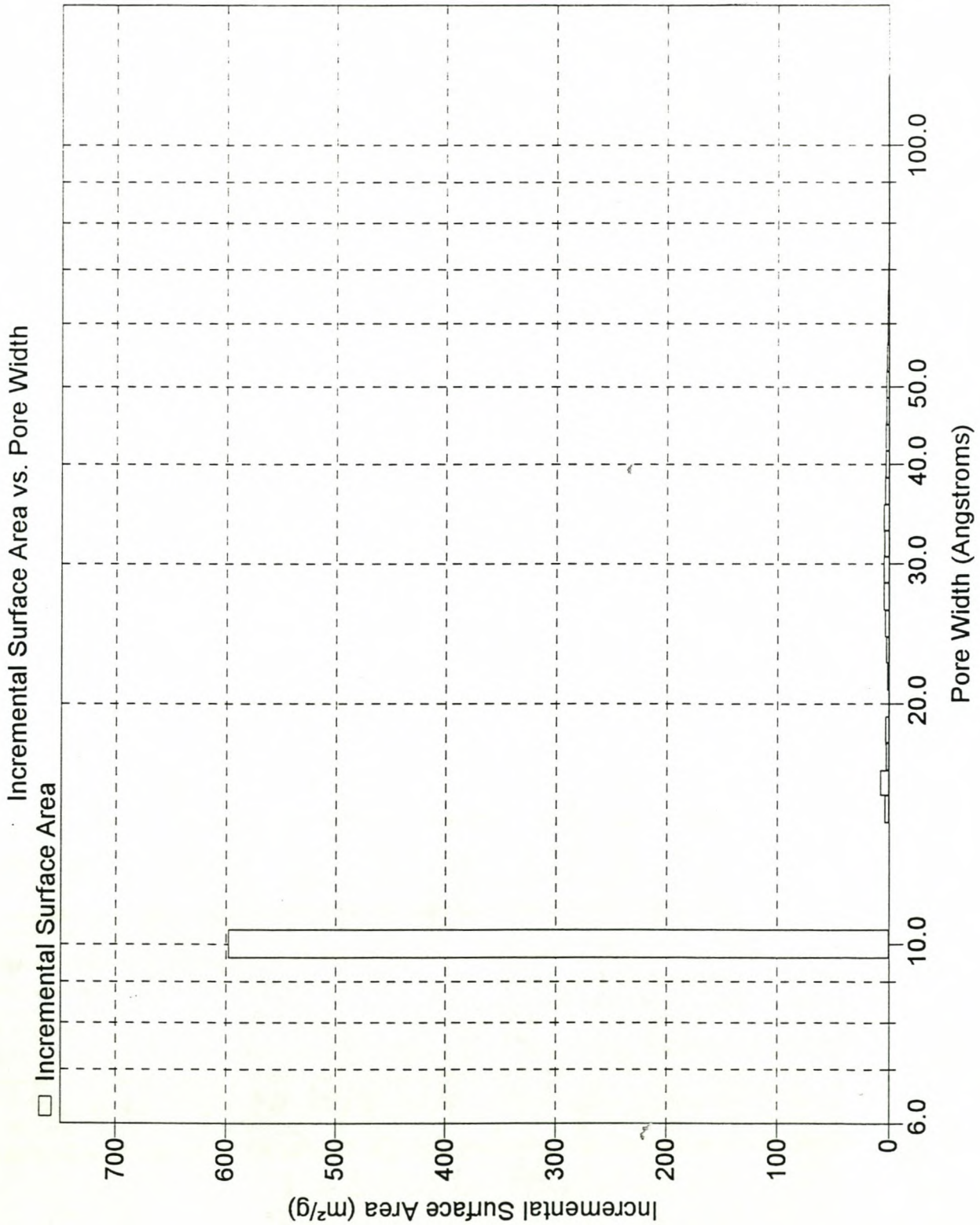

B4.2 Pore Area Distribution (6 – 150 Å): A900_0.0425_60

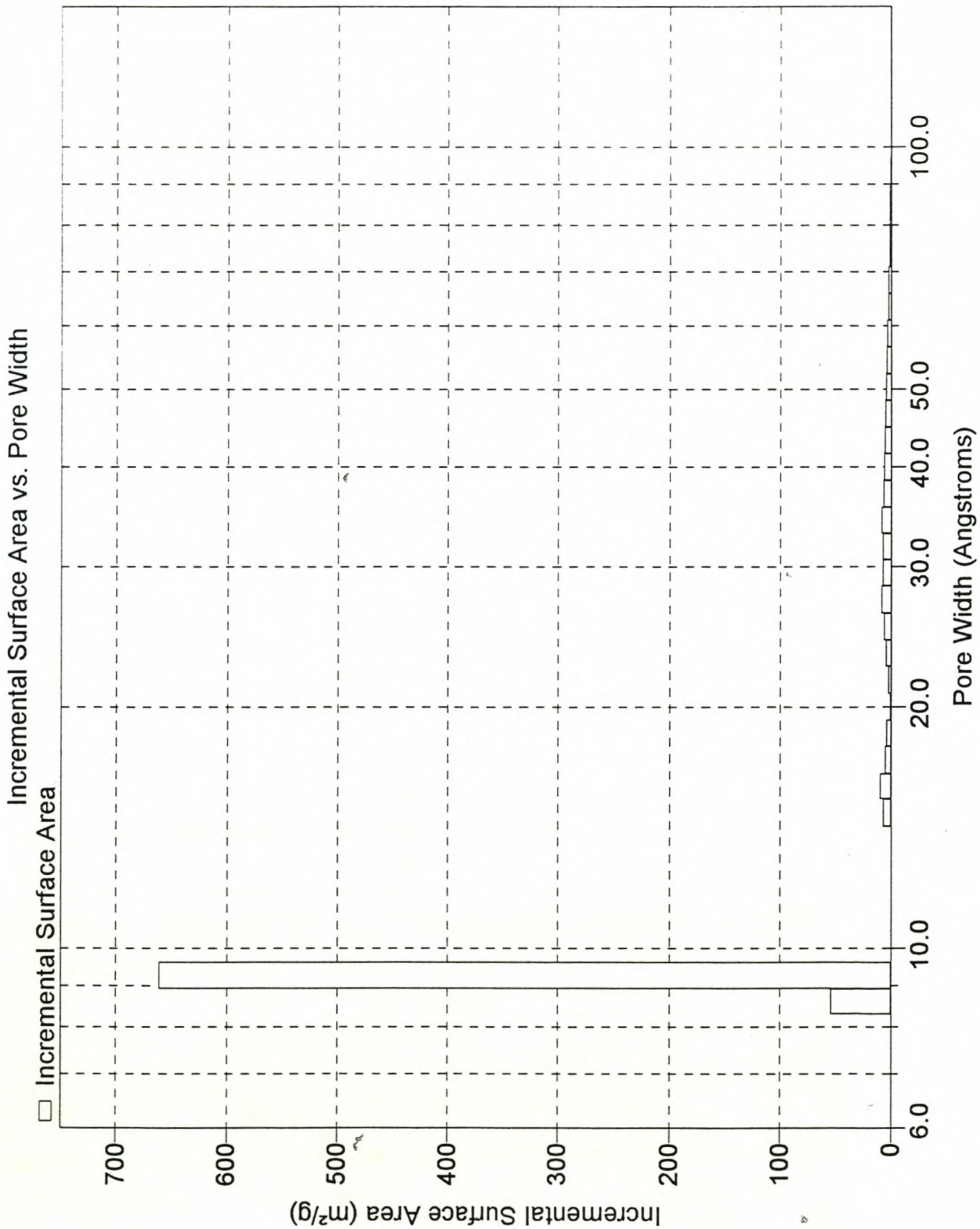

B4.3 Pore Area Distribution (6 – 150 Å): P875_0.0533_60

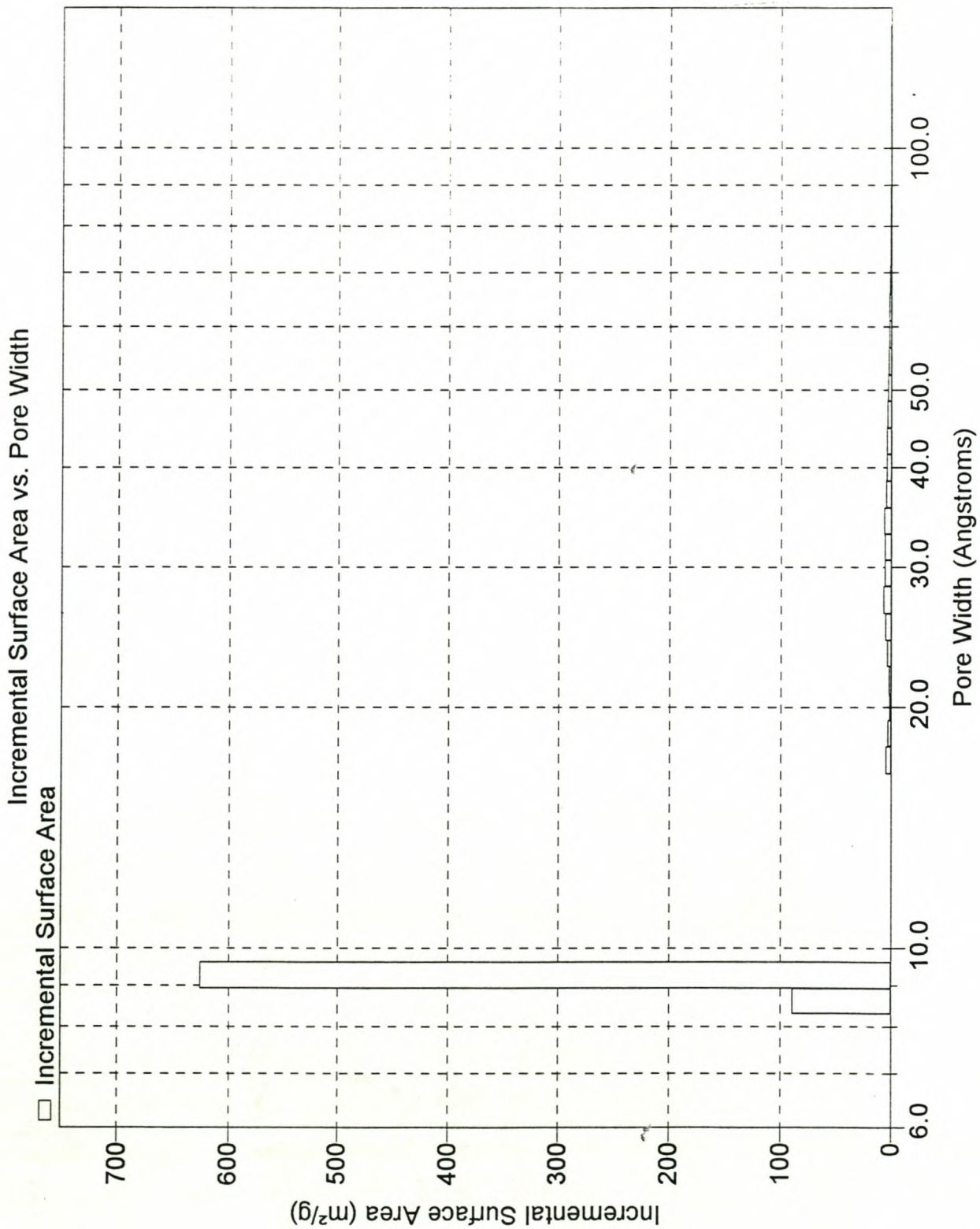

B4.4 Pore Area Distribution (6 – 150 Å): A850_0.0533_60

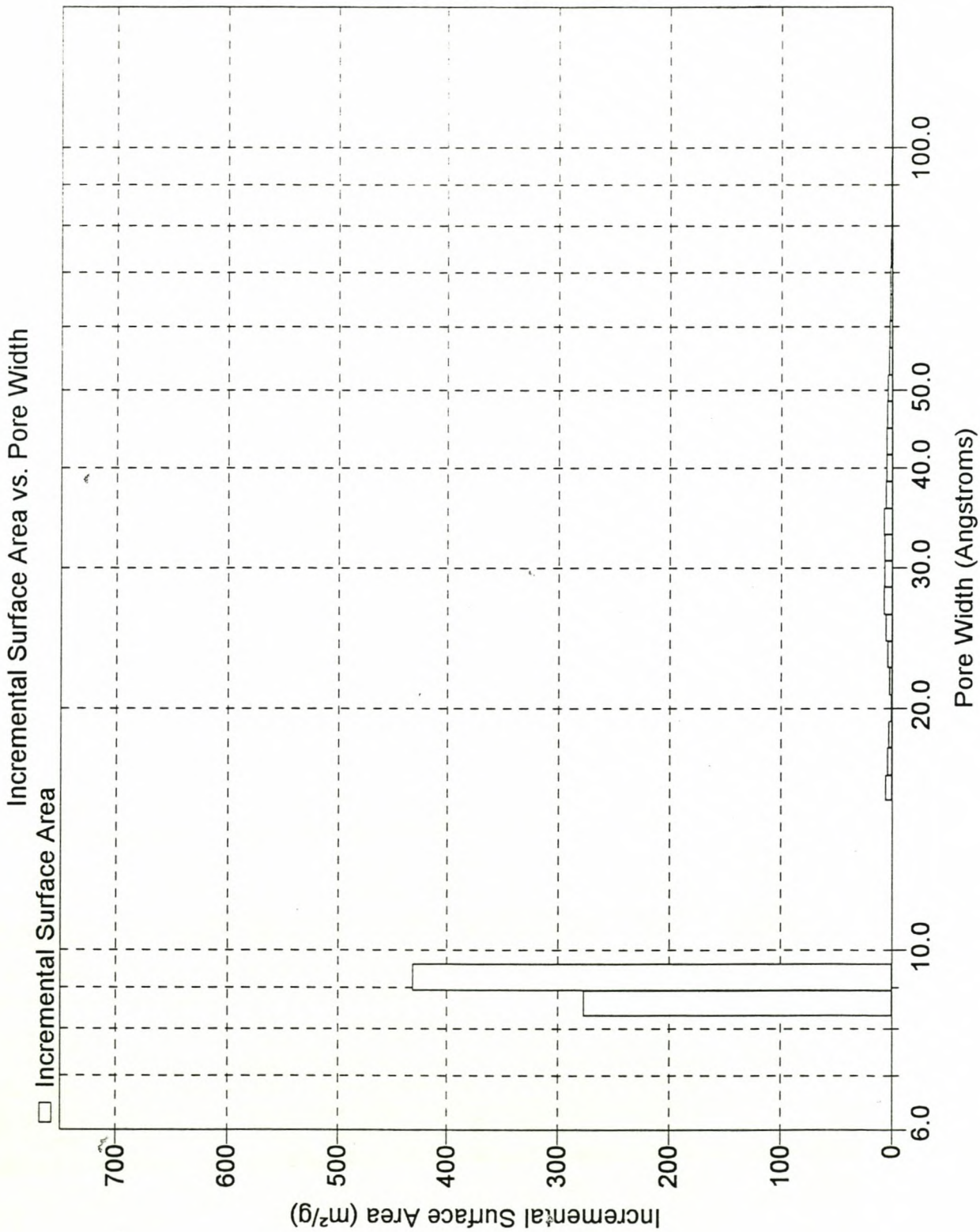

B4.5 Pore Area Distribution (6 – 150 Å): GRC 22

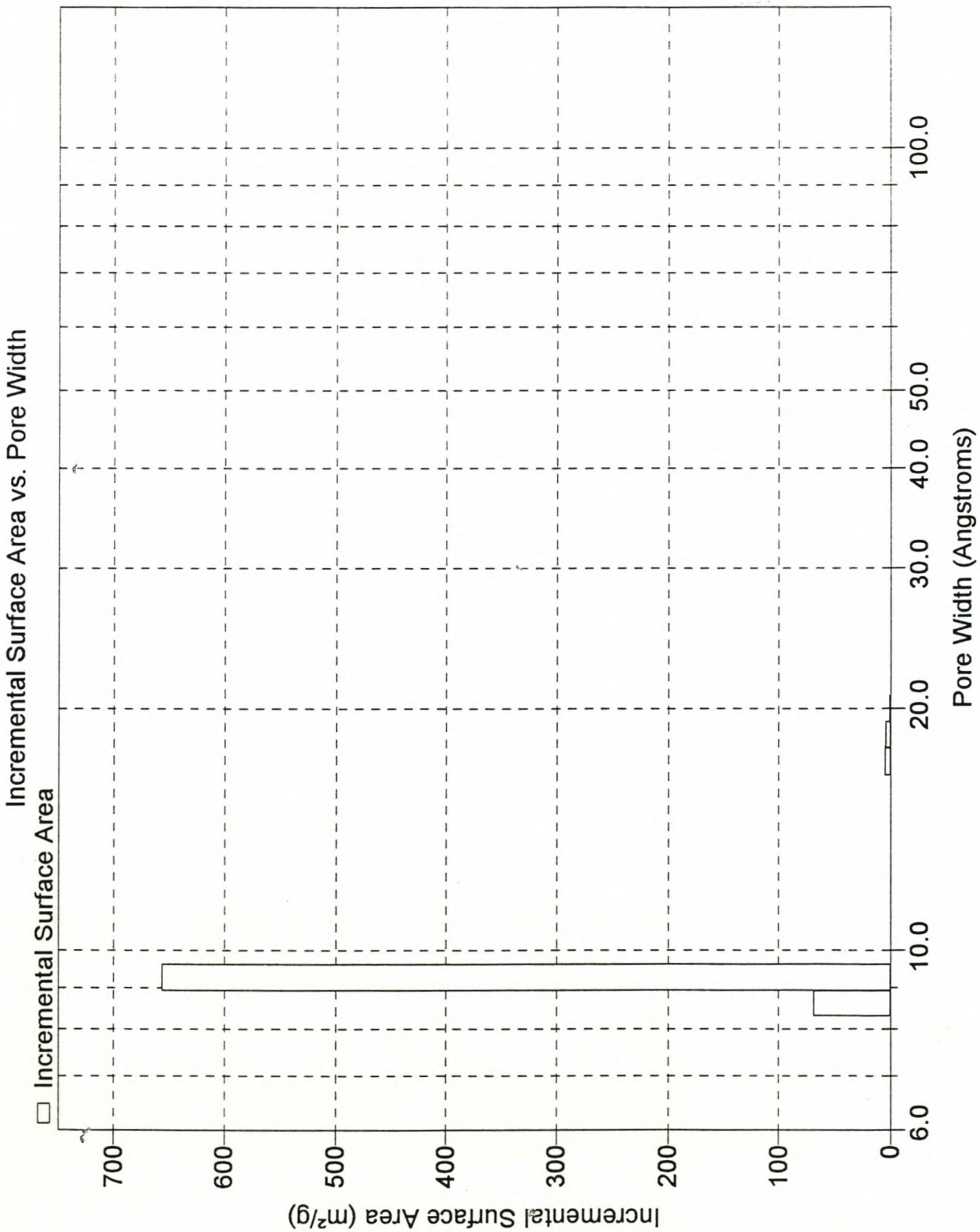

B4.6 Pore Area Distribution (6 – 150 Å): Chemquest 650

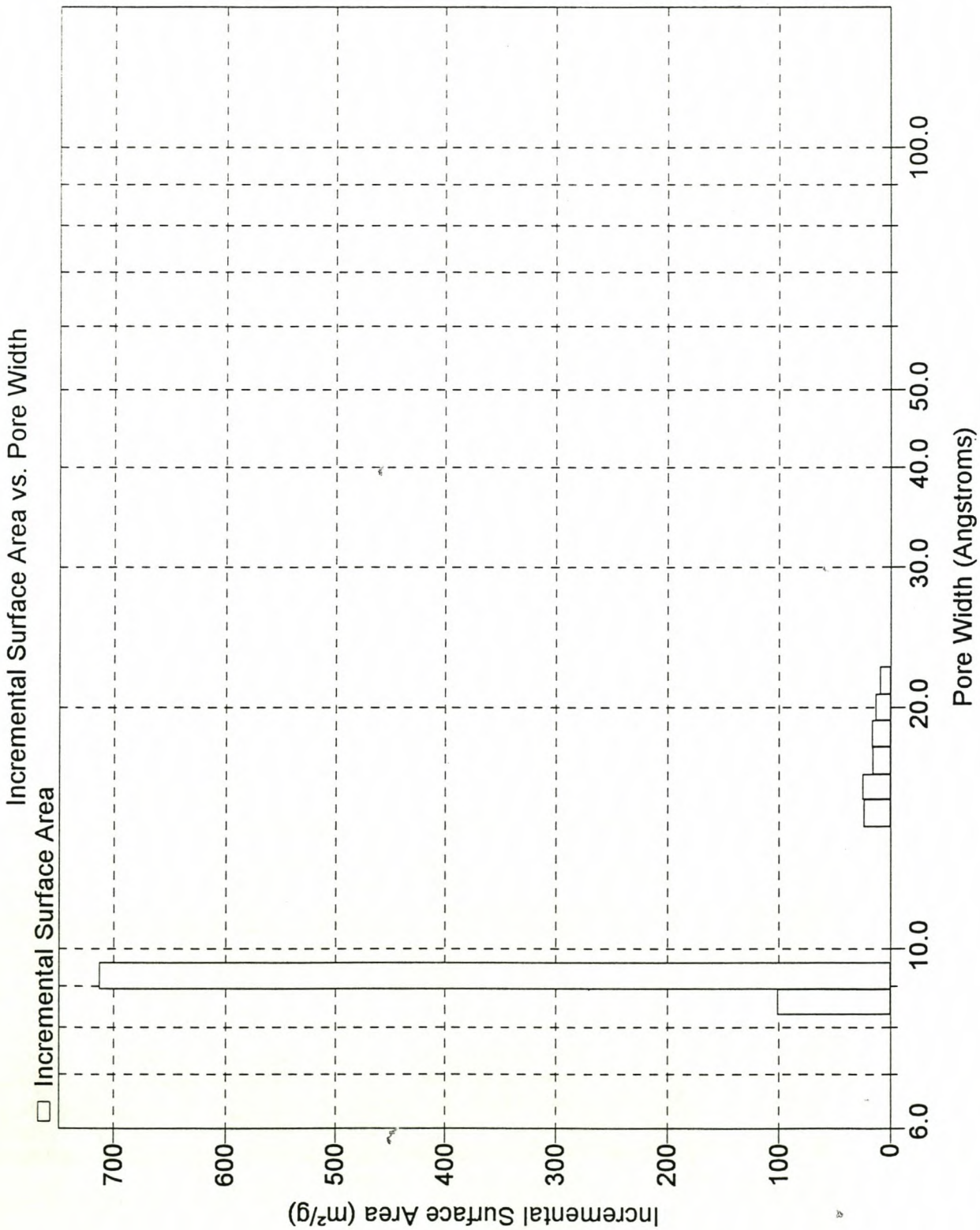

B4.7 Pore Area Distribution (15 – 200 Å): P900_0.0425_60

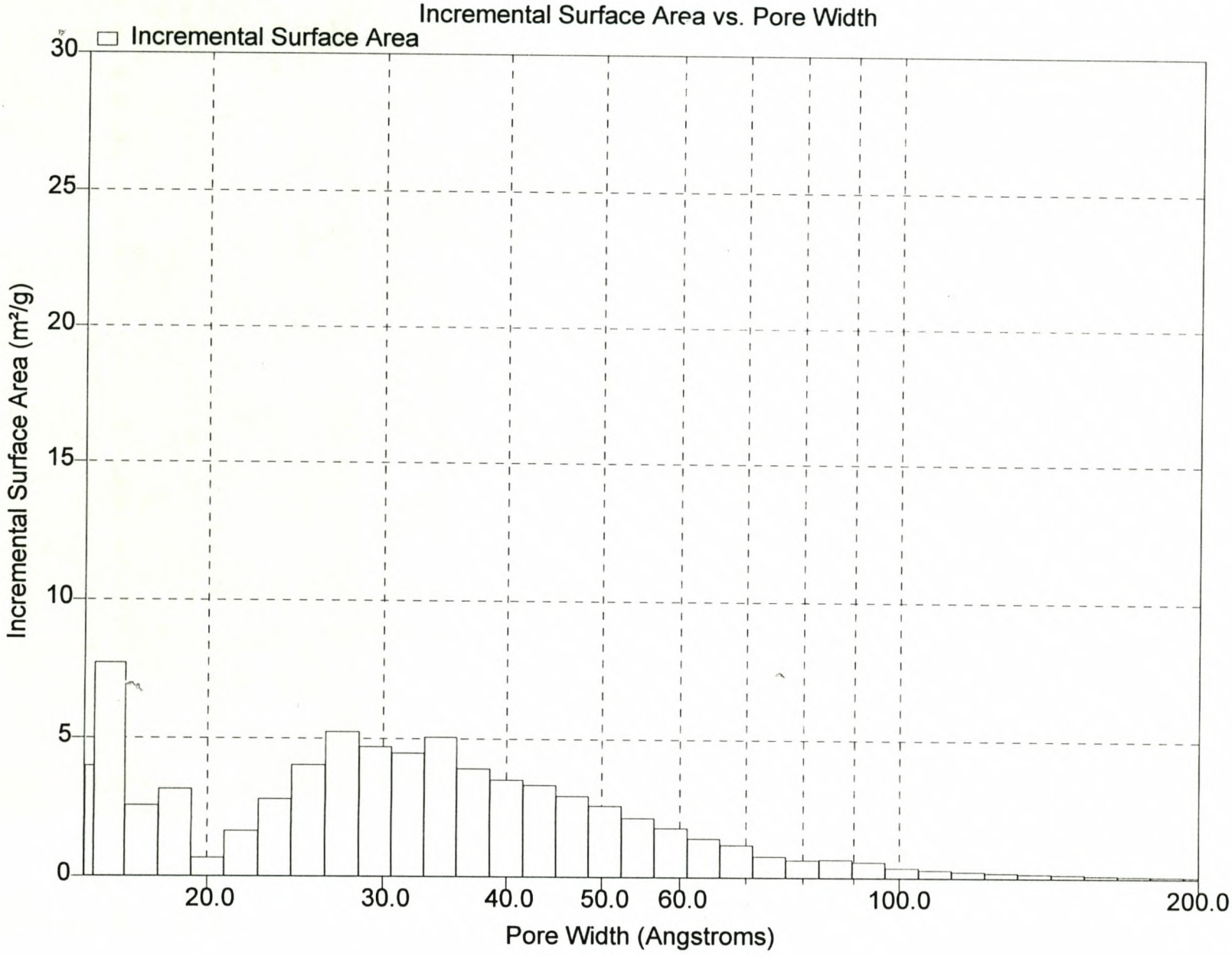

B4.8 Pore Area Distribution (15 – 200 Å): A900_0.0425_60

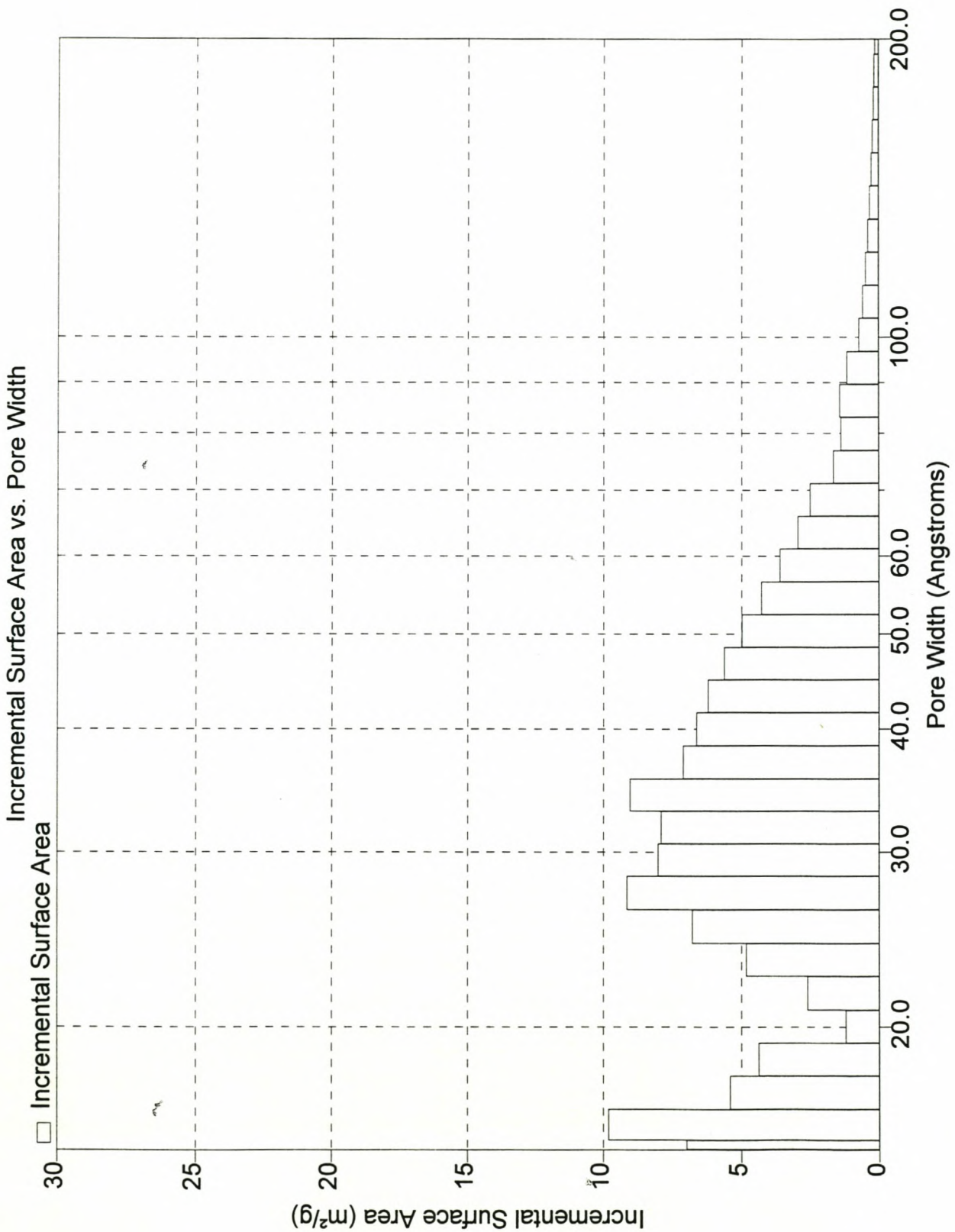

B4.9 Pore Area Distribution (15 – 200 Å): P875_0.0533_60

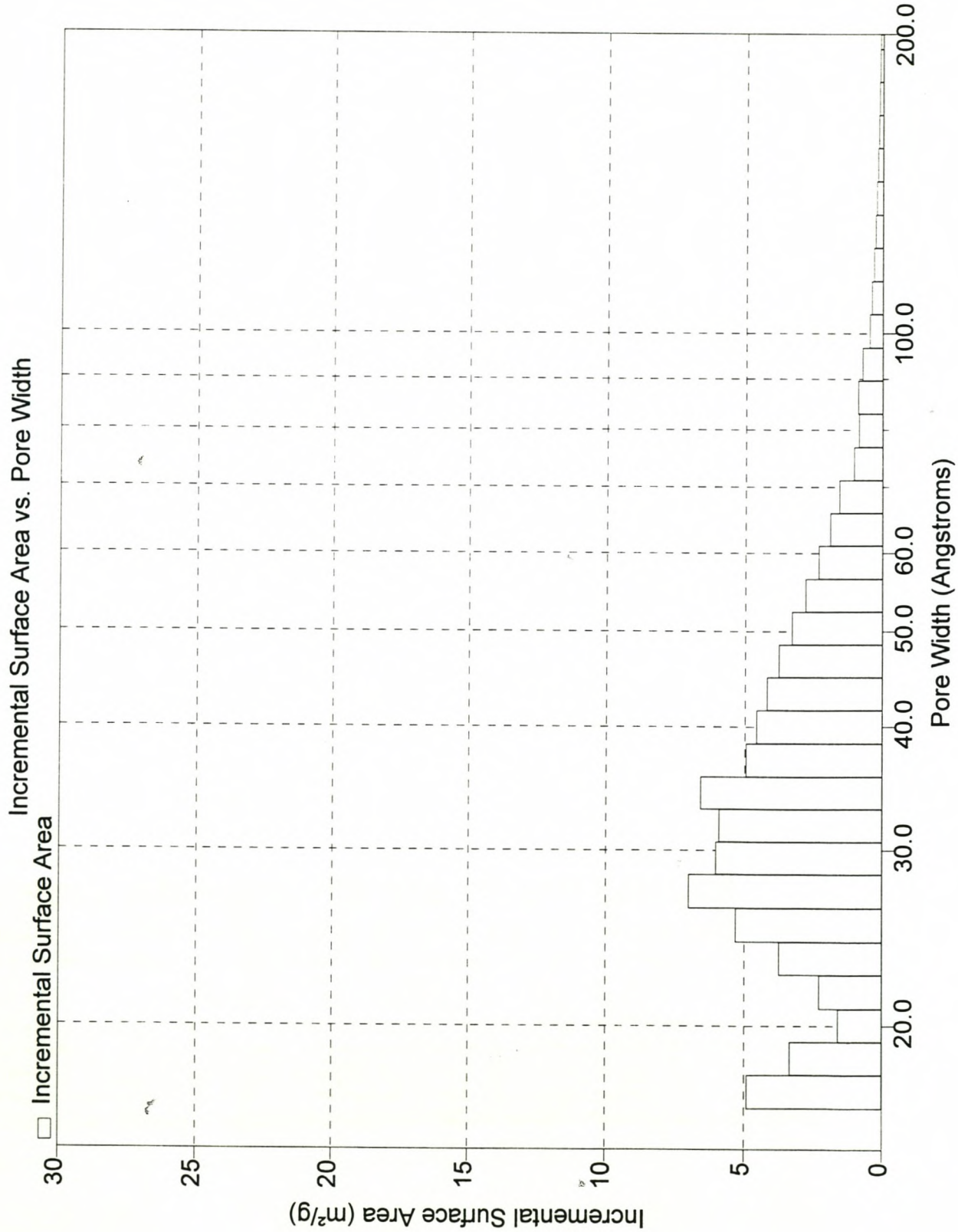

B4.10 Pore Area Distribution (15 – 200 Å): A850_0.0533_60

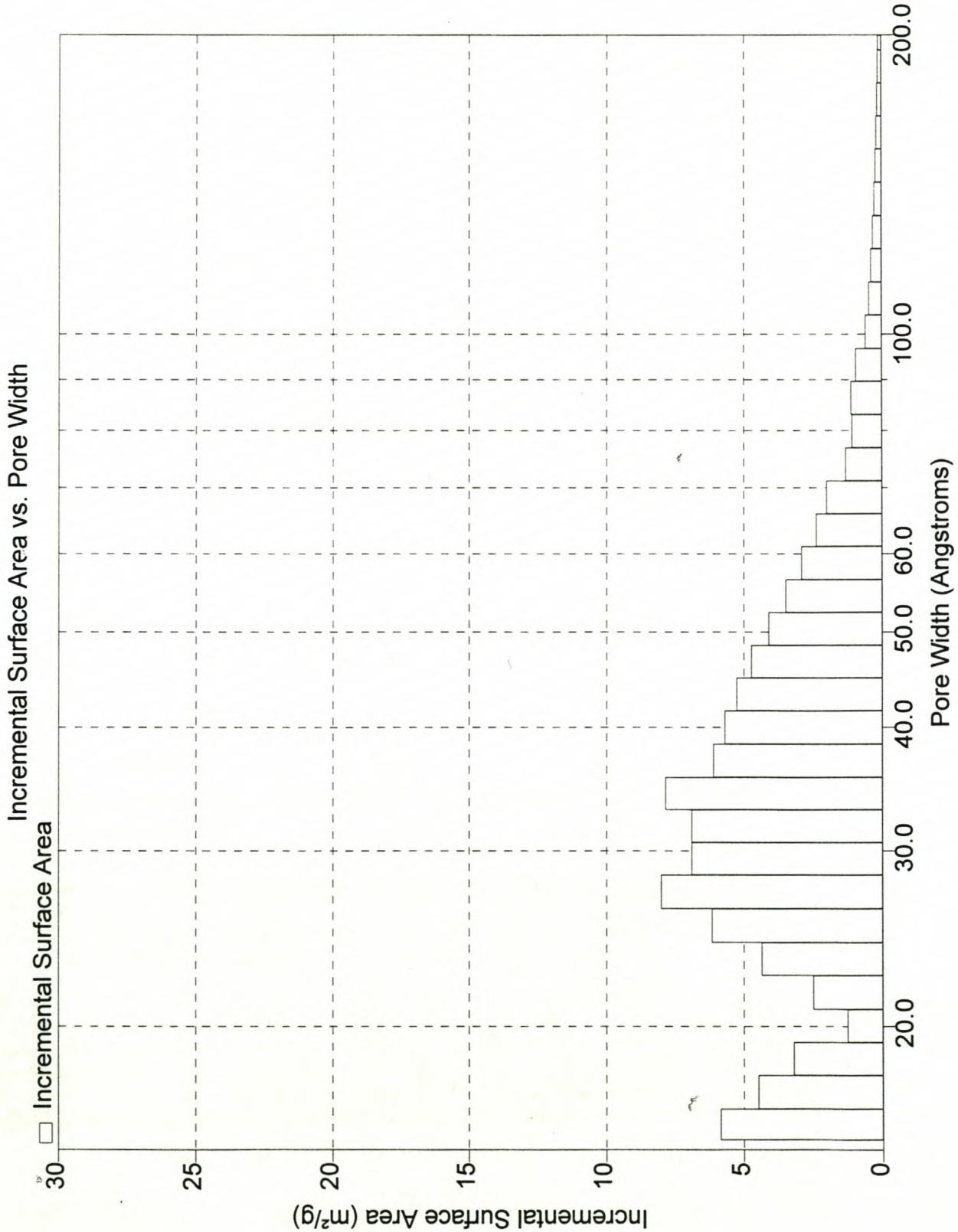

B4.11 Pore Area Distribution (15 – 200 Å): GRC 22

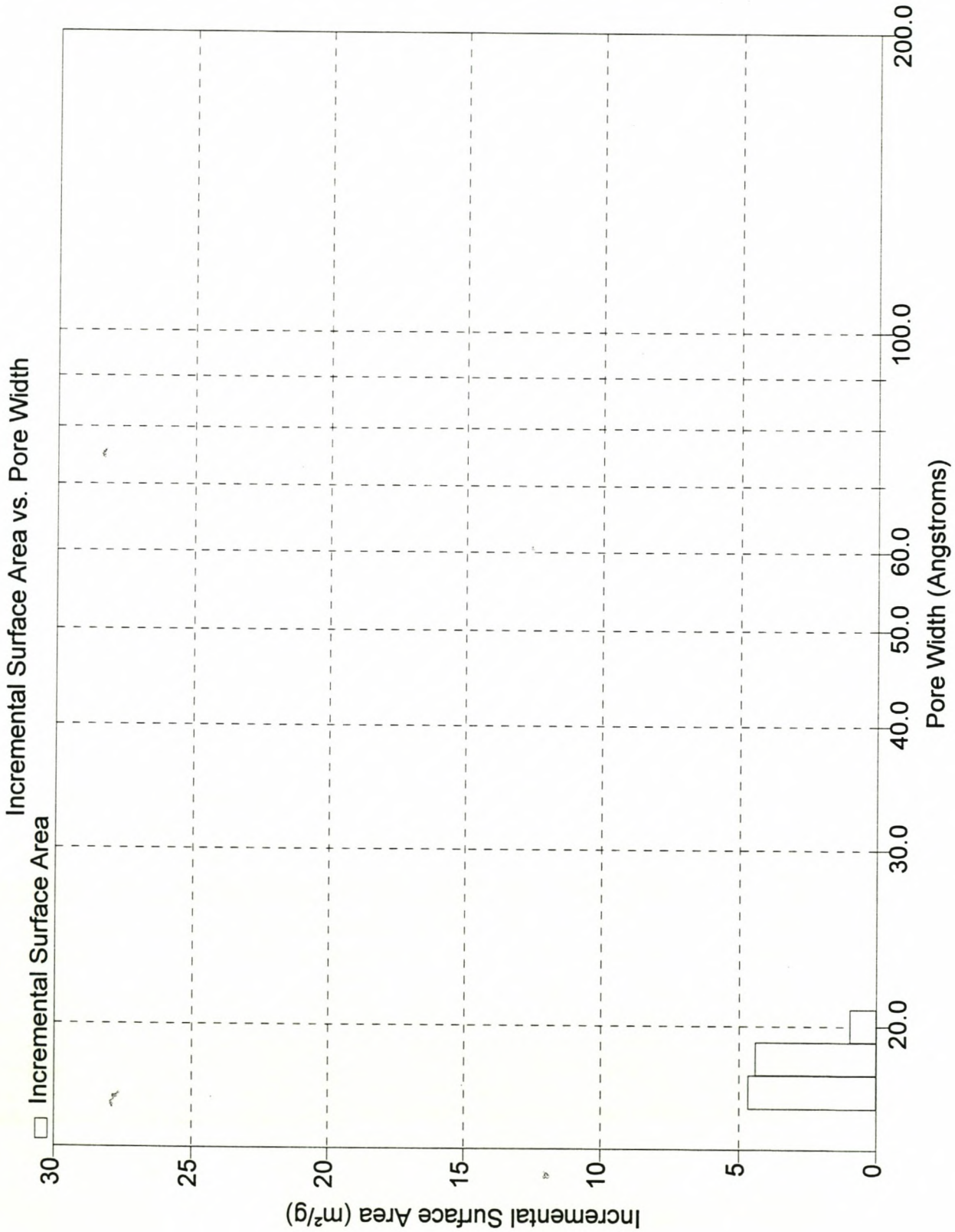

B4.12 Pore Area Distribution (15 – 200 Å): Chemquest 650

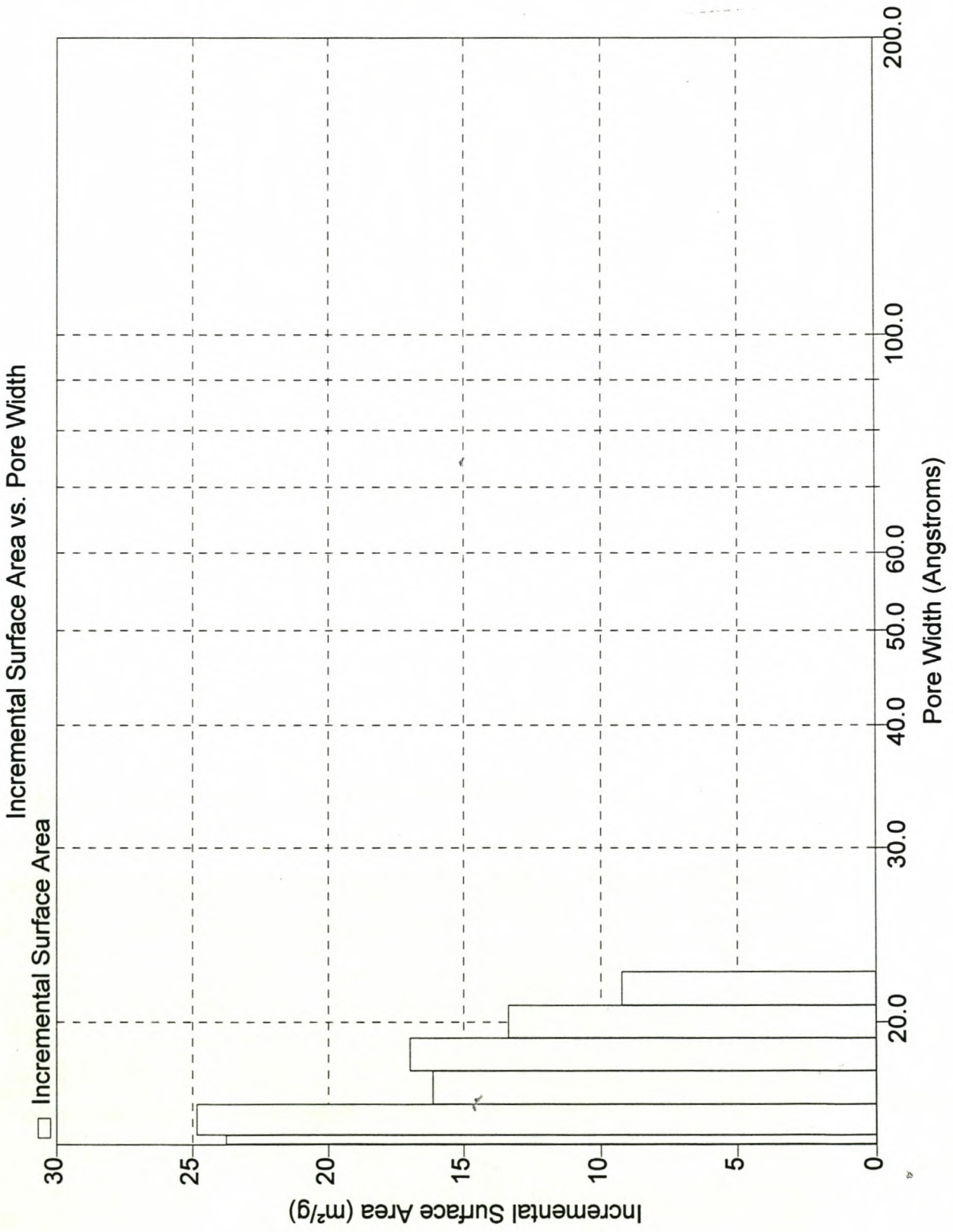

Appendix C: Phenol Adsorption

C1: Preparation of Phenol Solution

10 ppm Phenol solution

Transfer 0.01g of Phenol (100%) to a 1ℓ volumetric flask. Fill with ultra pure water.

Ultra pure water is used, because other organic species that might be present in the water may interfere with the UV analysis.

C2: Batch Kinetic Phenol Adsorption

C2.1 Batch Kinetic Phenol Adsorption P900_0.0425_60

0.25g Activated Carbon per 1000mℓ Phenol Solution

Particle Size 1400-1700 micrometer

Time [min]	Ci [ppm]	Ci/Co
0	9.94	1.000
5	9.73	0.979
10	9.60	0.965
15	9.45	0.951
30	9.10	0.915
46	8.56	0.861
60	8.16	0.821
90	7.43	0.747
131	6.81	0.685
171	6.25	0.629
221	5.25	0.528
278	4.49	0.452
341	3.85	0.388
415	3.37	0.339
497	2.97	0.299
612	2.52	0.254
727	2.39	0.240
899	2.04	0.205
1114	1.47	0.147
1265	1.31	0.132
1449	1.29	0.130
1863	1.17	0.118

C2.2 Batch Kinetic Phenol Adsorption A900_0.0425_60

0.25g Activated Carbon per 1000mℓ Phenol Solution

Particle Size 1400-1700 micrometer

Time [min]	Ci [ppm]	Ci/Co
0	9.94	1.000
5	9.75	0.981
10	9.50	0.956
15	9.27	0.932
30	8.82	0.887
45	8.26	0.831
60	7.90	0.794
90	7.10	0.714
123	6.55	0.658
180	5.51	0.554
237	4.53	0.456
300	3.84	0.386
371	3.48	0.350
455	3.20	0.322
570	2.58	0.259
686	2.29	0.230
854	2.14	0.216
1073	1.62	0.163
1221	1.48	0.149
1407	1.41	0.142
1690	1.31	0.132
1824	1.28	0.128

C2.3 Batch Kinetic Phenol Adsorption A850_0.0533_60

0.25g Activated Carbon per 1000mℓ Phenol Solution

Particle Size 1400-1700 micrometer

Time [min]	Ci [ppm]	Ci/Co
0	9.98	1.000
5	9.81	0.983
10	9.62	0.964
15	9.50	0.952
30	8.89	0.890
45	8.43	0.844
60	7.97	0.798
90	7.27	0.728
120	6.54	0.655
180	5.44	0.545
240	4.50	0.451
300	3.78	0.379
368	3.33	0.334
422	2.99	0.299
519	2.43	0.244
583	2.09	0.210
644	1.90	0.190
800	1.65	0.165
1106	1.29	0.129
1384	0.95	0.095
2807	0.72	0.072

C2.4 Batch Kinetic Phenol Tests: P875_0.0533_60

0.25g Activated Carbon per 1000mℓ Phenol Solution

Particle Size 1400-1700 micrometer

Time [min]	Ci [ppm]	Ci/Co
0	9.96	1.000
5	9.82	0.986
10	9.70	0.973
15	9.50	0.953
30	9.09	0.913
45	8.63	0.867
60	8.19	0.822
90	7.50	0.753
120	6.80	0.682
180	5.67	0.569
240	4.75	0.477
300	4.10	0.412
368	3.52	0.354
422	3.07	0.309
519	2.45	0.246
583	2.16	0.217
645	1.84	0.184
800	1.41	0.142
1100	1.24	0.124
1384	0.82	0.083
1537	0.78	0.078
2808	0.39	0.039

Appendix D: Calibration curves for experimental rotameter

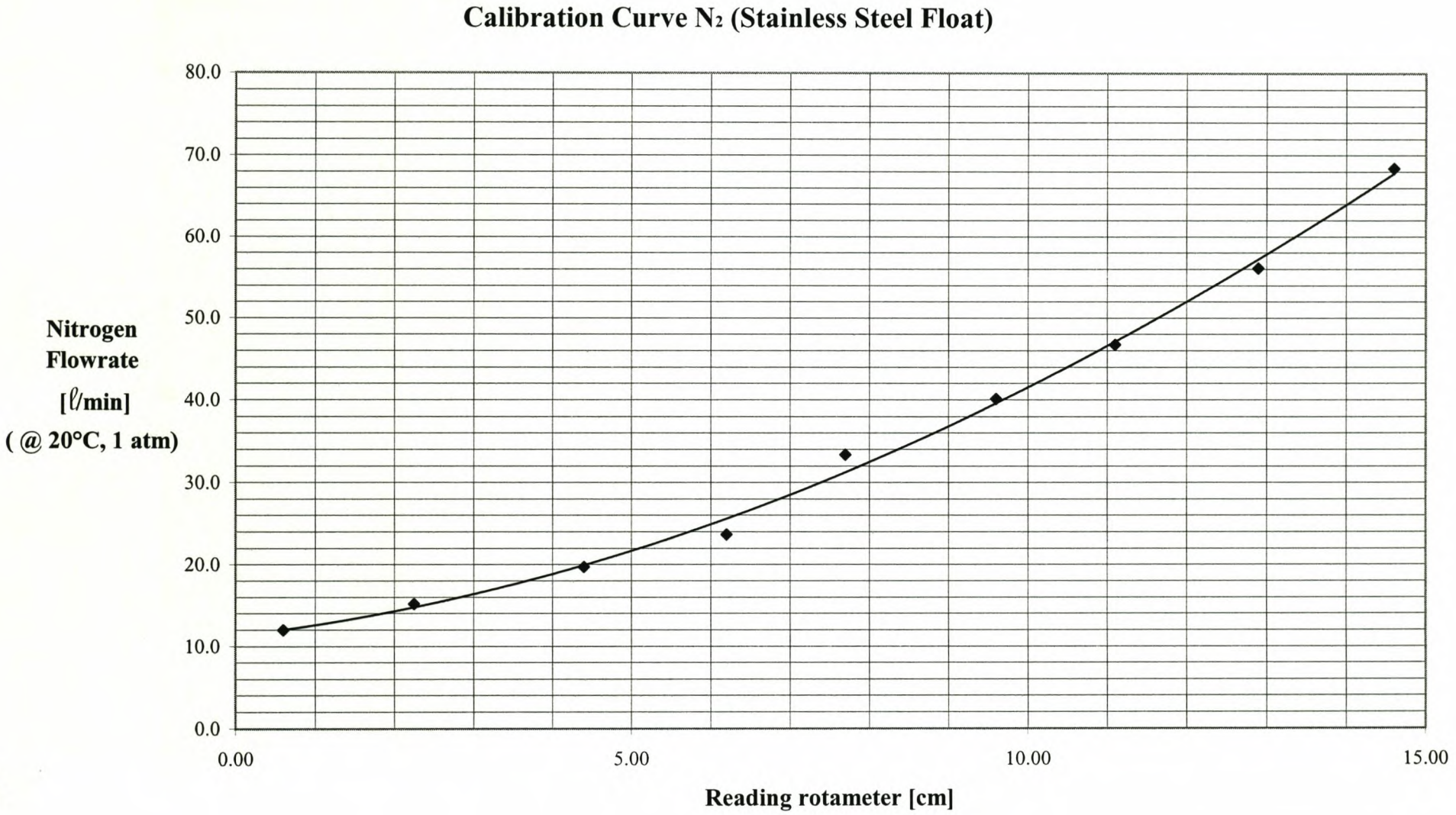
Calibration Curve N2 (Stainless Steel Float)
Nitrogen Flowrate [ℓ/min] (@ 20°C, 1 atm)
80.0
70.0
60.0
50.0
40.0
30.0
20.0
10.0
0.0
0.00
5.00
10.00
15.00
Reading rotameter [cm]

Calibration Curve N_2 (Aluminium Float)

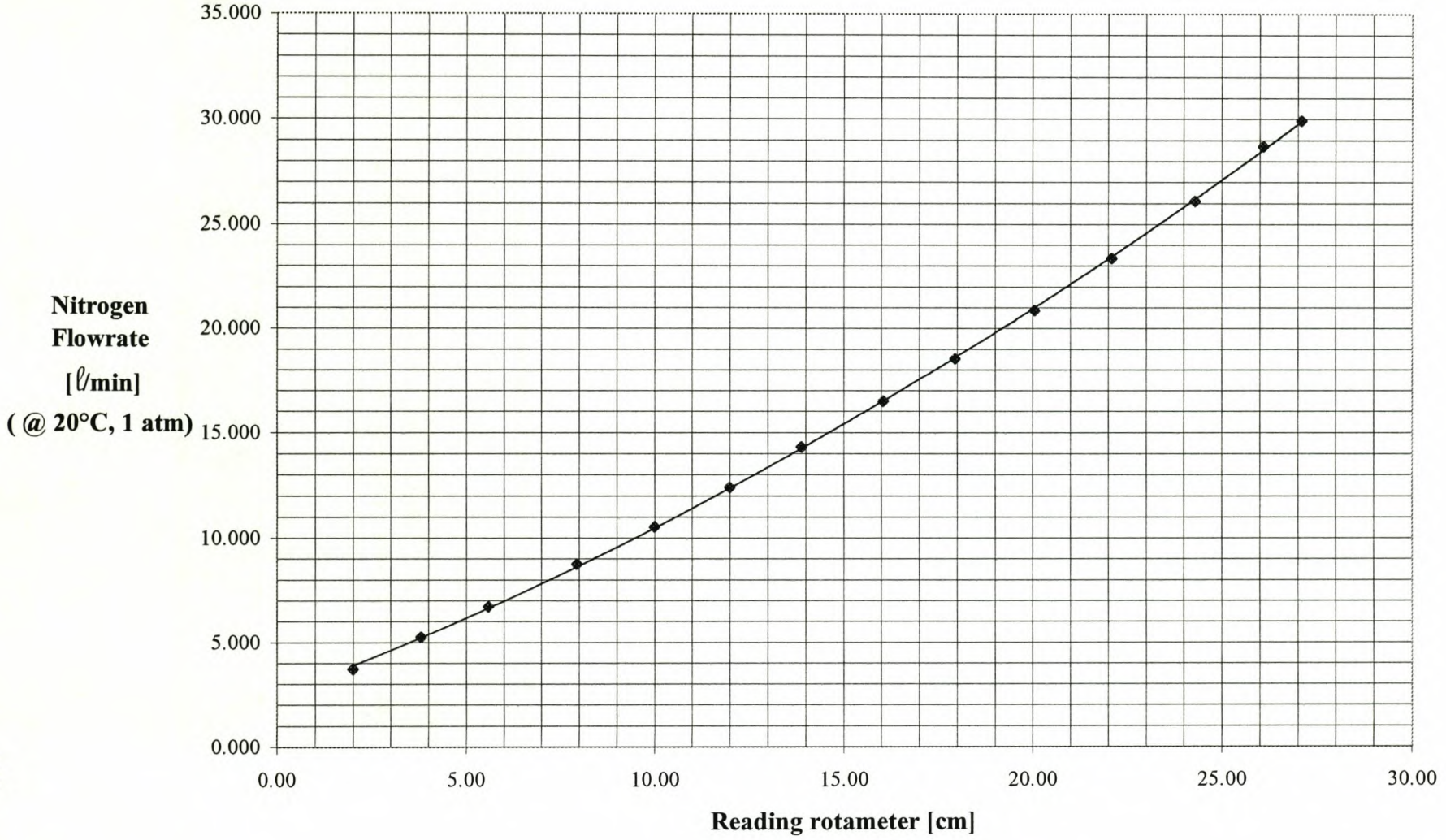

Appendix E: List of Symbols

A	Parameter of Freundlich Isotherm expression
C	Liquid phase concentration [g/m^3] or [kg/m^3]
C_e	Equibrium phenol concentration [mg/l]
D	Density conversion factor
d_p	Average particle diameter [m^2]
D_s	Effective surface diffusion coefficient (in mesopores) [m^2/s]
$\bar{D}_s$	Combined pseudo surface diffusion ($\bar{D}_s = D_s\psi$) [m^2/s]
F	Surface area correction factor
k_b	Rate coefficient for transport from the mesopores to the micropores [s^{-1}]
k_f	Film transfer coefficient [s^{-1}]
M_c	Mass of activated carbon [kg]
M_{CA}	Mass of sample after carbonization [kg]
M_{CS}	Mass of char before activation [kg]
M_{GAC}	Mass of sample after activation [kg]
M_{RM}	Mass of raw material [kg]
n	Parameter of Freundlich Isotherm expression
n_I	Number of activated carbon particles
q	Activated carbon gold loading [mg Au^+/g GAC] or [g Au^+/kg GAC] or [mg Phenol/ g GAC]
SA_{EXT}	External surface area/ Mesoporous area [m^2/g]
S_{BET}	BET surface area [m^2/g]
t	Time [s]
t_l	Film thickness [m]
V	Volume [m^3]
Y_c	Yield after carbonization
Y_T	Total yield percentage after activation (Raw material to GAC)

Greek Letters

α	Fraction of gold loading capacity available as mesopores
ρ_c	Apparent activated carbon particle density [kg/m^3]
ψ	Correction factor for surface diffusivity

Subscripts

b	Micropores
m	Mesopores
o	Initial
s	Liquid – activated carbon interface